TECHNICKÁ UNIVERZITA V LIBERCI
Fakulta strojní

Modifikace diamantového nanoprášku pomocí magnetronového PACVD procesu

Disertační práce

Studijní program: P2301 – Strojní inženýrství
Studijní obor: 3911V011 – Materiálové inženýrství

Autor práce: **Ing. Przemyslaw Ceynowa**
Vedoucí práce: prof. RNDr. Stanislaw Mitura, DrSc.

Liberec 2015

TECHNICAL UNIVERSITY OF LIBEREC
Faculty of Mechanical Engineering

MODIFICATION OF DIAMOND NANOPOWDERS BY THE MW PACVD ROTARY REACTOR CHAMBER

Dissertation

Study programme: P2301 – Mechanical Engineering
Study branch: 3911V011 – Materials engineering

Author: **Ing. Przemyslaw Ceynowa**
Supervisor: prof. RNDr. Stanislaw Mitura, DrSc.

Liberec 2015

Prohlášení

Byl jsem seznámen s tím, že na mou disertační práci se plně vztahuje zákon č. 121/2000 Sb., o právu autorském, zejména § 60 – školní dílo.

Beru na vědomí, že Technická univerzita v Liberci (TUL) nezasahuje do mých autorských práv užitím mé disertační práce pro vnitřní potřebu TUL.

Užiji-li disertační práci nebo poskytnu-li licenci k jejímu využití, jsem si vědom povinnosti informovat o této skutečnosti TUL; v tomto případě má TUL právo ode mne požadovat úhradu nákladů, které vynaložila na vytvoření díla, až do jejich skutečné výše.

Disertační práci jsem vypracoval samostatně s použitím uvedené literatury a na základě konzultací s vedoucím mé disertační práce a konzultantem.

Současně čestně prohlašuji, že tištěná verze práce se shoduje s elektronickou verzí, vloženou do IS STAG.

Datum:

Podpis:

Acknowledgements:

I would like to warmly thank my promoter prof. Stanislawowi Miturze for confidence, time, friendly help, patience and constantly motivate to work.

Thank, dr. Katarzynie Mitura for scientific support during the implementation of each stage of biological research and prof. Petra Louda and Prof. Kazimierz Reszka for the help and valuable comments in the field of materials science.

Dr inż. Annie Sobczyk-Guzenda for the valuable assistance to Do in gaining experience in the analysis of carbon materials.

My dear wife for help, understanding and great patience, children, family, friends, colleagues for all their support.

Work funded by the National Science Centre project No. UMO-2011/03 / N / ST8 / 06184

Contents

Contents 2

1 Introduction 5

2 Literaruture overview 8

2.1 Diamond 8

2.1.1 Natural Carbon 8

2.1.2 Carbon as a solid body 9

2.1.3 Diamond properties 11

2.2 The synthetic diamond 11

2.2.1 Single crystal diamond (SCD) 11

2.2.2 Microcrystalline diamond (MCD) 12

2.2.3 Synthetic diamond properties 13

2.2.4 Applications of synthetic diamonds 14

2.3 The diamond synthesis 14

2.3.1 High-pressure/High-temperature diamond 15

2.3.2 The diamond growth: CVD 16

2.3.3 HF CVD 17

2.3.4 MW CVD 17

2.3.4.1 CVD Plasma 18

2.3.4.2 The plasma discharge 18

2.3.4.3 The chemical environment of the CVD diamond 19

2.4 The diamond as a powder in the nano scale 23

2.4.1 Diamond nanopowders obtained by the detonation method 24

2.4.2 Nanodiamond structure obtained by the detonation method 26

2.4.3 Physicochemical properties of nanodiamond 27

2.5 Biological properties of carbon nanopowders 32

2.6 The overview of diamond nanopowders modifications 34
2.6.1 The mechanical modification 34
2.6.2 The plasma-chemical modification 35
2.6.2.1 Commonly used MW PACVD systems 35
2.6.3 Chemical modifications 36
2.6.3.1 Hydrogenation of the carbon powder surface 36
2.6.3.2 Oxidation reactions 36
3 The objective and thesis of the dissertation 39
4 Experimental 40
4.1 The design and description of the research station 40
4.1.1 The microwave discharge 40
4.1.2 Work schedule 41
4.1.3 Diagram of the „MW PACVD +R" system 44
4.1.4 The construction of MW PACVD + R system [5] 45
4.1.4.1 MW PACVD +R reaction chamber 45
4.1.4.2 The waveguide line 49
4.1.4.3 The microwave generator 51
4.1.4.4 The vacuum system 53
4.1.4.5 Gas distribution system 53
4.1.4.6 The system of control and regulation 54
4.2 Methods used to study the properties of diamond nanopowders 59
4.3 Modification of diamond powders 61
5 Description and the test results 65
5.1.1 Biological Studies 65
5.1.2 HR TEM 68
5.1.3 SEM 69

5.1.4 FTIR 71
5.1.5 Raman spectroscopy 80
6 Discussion of results 83
7 Conclusions 87
8 Abstract 88
9 Bibliography 90
10 Figures list 100
11 Tables list 103
12 Appendix 104

1 Introduction

Modern technologies, used in material engineering, are the source of modern biomaterials. At present, there is observed a significant increase in the interest of plasma chemical methods of nanodiamond modification thanks to which it gains new spectacular properties.

This dissertation concerns the modification of diamond powders (DPP – *diamond powders particles*) in order to achieve the specific physical and chemical properties that would be beneficial for various applications in biomedical engineering. That was the reason why the innovative MW PACVD rotary reactor chamber (MW PACVD – *Microwave Plasma Activated Chemical Vapour Deposition*) was designed and constructed. The material modified in the reactor chamber was tested for potential applications.

Diamond is the carbon allotrope that is metastable under normal conditions. Diamond, as a material, is well-known due to its amazing properties. It is the hardest known material, has the highest thermal conductivity, is chemically inert and has high resistance to wear. What is more it is as well a dielectric material and is optically transparent. This properties individually or in combination, make the diamond a useful material within a wide range of extreme conditions. Due to this reason, many people for over the last few centuries dreamed of synthesis of the artificial diamonds on an industrial scale. At the end of the millennium we have a wide range of methods enabling to create artificial diamonds.

Diamond microcrystals were widely used in the industry for the last half century. The diamond nanoparticles have been found both, in the products of plasma-chemical reactions, and in some meteorites about sixty years ago. Presolar grains were discovered for the first time and isolated by Lewis and his co-workers in 1987 [6]. There were many theories presented in order to explain the appearance of the extraterrestrial diamonds: chemical vapour deposition (CVD) out of stellar outflows, metamorphic shockwave driven by the supernova, UV etching of the coal grains and the mechanism of radiation. In 1987, for the first time, S.Mitura pointed out that nanodiamonds can be formed at a low pressure, with the use of electrons in the CVD process [1, 2], under similar conditions to those existing in the space.

The synthesis of the diamond under the static pressure was discovered in the late fifties. In years 1953-1958 studies, conducted independently by ASEA in Sweden and General Electric in the USA, were successfully completed [7]. In 1955 GE announced the capability to produce synthetic diamonds on the industrial scale [8,9] and patented the method of diamond synthesis [10]. This discovery initiated the studies on the use of the explosive energy for the synthesis of diamonds. In 1961 in the USA, for the first time, in the preserved graphite sample subjected to explosive material compression, was detected the synthetic diamond [7]. The detonation method of the nanodiamond synthesis was discovered in 1963 [8, 9]. V.V. Danilenko proposes and effectively implements the non-ampoule synthesis, with the explosion of the explosive material in the discharge chamber, instead of the ampoule synthesis. In this method, the graphite was placed directly in the cylindrical charge consisting of the mixture of trinitrotoluene and hexogen - TG40. The charge was wrapped in the water jacket to suppress the graphitization and to reduce the unloading speed of the synthesized diamonds.

Methods of diamond synthesis are described in chapter *2.3. The diamond synthesis*. The most common method is the previously mentioned detonation method. For the synthesis of diamond powders is required the energy that can be provided as well by the processes that are enumerated and described in this chapter: thermal processes (*High-pressure/High-temperature*) and plasma processes CVD (*Chemical Vapour Deposition*). Amongst the plasma methods, the special attention deserve CVD processes activated by the PA CVD plasma (*Plasma Activated Chemical Vapour Deposition*) inter alia MW PACVD (*Microwave Plasma Activated Chemical Vapour Deposition*) in which the plasma is generated with the use of typical power supply of the frequency of 2,45 GHz, which is characterized by the high density of electrons.

Currently, there is a great interest in the development of the diamond powder particles (DPP) modification methods, thanks to which they gain new properties [16]. Diamond powders are modified by chemical, mechanical and plasma methods [11-16]. The MW PACVD is one of the methods used for the modification of the DPP.

The technology of modifying the DPP by the MW PACVD method, by the use of the rotary reactor chamber, may be much more advantageous in comparison to commonly used methods that use the static reactors. It allows to carry out the modification process in

a continuous and cyclic way (through the repeated rotation of the reaktor chamber) at the level not reachable for the classical methods. At the same time, it will lower the costs, increase the efficiency and allow for the control of the level of DPP modification. Moreover, it may also lead to discoveries of the great significance in the field of material and biomedical engineering.

So far, this type of solutions, using the MW PACVD reactors, were carried out in the vertical orientation with the static reactor chamber. As a part of the dissertation was anticipated the project of such solution, the purchase of the necessary equipment and the ultimate realization of the prepared solution.

This dissertation concerns the basic research that were carried out in the field of the material engineering, more specifically in the technologies of plasma modifications of diamond powders. During the implementation was carried a careful analysis of the physical and chemical processes that occur during the process of DPP modification (first of all, the influence of the rotation of the reactor chamber on the level of the DPP modification). The research carried out are mainly design realizations and experimental studies. These are the original research works conducted in the field of obtaining and modification of the DPP, which make an invaluable contribution to the development of this discipline and, in particular, to the development of plasma methods. The new knowledge, about the impact of the innovative design of the MW PACVD reactor chamber on the plasma processes occurring in its inside, was acquired during the subsequent experiments with its use.

The literature data show that despite the large amount of works on modification of diamond powders by the MWPACVD method, there is a lack of any mention in the literature regarding this type of solution. The modification using the rotary chamber of the MW PACVD generator, remains an unclear issue worthy of further examination. In particular, determining the influence of the rotation on the DPP modification, selection of the powder and conditions of the modification, seem to be of utmost interest. The scope and the subject of the research would be the first study regarding the DPP modification by the MW PACVD rotary reactor chamber.

For the implementation this work was achieved project National Science Centre No. UMO-2011/03 / N / ST8 / 06184.

2 Literaruture overview

2.1 Diamond

2.1.1 Natural Carbon

Carbon occurs naturally both as a free element, in the form of graphite or diamond, and in combination with the other elements in a great number of chemical compounds. Many of the substances containing carbon are the foundation of life on Earth and form the basis of the whole branch of science called the organic chemistry. In the anthropological sense, carbon materials have been known since prehistory, they occurred in the form of charcoal, soot and even diamond, used for abrasive polishing, about 2500 BC [Lu *et al.*, 2005]. As shown in the records of the early years of civilization coming from Indochina dated approximately 4^{th} to 2^{nd} century BC, diamond played a particular role in the history of mankind. The classification of carbon as an element occured in late 18^{th} century where, for the first time, Antoine Lavoisier used name *carbone* derived from Latin *carbo*, meaning charcoal. The term diamond was proposed at the same time. The name diamond is the combination of Greek word transparent ^a^aupę or *diaphanes* and indestructible or invincible (aSapaę albo *adamas)*. The fact that diamond was the allotrope of carbon was proven by Lavoisier in France and Smithson Tennant in England, in the process of material combustion and later weighing the produced CO_2 [Tennant, 1797].

The natural diamond is formed from molten rock in a specific band in the upper part of the mantle, known as asthenosphere, comprised between 100 and 200 km below the surface of the Earth. During volcanic eruptions, material from this region is transported closer to the Earth's surface where, while cooling, creates specific rock tubes. The process of extracting these ancient volcanic rock tubes, named kimberlite (after the discovery of diamond-bearing rocks in South Africa near the town of Kimberley in 1870). It is worth to mention that they form a large part of the world's natural diamond resources. As a result of the kimberlite tubes erosion, natural diamond can also be found in deposited deposits of sedimentary and alluvial rocks [Hazen, 1999]. With some notable exceptions, most of the mined natural diamond is of poor quality, unresponsive to precious stones, despite that fact it is widely used in industry mainly for polishing, abrasive materials and cutting tools [Greenwood & Earnshaw, 2001]. This inherent deficiency of the natural diamond and significant efforts in improving the extraction and mining processes, make the natural

diamond highly desirable, expensive and luxury commodity. In this situation, the alternative of synthetic diamonds seems to be essential.

2.1.2 Carbon as a solid body

Carbon is the sixth element in the periodic table. It has an electron configuration $1s^2 2s^2 2p^2$, consisting of two electrons on electron shell K (orbital 1s) and four electrons on electron shell L (2 * 2s and 2 * 2p). Two electrons from orbital 2p are valence electrons [5].

Carbon atoms can be combined with each other by various types of bonds. Valence electrons of this element may create bonds of σ type (hybrid of σsp or σsp^2). Other p electrons create bonds of Π type or may create σsp^3 hybrids (depending on the excited state). The carbon bond of σ type is the strongest covalent bond occurring in nature [5].

Types of bonds occurring between two atoms of carbon:

- single C-C type σsp^3 of the length 1,54 A,
- double C=C type sp^2 of the length 1,3 A
- triple C=C type sp of the length 1,2 A.

Electron binding energies and spatial distribution of carbon atoms of various configurations significantly differ from each other. Thus, carbon as a solid body, occurs in various allotropes varieties (Tabel 1.):

- enantiotropic variety – thermodynamic stability depends only on the temperature; differs in the spatial arrangements of atoms (crystallographic system)
- monotropic variety – differs in types of chemical bonds and their energy

Apart from the above mentioned carbon allotropes, there are also other carbon materials of homeogenius structure – fullerenes, carbon nanotubes of homeogenius chemical structure and heterogeneous in terms of bond types (thin layers of carbon).

Table 1. The features of varietes of carbon materials [5]

	Material	**Electron configuration**	**Energetic structure in the temperature 0 *K***	**Type of crystal**
Carbon allotropes	carbyne	σspΠpΠp	Filled band σ Empty band σ^* Half-filled band Π	3D atomic-molecular
	graphite	$\sigma sp^2\Pi p$	Filled band σ Empty band σ^* Half-filled Π	3D atomic-molecular
	diamond	σsp^3	Filled band σ * Empty band σ^*	3D atomic
Other carbon materials	fullerens, carbon nanotubes	$\sigma sp^2\Pi p$	Filled band σ Empty band σ^* Filled band Π Empty band Π^*	3D molecular
	graphene	$\sigma sp^2\Pi p$	Filled band σ Empty band σ^* *Filled level* Π *Empty band* Π ↑↓ *Half-filled level* Π	2D atomic

Natural diamonds are classified according to the number of nitrogen atoms (N), which they contain, and in that way are determined their certain physical properties. Type Ia consists of 0.05-0.25% N and has the largest impurities within the crystal, while type Ib contains higher fractions of N in 1%. A little number of diamonds contain small amounts of (Ila), but some contain boron (IIb), that gives them very sought after blue colour.

2.1.3 Diamond properties

Diamond is well-known not only as the hardest of all minerals, but also has a large range of other extreme properties that are listed in the table below:

Table 2. Some extreme properties of natural diamonds [Field, 1992, Maj, 2000].

Criteria	*Diamond properties*
Structural	Exceptional mechanical hardness (~ 90 GPa) and wear resistance as well as low compression factor (8.3 X 10^{-3} m^2 N^{-1}); High modular mass (1.2 x 10^{12} N m^{-2}); High thermal conductivity (2 x 10^3 W m^{-1} K^{-1}, in room temperature (RT)); Low thermal expansion factor (1 x 10^{-6} K^{-1} at RT)
Electronic	High electric al resistance (~10^{16} Q m, ale 10^{-1}-10^4 Q m for additive material); Wide internal band gap (intermediate band = 5.4 eV, but Lower in additive materials); The surface shows a low or even negative degree of electron affinity
Chemical	Chemically and biologically inert; Corrosion resistant;
Optical	Transparent over a wide wavelength range from deep UV to far IR High resistance to radiation damage.

2.2 The synthetic diamond

2.2.1 Single crystal diamond (SCD)

Synthetic diamonds appear in many different sizes and morphologies. In extreme cases, small diamond crystals, which fulfil the function of diamond embryo, may grow to large, epitaxially single crystalline materials in the process of the gradual carbon deposition. The development of CVD methods enabled to improve the growth rate to the respective of 165 pm h^{-1}, working at high pressures - about 350 torr, which leads to high SCD deposition up to 18 millimetres [Liang et al., 2009]. Those homoepitaxil processes are widely studied with a particular emphasis on the growth and development of various crystal planes. However, these processes are not used within this thesis.

2.2.2 Microcrystalline diamond (MCD)

The diamond formed in the CVD processes in general does not take the form of a single crystal, mostly its structure consists of small crystallite diamonds appearing in the environment of no-sp^3 structures, on the borders between individual grains (term crystallite and grain is used interchangeably).

Diamond layers can be made of an infinite number of various grain sizes ranging from macroscopic crystals, almost like SCD, to nanocrystalline diamond NCD. Between these two extremes is a material known as microcrystalline diamond MCD or sometimes PCD: a polycrystalline diamond, in which the grain size is determined within the range of 100-10000 nm. In the layer section, MCS shows column structure made of single crystals up to larger ones depending on time of deposition/thickness of the layer.

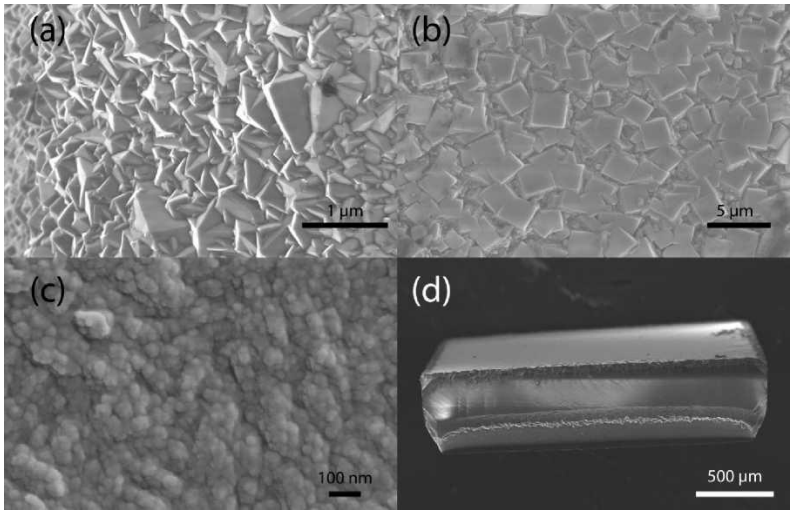

Figure 1. The range of different morphologies of a large single crystal of the synthetic diamond

(d, shows the last form) through <111> (a) and (b)<100>polished microcrystalline layer to nanocrystalline diamond (c). From (a) to (c) grown and (d) covered with the use of MW CVD

Like most of crystalline solids, the diamond can be described by its various levels that occur periodically throughout the whole crystal lattice. One of these planes is often privileged and spreads in the structure, thus making the surface more receptive to the deposition process (growth zone). Within the diamond, there are three dominant crystal planes that are determined by the Miller indices <111>, <110> and <100>.

In general, synthetic diamond surfaces or natural diamonds that are cut along a defined plane, have different properties due to different arrangements of carbon atoms. On

the MCD, those differences are visible while comparing the morphology of the surface <111> and <100> of polished samples (Figure 2. a and b). It can be noticed that <111>, in a dominant advantage, consists of diamond grains having pyramidal structure of more or less triangular facades, while sample <100> has square facades corresponding to the crystal lattice of plane.

Understanding the structure of these different crystal surfaces is crucial. The mechanics of deposition and the energy of the whole process will have an influence on relations in distribution of atoms and interatomic distance on any surface. Generally, the morphology depends on various mechanisms of the diamond deposition, which, in turn, result from the variation of plasma-chemical processes.

2.2.3 Synthetic diamond properties

In comparison to MCD, NCD layers have smoother surfaces, yet, because they contain a larger amount of sp^2 carbon, they are sometimes considered to be of inferior quality diamond, although they often show similar or even better physical properties. It is clear that when the grain size decreases, then the surface area of all grains increases and this causes the increase of non-diamond material content within the structure. The grain size in the NCD film is ranging from 5 to 100 nm, at the same time, the lowest sizes (<10 nm) were smartly called ultra nanocrystalline diamonds (UNCD), this material is substantially identical though has smaller crystallite sizes. Within the lower limits, the smoothness of NCD surface becomes comparable to single crystal diamond, with an average roughness factor of several nm, which is desired in a wide variety of applications. Thicker layers are usually formed as a result of grouping of individual diamond grains into larger structures, such as spherical shapes referred to as *Ballas diament*, and can be observed as clear islands on the surface of the substrate, if the deposition is stopped before the layer becomes continuous (Figure 2. c). As a result in NCD, in comparison to MCD, surface roughness is independent on the layer thickness, in case when re-nucleation of crystals occurs throughout the whole layer treated by depostion [Krauss et al., 2001, Williams et al., 2006]. The morphology of the diamond is highly dependent on the conditions under which it is deposited.

2.2.4 Applications of synthetic diamonds

Thanks to the sample properties of natural stone (see Table 1.) that are expanded in synthetic materials, the diamond has found many ways in which to be used, not only by its reputation but also as a very sought after stone. The scope of use of thin diamond layers has been described extensively [Gicquel et al., 2001, May, 2000, Yarbrough, 1991] with a particular emphasis on the electrical properties [Railkar et al., 2000, Williams et al., 2005], optical properties [Koidl i Klages, 1992], tribological properties [Erdemir et al., 1996], biological functions [Williams et al., 2007b] as well as use as biomaterials [Nebel et al., 2007], radiation sensors [Bergonzo et al., 2001] or for creating mechanical microelectronic devices [Auciello et al., 2004, Huff et al., 2006, Krauss et al., 2001]. It is obvious that the diamond is used in countless applications that are impossible to be enumerated at this point.

Currently, there is a number of situations where the diamond would seem to be the perfect material for a specific application. However, it is not used due to the lack of the ability to transfer laboratory knowledge to industrial-scale production and high costs, owing to which applications are currently too expensive.

2.3 The diamond synthesis

Methods of preparing synthetic diamonds have been known for over 60 years. Initially, diamonds were of a small size and defected, but with time, as the process of synthesis began to improve, diamonds of good quality features and sizes allowing processing, were obtained. They are obtained from:

- crystallisation from molten carbon solutions in metal,
- direct conversion of graphite into diamond,
- the production of diamond embryos,
- crystallisation from a liquid or gaseous phase of the carbon.

Currently, there are two methods used on the large scale: HPHT (High Pressure High Temperature) and CVD (Chemical Vapour Deposition).

The first method, high pressure high temperature is older and is used for greater scale. That method is based on heating the natural diamond, the brown one, to very high

temperature (above 2000 K) at a high pressure of about 7000 MPa. In such conditions the crystal lattice of the diamond is distorted and appear effects, which at the same change the colour of the diamond from brown to green or yellow.

On the other hand, the CVD method is based on the same technology as the one used for the production of microprocessors. That method is based on the growth of crystals in plasma at high temperature under the reduced pressure. In this way, with relatively low costs are obtained quite large, colourless, clean single synthetic diamond crystals. In terms of physical and chemical properties, as well as appearance, they virtually do not differ from natural stones and it is difficult to tell them apart, even while using standard gemmological methods. The diamond obtained by CVD method is exactly the same stone as the one mined in the mine, often surpassing in its purity or size. However, the price plays here crucial role – synthetic diamonds are much cheaper than their natural equivalents.

2.3.1 High-pressure/High-temperature diamond

Originally, it was thought that a considerable activation barrier of two carbon allotropes could be overcome by exerting great pressure on the graphite, creating in that way a more thermodynamically stable the allotrope diamond. However, the increase of the activation barrier under the pressure requires additional heating and thus high-pressure high-temperature (HPHT) - the method worked out by General Electric in order to obtain synthetic diamond [Bundy et al., 1955].

Typical process conditions imitate those appearing in the Earth`s crust, where are created natural diamonds at p ~ 150 kbar and T ~ 2000 ° C. These values may be reduced a little bit by the use of transition metal catalysts such as Fe, Co and Ti, which dissolve carbon and allow crystals of diamond to precipitate, when p and T are fulfilled and are on the border line, known as Berman-Simon line, in the phase diagram of carbon.

Modern solutions introduce large anvils and copper heating coils in which the mixture of catalytic metals, graphite and diamond grains is precisely regulated in order to achieve certain size of crystals depending on their application. The key parameter of this method is the temperature gradient in the whole mixture of carbon/catalyst, in which the

graphite is heated more than diamond embryos. Carbon dissolves in metal and deposits on grains, but the difference in temperature gradient ensures that it does not redecomposes to the catalyst.

There is a vast number of applications of HPHT diamonds that are produced by such companies like Du Pont and Element Six on the industrial scale. Despite the undoubted success of this method, the production is a little limited. Although the biggest sizes of the produced diamond reach the size of ~ 2 mm across, their production provides 90% of all industrial diamonds.

2.3.2 The diamond growth: CVD

While HPHT industrial diamonds are crucial for various applications, there are many other situations in which that material does not meet the required criteria. Using the technology of chemical vapour deposition, for forming thin diamond films on large surfaces and various types of substrates, makes the diamond the subject of research in many fields.

CVD processes can take many forms but all are based on the method of depositing active gas precursors on a solid substrate. The CVD process uses gas phase kinetics of binding metastable diamond structures in non-equilibrium system (Matsumoto et al., 1982, Spitsyn et al., 1981). Usually, this involves low-pressure process (~ 10-200 Torr) and high temperature of the substrate environment (~ 700-1200 K) consisting of a mixture of the activated gas phase, which contains some types of the hydrocarbon that reacts and deposits on the substrate.

Thermal or plasma discharges are commonly used to activate a mixture containing carbon – always containing certain quantity of hydrogen, which dissociates to form reactive hydrogen atom. Within environments rich in hydrogen, the etching rate of carbon (sp^2 graphite) is from 10 to 100 times faster than the sp^3 diamond and creates a situation in which thermodynamically metastable carbon allotrope (diamond) is kinetically privileged [Angus et al., in. 1968].

Modern CVD diamond techniques have evolved over the past 20 years in many different formats, however, out of two major types of reactors dominant influence had:

CVD activated by hot filament (HF CVD) and CVD activated by microwave radiation (MW CVD). The last technique was determined as MP CVD, MW strengthen by CVD plasma (MW PECVD) or MW activated by plasma (MW PACVD or CVD), but all MPACVD are synonyms and we will stick to MW CVD.

HF CVD and MW CVD methods are described below, taking into account the microwave activation to which this thesis is devoted. The deposition in direct current arc stream reactor is not presented, yet, that topic has been discussed in many publications [Dandy and Coltrin, 1995, Konov et al., 1995, Ohtake and Yoshikawa, 1990].

2.3.3 HF CVD

The activation of gaseous mixture comprising carbon in HF CVD reactors is obtained by means of thermal method based on using metallic fibres, typically tantalum, tungsten or rhenium, that are warmed resistively [Matsumoto et al., 1982]. Although the reactor construction determines the parameters of the process, the deposition of diamond typically occurs at fibre temperature ~ 2300- 2700 K and low pressure ~ 20 Tor. The substrate has to be placed relatively close to fibres (~ 4 mm) for the suitable heating and to be treated with sufficiently large H atoms streams to facilitate the growth of nucleating hydrocarbons. The additional heating is often accomplished by the use of the secondary substrate heater, in order to improve the dynamics of the process. The diamond is deposited on the substrate at the rate of about ~1-10 pm h^{-1}, although it depends, of course, on the process conditions. HF CVD systems are a little limited due to the fact that some reactants cause the oxidation or corrosion of the fibres. The fibres themselves may be a source of diamond films contamination. However, these reactors have the advantage that the fibre arrangements may be used for the diamond deposition on a relatively large surface area.

2.3.4 MW CVD

The mixture of hydrocarbon compounds and hydrogen can be effectively activated by a microwave discharge, then a mixture of reactive neutral compounds, ions and free radicals is produced [Kamo et al., 1983].

2.3.4.1 CVD Plasma

Plasmas cover a physical state in which some part of atoms or molecules, which were ionized to form a system in which electrons, ions and neutral charges coexist as a reactive medium. There is a separate type of charged particles within the plasma that gives it a wide variety of properties and allow the system to influence the electric and magnetic fields. In MW CVD systems, plasma is controlled by centring of the maximum of the electric field in the middle of the pressure discharge pipe or discharged directly above the substrate. The substrate is heated to ~ 1000 K by the plasma and exposed to the reactive agents in a discharge.

The first MWCVD reactor consisted of the quartz tube inserted into the rectangular microwave wave guard so that the maximum of the electric field was focused in the middle of the tube in order to allow the discharge in the gas mixture 1-3% CH_4 in H_2 [Kamo et al., 1983].

Another system of the reactor uses the antenna that inserts, through the quartz window, microwave energy into a chamber cooled by the water. This solution was presented and commercialized by ASTEX company (Applied Science and Technology, Inc.).

2.3.4.2 The plasma discharge

In the plasma derived by the absorption of the electromagnetic radiation (*EM*), the energy is transferred the most efficiently by light molecules, free electrons and protons and later on transferred to larger and neutral units through the secondary interaction. This results in a partition of energy between electrons of the temperature T_e, measured in electronovolts and by neutral gas molecules that are in thermal equilibrium at the particular gas temperature T_{gas}. The plasma excitation state is initiated by the coupling of the electric field with a small portion of free electrons in the gas until occurs the spontaneous form of discharge. The MW CVD reactor is designed in such a way that a standing wave, formed between the antenna and the ground, has only one peak that occurs just above the ground. The energy is transferred directly to the system as the electrons are continuously accelerated and decelerated, which leads to enhanced energy replacement with the inert gases background.

Below ~ 15 torr (~ 20 mbas) electromagnetically excitable plasma is characterized by T_e, which is dependent on frequency ω, and the amplitude of electric field *E*. At higher pressures Te affects dispersing the background particles and may reduce the electric field E/n, where n is density. This means that such a discharge may not be initiated at more than 20 Torr, since free electrons would have too low mobility to initiate next collisions. In the stable situation at increased pressure, there is a situation in which heating will lead to the decrease of n. At this point, the increased density of charged particles means the increased absorption of the electromagnetic field *EM*. However, at higher densities of the more conductive plasma, the microwave energy cannot penetrate deeply what leads to the decrease of its volume under high pressure. The pressure in the chamber *p*, and supplied microwave power *P*, may be mutually configured to give different parameters of energy density *Q*.

The indication, the power density of plasma (or a distance between hot fibre and the substrate), determines the temperature of the substrate in systems where no other additional heating of the substrate is used. There is the temperature window for optimum diamond deposition while using MW CVD method of the centre T_{sub} ~ 1000 K ± 250 K. Above this area, there are only graphite or amorphous carbon layers, and below ~ 750 K the diamond is not deposited. This limits the type of substances that can be used as substrates as they must be able to withstand the rough environment in the MW reactor. Therefore, the aim of modern research on the diamond synthesized by CVD method is to make possibile the deposition at lower temperatures T_{sub}. There was presented one of such methods of diamond deposition from the substrate at temperatures as low as 650 K, by means of halogen precursor particles and aluminium (T_m = 933 K) and the less effective deposition on zinc (T_m = 692 K) [Schmidt i Benndorf, 2001].

2.3.4.3 The chemical environment of the CVD diamond

In the last two decades, there has been noticed a considerable progress in understanding the chemistry and composition of the mixture of the gases used in the process of diamond films deposition. In particular, there has changed the attitude to

distribution parameter of the gases in the reactor`s space and in various process conditions [Butler et al., 2009, Hassouni et al., 2010].

1. Hydrogen

The presence of atomic hydrogen (H) is essential for carrying out the mechanism of the diamond deposition for both HF CVD and MW CVD technique, at the same time allowing processing metastable diamond allotropes into thermodynamically preferred diamond through etching of sp^2 carbon and its return to the gas phase. The full termination of growing diamond surface in the presence of H atoms is conducive to the formation of sp^3 tetrahedral crystal lattice that makes difficult the reaction of crossing carbon bonds (C-C cross-linking) on the surface. Even in the gas phase, atomic H is used for grinding long hydrocarbon chain that may be formed and disrupt the deposition process and decide that plasma, in which H_2 is not the main output component, comprises generally of more soot and creates more contaminated diamonds.

For MW systems, hydrogen creates stable, chemically active plasma of a wide range of pressure inside the reactor chamber and microwave energy, dominating chemical interaction between neutral particles and surface gases. In the typical gas temperature T_{gas} ~ 3000 K occurs MW CVD discharge [Gicquel et al., 1994, Kaminsky & Ewart, 1997, Lombardi et al., 2005] and about one third of H_2 will dissociate into atomic hydrogen forms $x(H_2) \sim x(H)$.

2. Hydrocarbons

In many cases, for the diamond deposition in MW CVD reactors, in typical conditions for MCD deposition, are used hydrocarbon sources of gas (very often it is methane CH_4 due to economic reasons) with diluted hydrogen. The hydrocarbon gas is quickly converted into C_2H_2 under the dispersion in the plasma, as much as low is the concentration of other C_1 and C_2 radicals in the centre of the plasma. In the production of MCD layers, the hybridization of fractions depends moderately on the gas activation method, in MW CVD is required ~ 5% CH_4 in H_2, while in HF CVD reactors ~1% is necessary to obtain analogous morphologies. For both systems, the increase of hybridized mole fractions $x_o(C_xH_y)$, causes changes in the morphology leading to transfer from MCD

to NCD and then, at higher $x_o(C_xH_y)$ to dispersion of non-diamond amorphous carbon (a-C) [May & Mankelevich, 2008].

In many experimental studies, it has been shown that the hydrocarbon identity in the mixture of power gas is irrelevant, whereas the key factors are: the ratio of H:C, and the concentration of CH_x (x = 0-3) growth particles above the substrate surface. The role of these growth particles is to transfer carbon from the plasma core to the surface of the substrate where they are incorporated into the crystal lattice. Methyl radicals are preferred as the growth particles, as was presented in many studies, show their presence above the substrate layer in a higher concentration than majority of other hydrogen radicals and surface reactions have preferred activation borders. The further evidence is the use of molecular beams containing CH_3 in quick diamond deposition [Lee et al., 1994, Loh et al., 1996].

3. Argon and other noble gases

There is a great interest in the addition of inert gases to the standard mixture of H_2/CH_4 with a particular reference to argon and nitrogen, when it comes to diamond deposition. The latter is also responsible for the pollution in layers of both natural and synthetic diamond and will be discussed a little later in the thesis. Argon (and to a lesser extent, other noble gases) was being added to the mixture of process gases in small quantities at the early stage of the experiment with the use of MW CVD method, as its presence helped to initiate and stabilize the plasma [Gicquel et al., 1994]. Adding Ar shown the increase in the speed of diamond deposition, however, it was at the expense of the quality of the diamond layer. There was observed a higher content of sp^2 [Han et al., 1997, Zhou et al., 1997]. Larger number of Ar mole structures in gas mixture during the MW CVD process, may have a strong influence on the morphology of NCD layers inducing the deposition above certain border value [Gruen 1999 Zhou et al., 1998]. Within those limits, the plasma rich in Ar may become unstable and reach the limit of $x_o(Ar) \sim 0.97$. This is due to the mechanism of ions recombination, in which Ar is less efficient than in systems where H_2 has the additional degrees of freedom of the dispersed electron bonds. Instead, Ar ions in reaction with H_2 create ArH+, that may receive electrons.

4. Oxygen

Adding oxygen to CVD reactors, usually in the form of CO and CO_2, has become an important and well-studied area providing new methods of obtaining various morphologies, often at low substrate temperatures. This, thus, provides a broad range of substrate materials and the lower energy consumption. The energy efficiency is an important factor when it comes to commercial applications where reactors may work for a week time at e.g. the production of thicker SCD layers, where the cost of electric energy becomes significant. As atomic hydrogen (H), oxygen is also used to reduce sp^2 carbon during the deposition process that improves the quality of diamond [Kawato & Kondo, 1987], but also reduces the amount of hydrogen incorporated to the sp^3 crystal lattice [Tang et al., 2004].

The mixture of CO_2 and CH_4 successfully enables the production of diamond films at the temperature T_{sub} as low as 710 K. Scanty molar fractions of O, O_2 and OH within these systems, under optimal growth conditions, show the importance of CO in low temperature diamond growth [Petherbridge et al., 2001].

These works also show that the window for diamond deposition is located in a small range between 50-52% CH_4 in CO_2. Simultaneous measurement of radical CH_3 with the use of mass spectrometry method, leads to the conclusion that these were the key growth particles in the H_2 / CH_4 system, in which comparisons were made. While comparing many similarities of the activated surface of the diamond growth in various gas mixtures, with H_2/CH_4 system that is activated by the addition and acquisition H atom. It is believed that CO play a similar role to H atoms and is being able to do the same but in a lower temperature [Petherbridge et al., 2001].

The CO_2 / CH_4 system, both with and without additional H_2, is currently widely used for the deposition of the diamond layer at a low temperature Tsubz due to the reduced activation barrier in comparison to common mixtures of H_2 / CH_4.

5. Summary

The individual components exposed to neutral Argon (Ar), which acts in a similar manner to the catalyst, may be gathered and presented in a phase diagram C - H - O called the Bachman triangle [Bachmann et al., 1991]. This phase diagram of the empirical origin

is divided into areas: the area without the deposition phenomena, the area with the diamond deposition and the area with non-diamond carbon deposition. It is a useful tool to predict the results of the use of given gas mixture.

It also shows that in fact the diamond is deposited regardless of activation method and hydrocarbon precursor, although in the diamond deposition system the dynamics of growth and content of sp^2 may vary.

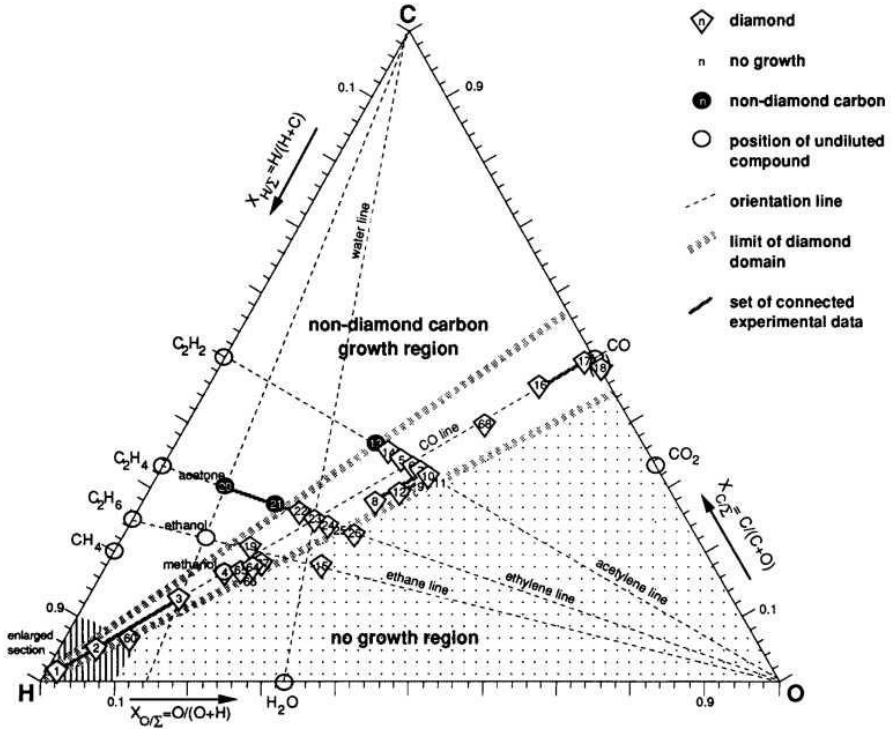

Figure 2. CHO phase diagram summarising 70 experiments with the use of gas mixtures for diamond deposition and with the use of CVD method [Bachmann et al., 1991].

2.4 The diamond as a powder in the nano scale

Nanodiamond is a term referring to the description of a variety of structures including diamond crystals with a diameter of several nanometers. Carbon nanoparticles include not groups of carbon nanoparticles found in natural environment inter alia interstellar dust or meteorites but also those synthesized artificially in the detonation process or by chemical vapour deposition CVD.

The core classification system of carbon nanostructures is based on the division depending on shape and spatial variations in the layout. This determines a clear picture of carbon structures in the nanoscale [17,18]. Taking as a division criteria the size, there can be determined: zero-dimensional (0D) structures – fullerenes, one-dimensional (1D) structures – carbon nanotubes, two-dimensional (2D) structures – graphene, three-dimensional (3D) structures – nanocrystalline diamond. Categorization according to the carbon allotropes, in the literature, is still ambiguous. An attempt to classify carbon allotropes based on types of chemical bonds was made by R. B. Heimann in 1997 [20].

Parts of the detonation diamond are probably one of the most promising materials if taking into consideration their physiochemical properties and the degree of surface development. As a result, all the time there are new possibilities for application of diamond nanopowders.

2.4.1 Diamond nanopowders obtained by the detonation method

The most common and the fastest growing method of obtaining diamond nanopowders may include the detonation method. It is performed in a series of technological processes strictly controlled when it comes to the time.

The initial step – loading explosive materials with an electric detonator. Depending on the used technology, the detonation material is installed in the upper part of the detonation chamber in a container with water or ice. The final stage is connected with the chemical cleaning, washing contaminants and acids residues.

In this process the most widely used is a mixture of trinitrotoluene-hexogen (2,4,6-trinitrotoluene, TNT/cyclotrimethylenetrinitramine, RDX) at the ratio 40/60 or 70/30. It is characterized by a negative oxygen balance which means having an oxygen content lower than the stoichiometric value, thus complete hydrogen binding by oxygen to water is possible, and in the process appears elemental carbon. The explosive mixture is both a source of energy and the elemental carbon. The weight of the mixture varies from 0.5 do 2.0 kilograms and depends on the cooling conditions of detonation products: volume, pressure, gas composition and strength characteristics of materials that the chamber is made of. The process of detonation of explosive materials within the chamber is accompanied by a high pressure (from 20 to 40 GPa) and the temperature of 3000-

4000K. These conditions correspond to the thermodynamic stability for the diamond and are sufficient to initiate the process of condensation (Figure 3.) [17–19,21].

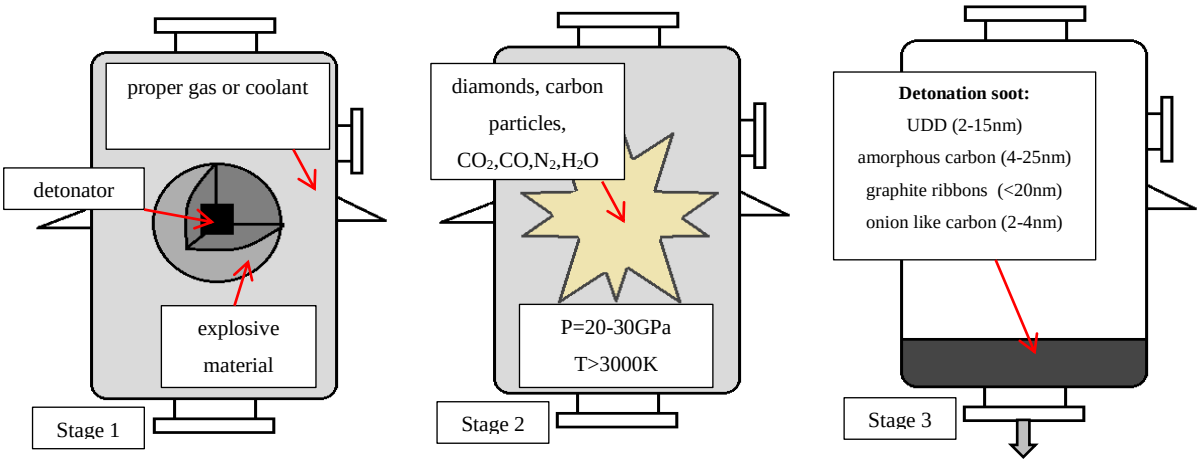

Figure 3. Stages of the detonation synthesis process of diamond nanopowders [17]

In the detonation process there have to be fulfilled two main technical conditions concerning the synthesis on diamond nanopowders:

- the composition of explosive materials must deliver thermodynamic conditions conducive to the formation of the diamond;
- the composition of gas atmosphere must provide the necessary rate of extinguishing (with an adequate thermal capacity) to prevent diamond oxidation.

The product must be cooled at a high speed in order to avoid the conversion of diamond into graphite during the process. The generated kinetic energy is converted into heat energy, which in turn contributes to a very high temperature in the chamber. After suppressing all the shock waves inside the chamber, the temperature inside is close to the detonation temperature and is about 3500 K. After cooling, the product temperature does not exceed 500–800 K.

The detonation synthesis is usually carried out in the chambers, with a volume ranging from 1 to 20 m^3, made of corrosion and shock resistant steel. The efficiency of the process depends, on a large extent, on the composition of the explosive mixture (explosive material). In the process of detonation is obtained the grey powder with the size of grains ranging from 4 to 20 nm, which consists of diamond core (sp^3), surrounded by amorphous carbon coating in the onion-like shape (Figure 4.). In fact, nanodiamond powders create

strongly linked agglomerates that allows them to reach sizes larger than it would arise from the theoretical calculations [3,22,23].

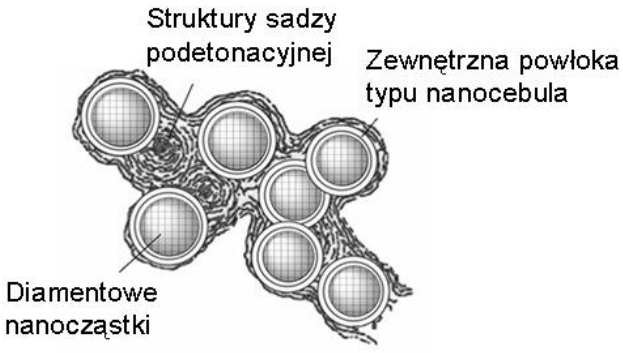

Figure 4. Model of possible structure of diamond particles obtained by the detonation process [5]

2.4.2 Nanodiamond structure obtained by the detonation method

Surveys on *nanodiamond* structures were mainly focused on bonding construction in the crystal lattice, in particular on distinguishing the promotive cell. In 1924, Decker suggested the sybthesis of tricyclic $C_{10}H_{16}$, made of three condensed cyclohexane rings [24].

The method of obtaining nanoparticles determines its various sizes. The size of particles obtained in the detonation process depends not only on the type and the quality of the explosive material, but also on the geometry of the detonation material. This monodisperse particles measure from about 4 to 10 nm [17,18,25,26].

Several experimental and thermodynamic factors affect the size of particles obtained in the detonation process, the main one is the duration of the process. Inside the chamber, there is a pressure conducive to formation of diamond particles out of amorphous carbon [17,25,26]. In the situation when the pressure drops, and the temperature is still high, on diamond particles is formed a layer of graphite. The cooling rate of the reactor after the process is of paramount importance when it comes to obtaining samples of the greatest possible purity.

Diamond nanoparticles obtained in this process outside sp^2 phase layers on the surface, may contain various functional groups and oxygen [26,27]. They are formed

mainly as the result of the reaction of newly formed diamond crystallites with a coolant or in the purification process with the use of concentrated mineral acids.

As a result of the detonation process, there is obtained diamond material of very strong particles agglomeration [22] that is not dispersed in the organic and water solvents. One of the scattering method, directly affecting the electrostatic forces, is the use of the ultrasound. This method is, however, insufficient due to the fact that the nanodiamond core - strongly associated with the graphite structure (on the surface), is not covered by sonification. The graphite layer closely surrounds the agglomerate surface consisting of several nanodiamond particles. As a result the obtained material is of much larger size than the one expected from nanomaterials [22,27–29]. Additionally, on the surface occur functional groups that may as well affect the phenomenon of strong nanodiamond agglomeration [30].

The experimental results of Raman spectroscopy confirmed that the outer layer in the type of onion consisting of bonds sp^2 [31]. The composition and the ratio of sp^2/sp^3 strongly depends on the synthesis conditions. Palosz et al. reported that nanodiamond consists of an organized atom structure in the core surrounded by the structure of the nature of soot graphite [32].

2.4.3 Physicochemical properties of nanodiamond

On the properties of particles of detonation diamond nanopowders the main influence have [18,22,33]:

- small size (from 4 to 10 nm diameter),
- shape,
- the content ratio of carbon atoms of bond hybridisation sp^2/sp^3,
- surface structure,
- types of occurring pollution,
- degree of chemical purification.

In order to obtain more information regarding specific properties of diamond nanopowders it is necessary to select the appropriate test method [17].

All carbon powders, at high angles in Bragg equation, have the same X-ray diffraction. The differences can be observed in case of low angle areas that is confirmed by the identical degree of long-range order in the crystal lattice of nanoclusters. Diffraction peaks for angles 20 = 43,9, 75,3 and 91,5 degrees, correspond respectively to reflexes from surfaces (111), (220) and (311). They originate from diamond of similar crystal lattice of a parameter a0 = (3,565 ± 0,006). The presence on diffractograms strong background confirms the presence of significant amounts of the amorphous carbon. The presence of a strong peak from the surface (002) for angle 20 = 26, determines the content of graphite in carbon powders [34,36,37]. An additional broad peak derived from graphite may also occur for the angle of 20 = 25,1o and may indicate the presence of nanographite of onion-like structure [36].

X-ray diffraction method, not only provides information about the phase composition, but also allows for analysis of the other physical properties. For defining nanoclusters of medium size are used various measurement methods. Scherrer formula – commonly used to determine the grain size of crystalline materials – does not take into account the potential deformations of the crystal lattice. As a result, it may lead to understated values of crystallite sizes. Williamson – Hall method allows for the simultaneous measurement of the nanoclusters size and structure deformation. The analysis of broadening the diffraction peaks, with the use of this method, is proposed in the thesis [37]. Another method is the analysis of virtual structure parameter (X - Ray Alp) – the structure of analyzed particles is examined as two separate phases: the core and the layer.

According to Niedzielski, long term arrangement within particles of nanometric sizes is limited by the size of crystallites, which size is smaller than the length of coherent dispersed beam [3]. As a result, the Bragg equation is not possible to be applied in this case. The nanocrystal cannot be treated as a homogenous object and its structure cannot be determined by one set of structure parameters.

Another commonly used method is the analysis of X-ray diffraction profiles used to determine the crystal size and defects of the structure. Linear profile analysis consists of adjusting Fourier coefficients of the obtained profiles allows to determine the heterogeneous states of tension (defects in crystal lattice). The state of tension and defects occurring in the core and subsurface area of diamond nanoparticles [38-40] is possible to

be determined with the use of combination of two methods: alp method and linear profile analysis.

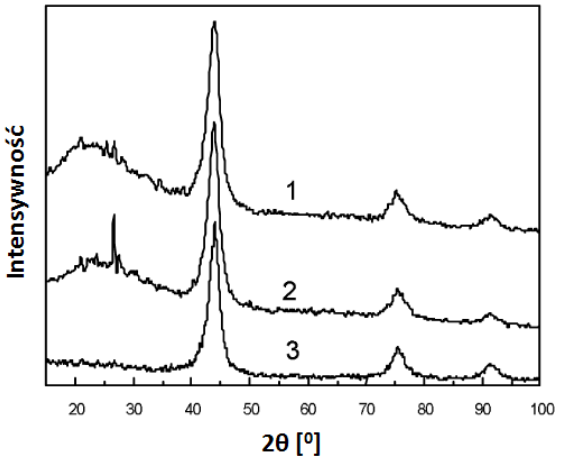

Figure 5. Diffractogram of diamond powders obtained by detonation of mixture of TNT-RDX in the amount of 50 / 50 in various environments (1-N_2, 2-NH_4CHO_3, 3-H_2O) [35];

Raman spectroscopy is a popular method of analysis of nanostructured carbon materials. Carbon allotropes – diamond and graphite present different, however, characteristic for themselves Raman spectra. This fact causes that their quick and easy identification is possible also in case of amorphous layers, diamond-like and extraterrestrial matter [41,42]. First row spectra for diamond monocrystal (sp^3 hybridized carbon) show a narrow;diamond powders, due to the nanocrystalline lattice, may be asymmetrically widen and there may appear frequency shift (occurrence of grain boundaries and structural defects) [44]. Raman spectrum of crystalline graphite shows a single narrow peak at 1575 cm^{-1} [45]. In case of sp^3 hybridized carbon, any changes in the structure and grain size determine the appearance of additional peaks in the range of 1360 cm^{-1} and 1620 cm^{-1}. The disordered finecrystalline lattice occurs mainly as a result of mechanical fragmentation or in the process of diamond graphitization, which may also be accompanied by the formation of amorphous phase (intensive background in the range of 1000 - 1500 cm^{-1}) [36]. sp^2 and sp^3 hybridized carbon shows various resonance conditions depending on the wavelength of excitation. It affects the shape and intensity of the Raman peaks. The low ratio of peak intensity derived from diamond and non-diamond phases, in the visible range, increases with the decrease of the wavelength to the UV range (to the benefit of the diamond phase) [46]. In the analysis of the disordered amorphous forms of carbon powders, containing in the structure C - C bonds of sp^3 hybridization, in the UV spectrum appear additional peak „T”:

- in the range of 1060 cm^{-1} for unhydrogenated structures
- in the range of 980 cm^{-1} for hydrogenated structures

The intensity, the degree of dispersion and the transfer of individual peaks in the Raman spectrum for different excitation energy is a distinctive and indisputable feature of the particular configuration of carbonous material [47,48]. In this case it seems fully justified to apply Raman laser spectroscopy, as a tool used for the analysis of various components of the examined sample, and a multi-scope Raman spectroscopy for the complete analysis of both crystalline and amorphous, as well as disordered, forms of carbon allotropes [3].

According to Niedzielski [3] still unresolved is the scope of Raman spectrum in the range of 1500 - 1800 cm^{-1}, in particular the broad peak at 1640 cm^{-1}. Recent studies indicate that this peak is most likely the result of superposition of the peak of 1590 cm^{-1} , which is characteristic for sp^2 carbon, and the peak of 1640 cm^{-1} showing the presence of the powder of function groups O - H on the surface. The additional arm, which occurs on the other side of the peak of 1640 cm^{-1}, is most likely to be caused by the appearance of vibrations derived from C=O groups located in 1740 cm^{-1}. It is of the utmost importance to determine the effect from O – H functional groups on the Raman spectrum of carbon powders and other carbon nanomaterials, especially in situations where water is used as a coolant.

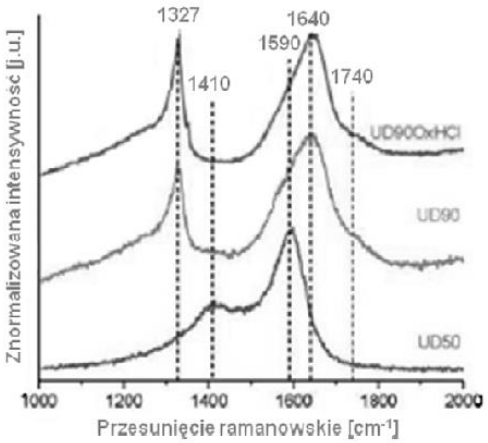

Figure 6. Raman spectroscopy of nanocrystalline diamond powders [49].

When it comes to the analysis of diamond powders, widely used are such techniques as transmission technique and scanning electron microscopy technique.

HRTEM (high resolution transmission electron microscopy) is a commonly used technique in the examination of single clusters of ultra dispersed diamond powders [37,42]. It is also used in the tracing graphitization processes of diamond powders. The research conducted with this method indicated that the onion-like carbon structure (grapheme planes) are formed of the surface of the powder.

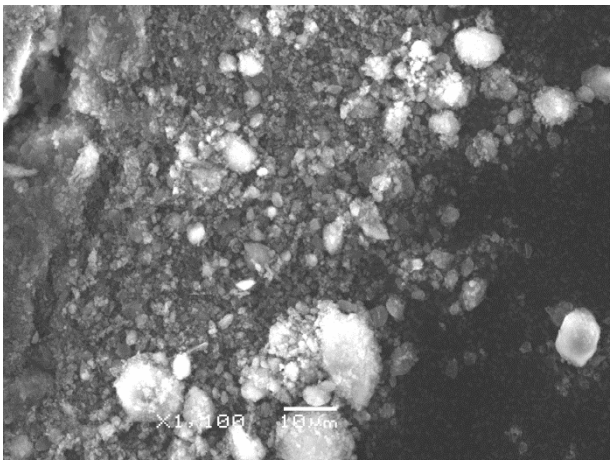

Figure 7. Diamond nanopowders surface examined by SEM

The specificity of the methods using for analysis relatively small surface area, in case of diamond powders show that the examined area, in general, is not representative for the powder as a whole. Thus, HRTEM analysis are conducted in conjunction with other techniques e.g. Raman spectroscopy [36,37,50].

Diamond powders, due to their relatively large specific surface area of about 200 -300 m^2/g", reveal good absorption capacity [34]. In order to improve application properties it is needed to possess the knowledge regarding the surface structure and functional groups appearing on the surface. These necessary information is provided by the studies of infrared spectroscopy. The need for the analysis of functional groups on the powders surface is due to several factors. First of all, because of the high reactivity of the particles, containing oxygen and hydrogen, covering the surface. Additionally, carbon powders purification process is accompanied by a high temperature and a range of reagents. Such situation causes the formation of functional groups on the powder surface that are relevant to oxidant and the gas atmosphere during the heat soaking process [18,51].

On the surface of carbon nanopowders exist various functional groups that allow its modification by intentional attachment of additional functional groups of compounds. It

leads to the conclusion that it will be possible that diamond powders suitably functionalized will become drugs.

The analysis of carbon powders with the use of AFM technique is not a simple matter. The main technical problem here is the necessity of depositing and attaching the tested material to the surface that is equal atomically. Additionally, the measurement itself is a complicated matter as the measurement tool (the microscope blade) is significantly larger than the geometric structure of the examined particles. Very often there occurs situation in which the attempts do not deliver results due to high mobility of the examined particles.

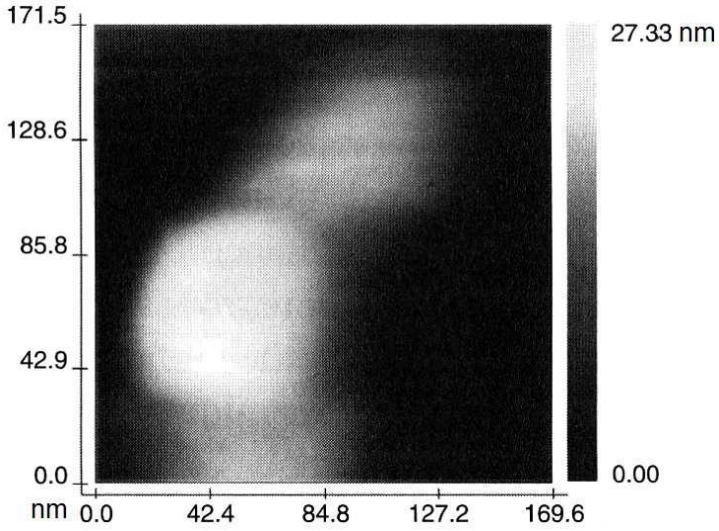

Figure 8. AFM image of detonation diamond conglomeration on the silicon surface [28]

2.5 Biological properties of carbon nanopowders

Materials that will have bio-medical application are to fulfil strict requirements. The main criterion is its biocompatibility. This term describes the abilities of certain biomatter to perform functions in relation to medical applications without causing to the recipient local or systemic adverse effects. They generate the most appropriate and beneficial cellular or tissue reactions. This phrase covers haemocompatibility, histocompatibility, lack of toxicity and lack of effect on the immune system of a living organism [65].

The non-exhaustive literature data taking on an assessment of the biological properties of carbon powders obtained by CVD, indicate the necessity to trace a little bit

richer resource that would include as well results of tests conducted on rabon layers (diamond and diamond-like). Generally, in order to determine the biocompatibility of carbon layers were used both in vitro and in vivo method.

The evidence of haemocompatibility of nanoocrystalline diamond layers are the results of Niedzielski research that indicate the lack of dynamic balance disorders of blood coagulation system while in contact with this layer. The nanocrystalline diamond in contact with the whole blond does not tend to activate coagulation factors i.e. it is not thrombogenic. This coexistence is not bringing any damage to the tested layer since the blood plasma does not influence it in a negative way [62].

The measurement commonly used for evaluation of the inflammatory conditions caused by biomaterial, is the in vivo test with the use of macrophages. At the time of inflammation, macrophages start to release the enzyme (NAG – N-acetyl-β-D-glucosaminidase), which level is adequate to the level of invasiveness of the biomaterial. An attempt to determine the level of this enzyme was taken by Thompson et al., who in the results showed no difference between quantitative doses of enzyme released for macrophages grown on pure Petri dish as well as on dished covered by DLC [66].

Another indicator of inflammatory conditions formed as a result of contact with biomaterial is its tendency to be colonized by bacteria. High resistance of NCD layers to be colonized by Escherichia coli bacteria, in comparison to titanium alloys (Ti_6Al_4V) and steel (AISI 316L), was revealed by the study of Jakubowski et al. [67].

The histocompatibility of DLC layers was evaluated by in vivo examination. Mitura team traced the changes in the muscle and bone tissues of guinea-pigs that were implanted 316L steel discs coated with NCD layer. No pathological changes were observed in the (tested) internal organs: liver, spleen, kidneys. In the place of the implant, there was no inflammatory reaction or products of corrosion. Around the implant was formed the capsule of connective tissue rich in fibrocytes, fibroplasts and collagen fibres [68]. CoCr alloy implants covered with DLC layer implemented in bone and muscle tissues of rats and sheep were also surrounded by the fibrous capsule. The histopatological analysis of tissues surrounding the implants, performed after the removal (after 12 weeks time.) revealed the lack of inflammatory factors or cell apoptosis [69].

Promising, although a few, are the studies of carbon powders produced by the use of the same methods as the layers described above, which allow to treat them as crystal collections of these layers.

The works carried out by K. Mitura prove that nanocrystalline diamond powder does not cause reaction of irritation (allergic) on the skin of patients-volunteers (with positive allergic history) whereas its application on originally sensitizing materials makes that it becomes a barrier protecting living cells from the impact of metal ions. Curbing toxic processes in the environment of the living organism is the proof of the bioactivity of nanocrystalline powders [60].

All reports in the literature described in this overview, provide a positive classification of carbon materials, produced in the CVD processes, as biomaterial.

2.6 The overview of diamond nanopowders modifications

Taking into account the peculiar properties of layers and carbon powders obtained by the detonation method and the growing interest in the use of such properites as: biocompatibility, bioactivity, there are also attempts made to modify the processing and transformation [61] of carbon powders (diamond and non-diamond). Choice of the modification is determined by the assumption concerning the end result i.e. the need to obtain a product of a strictly specific purpose.

2.6.1 The mechanical modification

The comminuition (grinding is a form of the size comminuition) is the process of separating the solid body by the forces destroying its natural internal cohesion. If in the process are used external forces then it is called physical (mechanical) comminuition. The use of even a small force causes a certain deformation of the grain and rises stress. There appear local areas of compression and stretching areas of atoms that build the grain (shear forces). The enlarged pressure force is accompanied by the transfer to the grain the increasing energy, which results in the stress intensification up to a critical moment, when the forces will exceed cohesion forces (i.e. the grain cohesion) what results in cracking bonds within the grain and its disintegration [70].

The mechanical comminuition includes: crushing, breaking, grinding, cracking and shearing. Mostly, the purpose of comminuition is to enlarge the surface area of the crushed material or to obtain the product of specified size of particles [71].

Grinding is the first process that material containing sp^3 phase (diamond powders) is subjected to immediately after it is obtained [64]. When the suspension of detonation diamond is subjected to attrition milling (mechanical-chemical clearing) [65], or BASD method (beads assisted sonic disintegration – sound-aided drip grinding) [72] are obtained stable colloidal solutions with a high nanodiamond concentration with particles closing with OH groups.

The prolonged time of milling the dispersed nanodiamond powder leads to the formation of sp^2 carbon in it, probably as a result of recombination between the free (Hanning) bonds generated by mechanical action [73].

2.6.2 The plasma-chemical modification

Former, presented in the literature, plasmo-chamical modification of products obtained by CVD and PVD methods, concerned the carbon layers and were based on implementing additional elements (chemical elements) into the layers structure during the manufacturing process.

Depending on the requirements, apart from the carboniferous gas (methane or acetylene), in the process of layers preparation, were used hydrocarbons: hexafluoroethane (C_2F_6) trifluoromethane (CHF_3) carbon tetrafluoride (CF_4), which incorporates fluorine [74-77], tetramethylosilane ($Si(CH_3)_4$), which incorporates silicon [75], as well as O_2 and CO_2 increasing the number of carboxyl groups on the surface of the layers [78].

2.6.2.1 Commonly used MW PACVD systems

There are known solutions that use the static chamber of plasma chemical reactor, which are widely used in the process of layers modifications by plasma activated chemical vapour deposition (PACVD).

The kit for the surface modification in plasma chemical processes, with the use of microwave generators, consists mostly of the static reactor chamber located vertically to the upper entrance of the waveguide (the quartz glass window), the waveguide line

equipped with E-H stub, circulators and the main part – the microwave generator. The plasma - chemical processes, using the microwave generators, require lower pressure. The reactor chamber is an airtight chamber equipped with such elements as: the quartz window that forms the input of the electromagnetic wave, the door for loading the cartridge, the coupling of the vacuum pump and the inlet for reactive gases.

2.6.3 Chemical modifications

2.6.3.1 Hydrogenation of the carbon powder surface

The typical stage preceding the experimental studies on layers and diamond powders is to subject them to the process of hydrogenation. In case of CVD methods, the process is carried out by the use of the introduced reactive gases (source of carbon and hydrogen) during the deposition of the carbon layers. An example of this is the presence of the a-C:H layer. One of the methods of creating C-H bonds on the diamond surface involves the use of hydrogen gas at elevated temperatures. This method, using gases at the temperature of 850^{o}C, was used by Spicyn et al. obtaining, apart from the expected C-H bond, the increase of OH groups [79].

In organic chemistry, hydrogeneration is typically carried out using a metal catalyst based on e.g. palladium, platinum or nickel, however, difficulties related to the removal of the catalyst are the reason for the lack of interest and, as a consequence, reports on catalytic hydrogenation [80].

One of the options of increasing the reactivity of the hydrogen gas is the hydrogenation in the plasma reactor. Loh et al., with the use of microwave plasma reactor, in the temperature of 8000°C within 60 minutes, air hydrogenated the oxidized detonation nanodiamond powder [81].

2.6.3.2 Oxidation reactions

The oxidation is a process based on the passing of electrons from atoms or groups of atoms often called the deselectronation process. The basic charge conservation requires that the oxidation is accompanied by the reduction and the amount of the electrons exchanged in both processes is equal. Oxidants may be atoms, ions or molecules that have the ability to adopt electrons. In the oxidation process the oxidants are reduced. Reductans,

on the other hand, are: atoms, ions or molecules that have the ability to give electrons to other atoms, ions or molecules what results in the reduction of these substances. In the reduction process, the reductants are oxidized as well [82].

For the future functionalization of the nanodiamond it is desired that the end of its surface is formed by carboxyl or ketone groups. In order to achieve the maximum oxidation level it is necessary to establish a homogeneous COOH layer on the diamond surface. This is inevitably accompanied by the material loss and the reduction of the diamond core, as well as the rise of carbon dioxide and monoxide (CO_2, CO) as the oxidation products [83].

The reactivity of the disordered sp2 carbon towards the oxidation is much higher than the diamond [85]. Thus, the diamond oxidation not only introduces oxygen groups on its surface, but also purifies the material phase.

Another way of placing on the diamond the oxygen contained in the surface groups is the use of the oxidized air. Gogotsi et al. controlled the ratio of sp^3/sp^2 by careful air oxidation of nanodiamond, at high temperatures. The selected temperatures are important for selective carbon oxidation with non-diamond hybridization. In the temperature at range of 400 – 425^oC occcurrs the etching process of sp^2 configuration of carbon and on the uncovered diamond is placed a large amount of oxygen surface groups. Above the level of 450^oC all types of carbon undergo the oxidation process, although both the sp^2 phase and diamond phase are reduced [84].

The application of the oxidized air was also used to reduce the size of the diamond particles. In 2004, Gordeev and Kochagina reported various reactivity (associated with the reduction in size) of nanodiamonds of different origins towards air oxidation [86].

The relevant ends of the surface of the diamond from the viewpoint of functionalisation apart from carboxyl and ketone groups, are hydroxyl groups. In 2006, Krueger et al. applied the borane reduction of existing oxygen surface groups carrying molecules of C=O [87]. There was obtained the hydroxylated diamond bearing 0.5 mmol g^{-1} of OH groups. The use of borane gives some additional benefits as well. The reaction of disordered graphite material with borane, lead by acid treatment, may reduce the unsaturated fragments, such as double bonds of saturated structures of sp^3 carbon

hybridization carrying hydrogen atoms (this is salso a simple way to introduce the C-H bonds without the use of gas).

In order to fully reduce any kinds of acid derivatives, highly reactive complex hydrides may be used. Teams of Zheng et al. and Ciftan et al., for the reduction of C=O groups that are on the surface of diamond of various origin, used lithium aluminium hydride ($LiAlH_4$) [88, 89].

Garcia et al. subjected the nanodiamond powder, obtained by the detonation method, to oxidation with the mixture of the above-mentioned reagents in a strong acidic solution. The aggressive action of the reagents used in the Fenton reaction served to remove the unwanted „soot matter" covering the diamond nanoparticles and a simultaneous increase of density of hydroxyl groups on their surface, which could be used as sites for the fastening of covalent bonds of alkyl chains or aromatic rings [90].

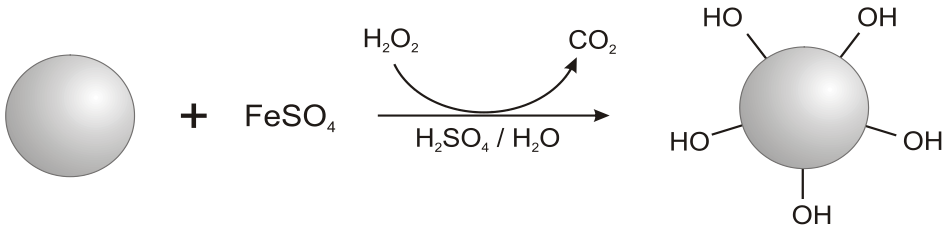

Figure 9. Graphical record of the Fenton reaction carried out in the nanodiamond powder [62].

In the process of primary nanodiamond cleansing, all of the above mentioned methods would not lead to the complete elimination of C=O structures. If it is intended to remove surface groups containing oxygen, it is recommended to previously hydroxylate it by the method comprising OH radical, meaning Fenton reaction, BASD (beads assisted sonic disintegration), attrition milling in water or photochemical hydroxylation.

Reactions of oxidation-reduction called redox processes, are known, for example, from everyday life e.g. corrosion of metals, combustion of coal, natural gas and liquid fuels. These reactions are also the basis of many processes occurring in the living organisms, such as breathing or photosynthesis [72].

3 The objective and thesis of the dissertation

At present is observed a significant increase in the interest of plasma chemical methods of nanodiamond modification thanks to which it gains new properties. Modern technologies, used in materials engineering, are the source of spectacular biomaterials.

Nanodiamond studies are mainly focused on the biological properties and the possibility of their usage in the biological environment. There are published more and more scientific works describing methods of functionalization of nanodiamond surface to connect it with biological elements such as e.g. DNA. Those works, however, in most cases are related to the conventional CVD systems.

The subject of this dissertation is the modification of nanopowders by the MW PACVD rotary plasma chemical reactor chamber. This thesis presents the concept of MW PACVD plasma system for modification of diamond nanopowders, equipped with a rotary drum placed in the reaction chamber.

On the basis of the literatutre overview, as well as on the results of preliminary test in the modification of diamond nanopowders, there was formulated the dissertation thesis:

> *„It is possible to modify the diamond nanopowders by the use of an innovative construction, the MW PACVD rotary plasma chemical reactor chamber*."

Such posed thesis clearly defines the objectives, which is:

- *Plasma-chemical methods of the surface modification, used in materials engineering, allow to create the biomaterial of the required properties.*
- *Design and implementation of the plasma-chemical MW PACVD system for the modification of diamond nanopowders.*
- *Indication of differences in the properties of the modified biomaterial.*

4 Experimental

According to the definition of the objective and the scope of research, in this chapter is described author`s original system for plasma modification of diamond nanopowders, MW PACVD + R, in which, for the first time was used the rotary drum inside the reactor chamber. Solutions of such type are not commonly used and literature studies indicate that, on the day of writing this dissertation, there is no information concerning a similar construction. The first section is devoted to the design and construction of the system, the subsequent stages of implementation and presentation of innovative solutions used during the work (*Section 4.1 The design and description of the research station*). The next section describes the methods used for the studies of diamond nanopowders (*Section 4.2 Methods of testing properties of diamond nanopowders*). In the final chapter is presented the realization of the exemplary modification of diamond nanopowders using the MW PACVD + R system (*Section 4.3 Modification of diamond nanopowder*).

4.1 The design and description of the research station

4.1.1 The microwave discharge

The microwave discharge, in contrast to the other types of discharges used in the process of obtaining carbon coatings or nanopowders, does not require any electrodes to excite the plasma within the discharge place. The plasma discharge in the gas occurs as a result of absorption of microwave energy, which is cumulated and localized in a certain volume of gas. The source of microwave radiation are, the so called, magnetrons and klystrons, working mostly at a frequency of 2,45 GHz. The microwave discharge energy from the source to the reactor is supplied, in the form of electromagnetic radiation, by appropriate waveguides.

The most important features, distinguishing the microwave plasma from plasma obtained in other types of discharges, include: high level of ionization of the plasma, high concentration of active particles including atoms and excited particles, photons of visible light and infrared range, high density of plasma $n_e > 10^{11}$ cm^{-3} and the energy of electrons. An example may here the argon plasma of microwave discharge (2,45 GHz) with the energy of electrons of about 10 eV with respect to the plasma of RF discharge (13,56 MHz) of about 4 eV, or DC plasma of about 1-2 eV.

4.1.2 Work schedule

The works were divided into subsequent tasks implemented within the framework presented below:

A. Drafting the device for modifying the diamond powder by MW PACVD rotary reaction chamber

The initial stage of the implementation was mainly related to the preparation of MW PACVD system. It dealt with a number of solutions commonly applied in this field, both in science and industry. Finally, was raised the final concept that fulfilled the basic assumptions. As a result, for the purpose of visualisation and testing was created a 3D model of the microwave line with the magnetron head and the vacuum chamber equipped with a rotary drum inside.

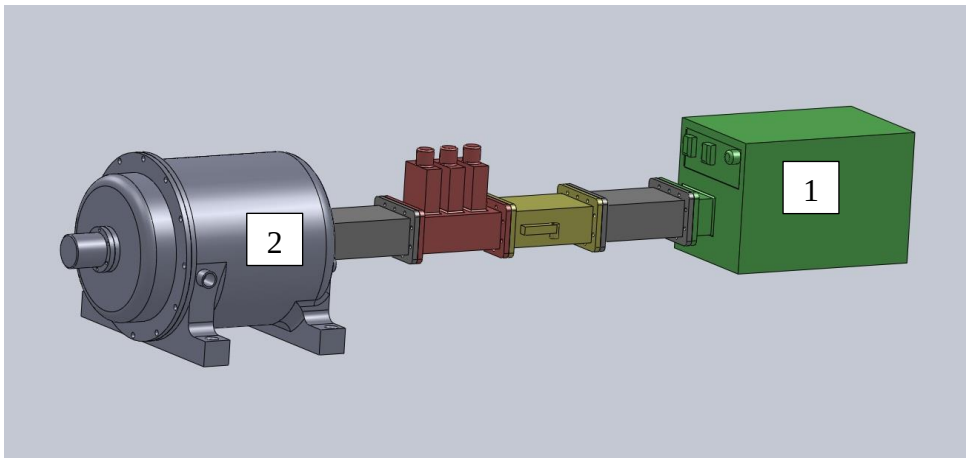

Figure 10. 3D model of the waveguide line with magnetron head (1) and vacuum chamber equipped with a rotary drum inside (2)

B. The choice of elements for the construction of the device for modification of diamond powder by MW PACVD rotary reaction chamber

The next stage was the selection of the appropriate elements constituing the system being carried out. The main emphasis here is placed on the choice of suitable source of electromagnetic energy (MW generator). There was selected the magnetron head TMx12 from Alter (frequency - 2,45 GHz, power – 1,2kW) along with the power pack SM 445G (stabilized power pack with the possibility of both continuous and switched work). There were chosen as well the elements of microwave line such as column stub (AG340M3) and the gauge of the electromagnetic wave, both standing and

reflective one. At this stage was also predicted the selection of the appropriate components of vacuum systems and was planned and designed the modernization of the possessed vacuum chamber.

C. Installation, control and calibration of the device for modification of diamond powder by MW PACVD rotary reaction chamber

The further step was the installation, start up and calibration of the system for plasma (MW PACVD) modification of diamond nanopowders. It was the stage of the intensified development work and laborious adaptation of the chamber.

At this stage were made the necessary conversion works of the reactor chamber:

- it was adapted to cooperate constructively with the waveguide line (the waveguide connector equipped with the quartz window – original idea and project, manufactured by TEPRO)
- it was equipped with the relevant vacuum spigot (TEPRO)
- inside was installed the rotary drum
- there was solved the problem of transferring the rotation of the drum on the verge of vacuum – atmospheric pressure (original solution and implementation)
- there was installed the temperature control system that uses the PID driver and resistance heating tapes
- it was checked for leaks and proper performance of individual components
- there was tested the rotary drum system

There was carried out a vacuum system using the possessed rotary pump and the number of small vacuum elements. In order to achieve greater control over the automatisation of the process and the process itself there was anticipated the use of solenoid valves.

The entire system is equipped with a number of necessary measurement tools and autonomous metrics for the control of the basics parameters of the process and the accompanying changes of the external environment (the harmfulness of the microwave

radiation). As the part of the task assumptions, there were installed the main particular components such as: the vacuum system with the pump and solenoid valves; the microwave line with magnetron and the power pack; the vacuum rotary chamber with a rotary drum along with the system of spigots, the quartz window and the temperature control system; the system of measuring devices and controls along with the controlling microcomputer (Raspberry Pi).

Due to the nature of microwave radiation crucial for the functioning of the system turned out to be the adjustment. The propagation takes place within the inside of the chamber and is controlled by the possibility of shifting the rotor in the inside of the chamber. The system was placed on the shelves especially prepared and constructed for this purpose, taking into account the required parameters of the length of the wavelength line. There was prepared and completed all the power wiring.

The process of generating the stable plasma, with the assumed process parameters, does not cause major problems. The system of the drum rotation was the key, and at the same time, the most difficult element, of the vacuum system, that was to be implemented. After the preliminary tests, it turned out that that the implemented original solution fulfil its task.

Figure 11. The photography of the author while removing the lid of the vacuum chamber.

The system is the adapted to perform the process of the plasma modification of diamond nanopowders automatically (except for the stage of loading the material that is to be modified). For this purpose was used the constructed control system based on Raspberry

Pi microcomputer. This system enables the remote control of the process from any place in the world via the Internet and the web browser, or the smartphone application. The basic parameters of the process can be viewed and archived with the use of SQL information technology.

D. The modification of diamond powder by the MW PACVD rotary reactor chamber. The selection of the optimum modification parameters.
This stage is described in details in section 4.2 (Modification of diamond powder).

E. Analysis of the modified diamond powder
This stage is described in details in section 4.3 (Analysis of physiochemical properties of nanodiamond powders).

4.1.3 Diagram of the „MW PACVD +R" system

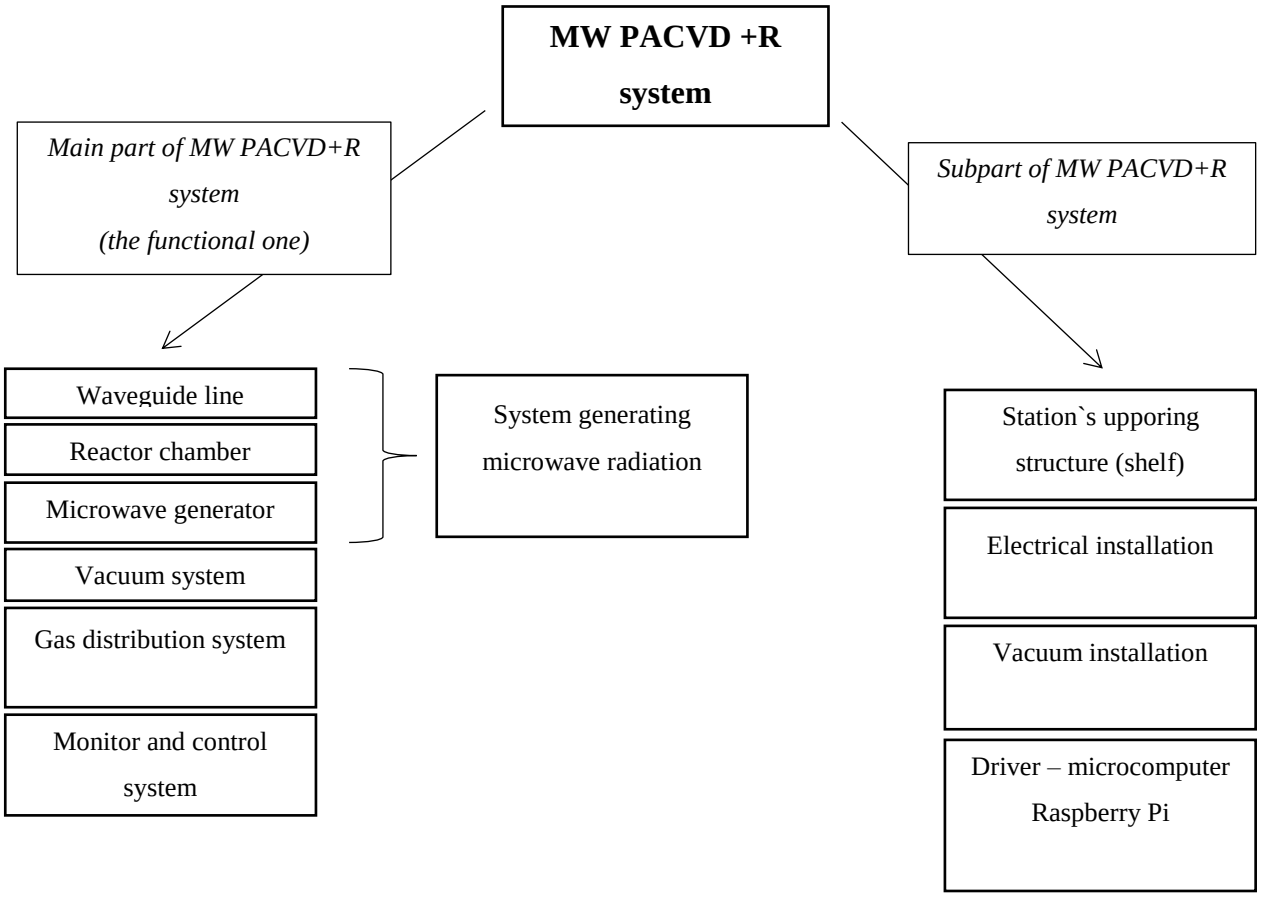

Figure 12. The block diagram of MW PACVD + R system

4.1.4 The construction of MW PACVD + R system [5]

4.1.4.1 MW PACVD +R reaction chamber

The initial concept involved the use of the vacuum chamber (Figure 13.) equipped with a quartz window, the inlet of the reactive gases (6), and the vacuum pump connector. The chamber was supposed to be water cooled and was to be equipped with the system of elements allowing the free rotation of the inner drum (3) e.g. with the use of the stepper motor (7). The basis of the construction would be the typical ECR chamber (electro cyclone), due to that in the construction were predicted such elements as: electromagnets (2) – introducing the excited plasma creative gases (plasma) in the spiral movement directed towards the narrowing of the chamber and the nozzle of reactive gases (6). The quartz window was to be equipped in the main axis of rotation. During the rotation of the drum, the material subjected to the modification is to be located, repeatedly and cyclically, in the area of microwave plasma. The chamber, in contrast to the presented drawing, will have the horisontal orientation.

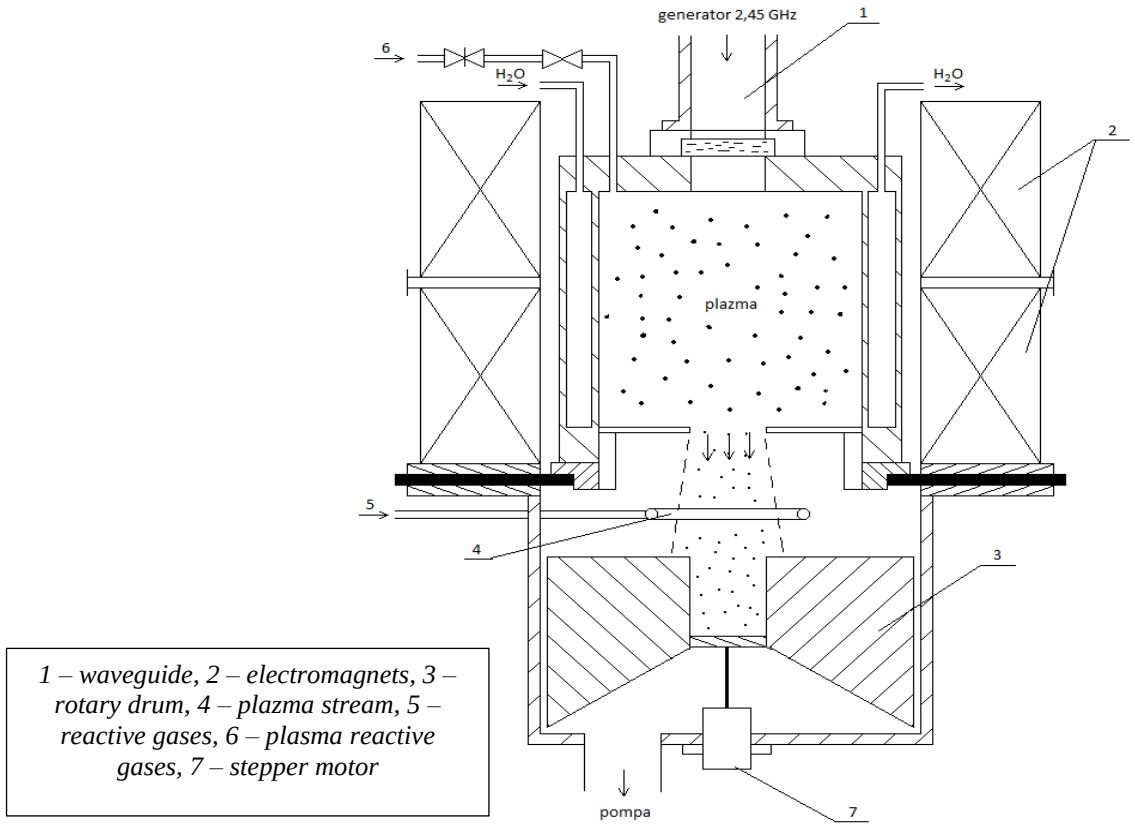

Figure 13. The initial concept of MW reactor chamber with the rotary drum.

In the implementation phase there was presented the concept of vacuum reactor chamber MW PACVD + R, which later on has changed. It took a little bit simplified form, yet, fully realizing the rotary assumptions in its inside. The chamber used in the system is presented in the figure below (Figure 14.)

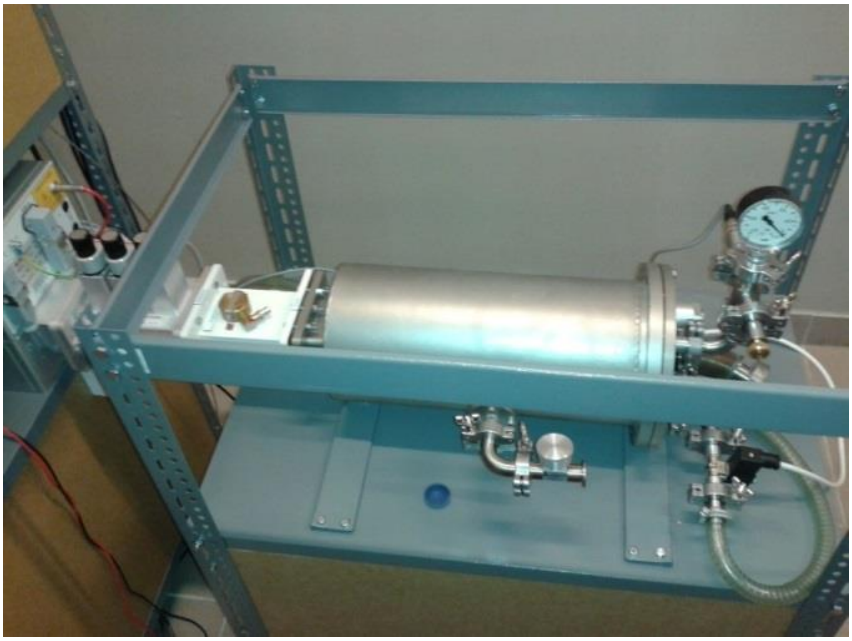

Figure 14. MW PACVD vacuum reactor chamber

The rotary drum, located in the inside of the chamber, was made of 2mm stainless steel according to the project placed in the appendices (Appendix 1.). Dimensions of the possessed chamber, as well as the specificity of the process with the use of the microwave radiation, determined the main dimensions. The diameter of the drum inlet is sufficiently larger than the dimension of the longer side of the waveguide in its internal cross-section, so that the electromagnetic wave, lead inside, does not come across any barrier and is neither destroyed nor reflected. In addition, the depth of the drum is not accidental, it fulfils the requirement of the four times length of the quarter wavelength for the electromagnetic wave with a frequency of 2,45 GHz. In order to ensure the accumulation of the poured nanodiamond powder inside the chamber were designed and manufactured special v-shaped splines shown in the figure below (Figure 15.).

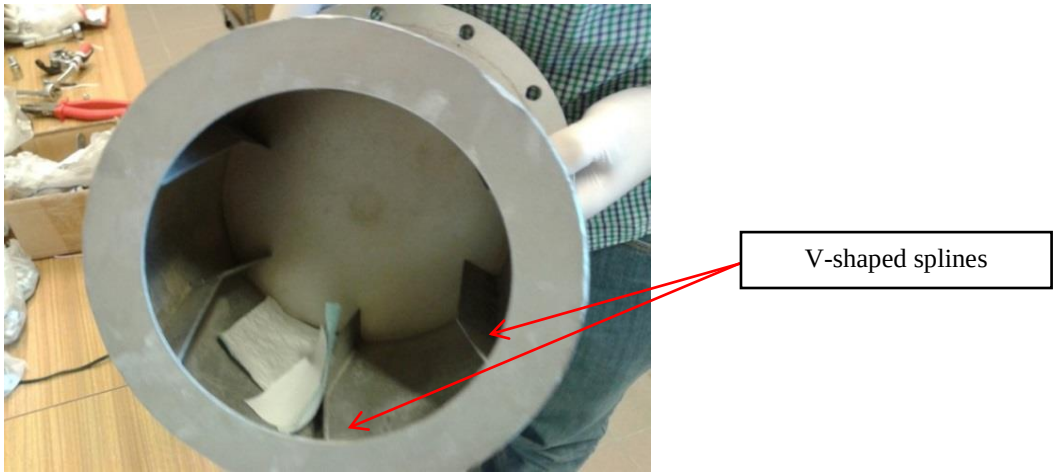

Figure 15. Photography of the rotary drum.

For the main assumption of the construction, the key factor was to vacuum-transfer the propulsion allowing free drum rotation while keeping the tightest possible vacuum environment inside the reactor chamber. The author realized this element himself with the use of standard components of vacuum installation. For the purpose of this solutions were made teflon bushings and the steel, bend axle. The bending of the axis is necessary to transfer the torque moment on the drum located inside the reactor chamber.

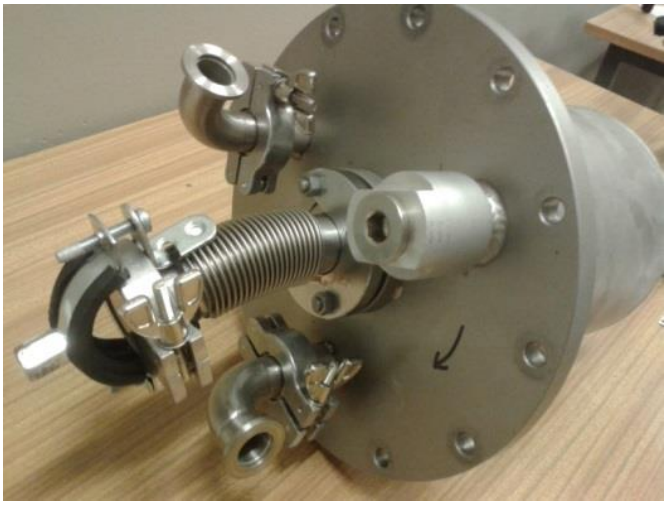

Figure 16. Photography showing vacuum ratio of the rotary drum.

MW PACVD systems do not have the electrons that provide the generation of the electromagnetic wave within the chamber. The microwave energy is supplied into the reactor chamber through the quartz window directly from the waveguide. This element, due to its characteristics, passes the widest possible spectrum of the electromagnetic radiation and, what is more, it can meet the requirement of tightness – the maintenance of

the appropriate conditions of the reduced pressure in order to initiate the generation of the plasma. To secure the quartz glass against any undesirable effect of compressive forces (tensions in the crystal lattice) and to improve the tightness of the connection were used special gaskets made of silicone rubber 70oSh.

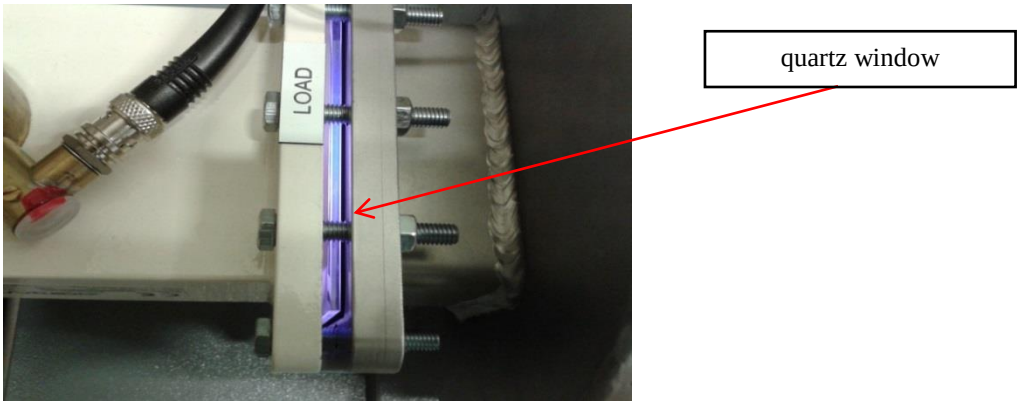

Figure 17. Photography of the quartz window during the process of plasma generation.

With the use of the vacuum culvert was created the propulsion system of the rotary drum. Such solution ensures the safety of the person who operates the system and is set to harmful electromagnetic radiation.

Below is the photography showing rotary drum propulsion system (Figure 19.)

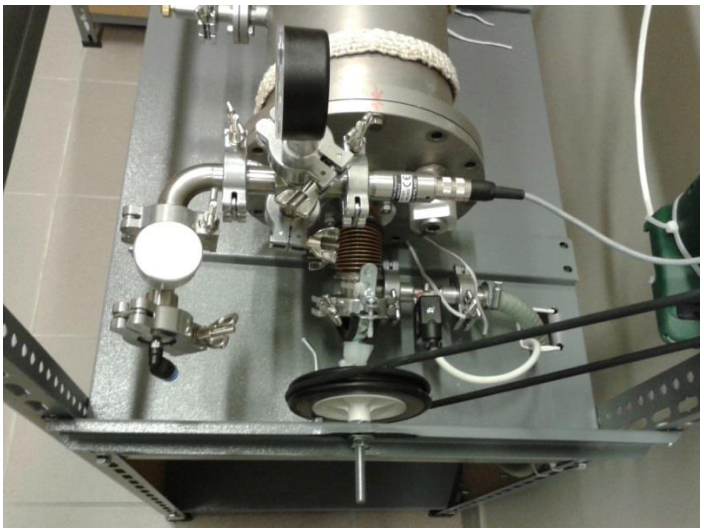

Figure 18. The rotary drum propulsion system.

4.1.4.2 The waveguide line

The waveguide line is made of such elements like: tricolumn microwave stub of type E and Bi-directional measuring device of the electromagnetic wave. The line is finished by an element of the quartz window which is the boundary element of the vacuum system (inside of the reactor chamber). The used components are standardized and all correspond to the type of WR340 waveguide, they are intended to work with electromagnetic waves of the operating frequency of 2,45 GHz and the acceptable power of 6 kW.

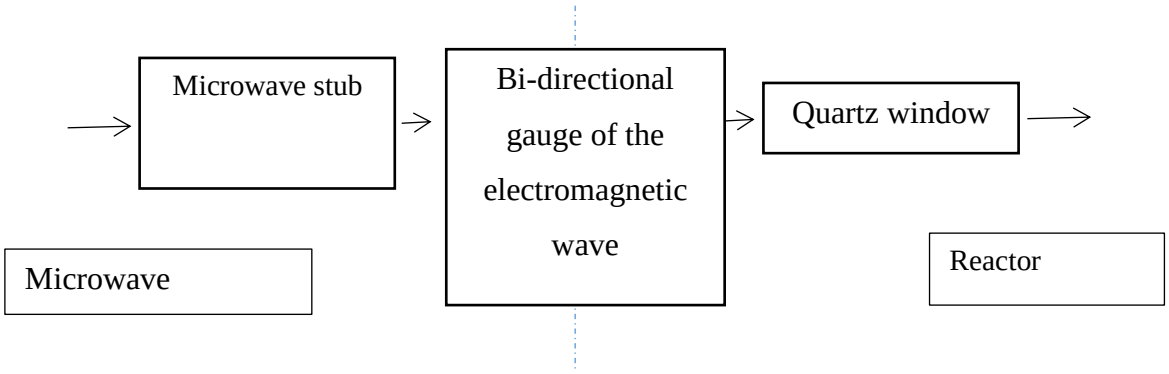

Figure 19. The diagram of the waveguide line.

The presented microwave system, like all systems based on the power generation of the same characteristics, may be considered as the transmitter-receiver. The transmitter, in this case, is the magnetron generating the electromagnetic wave propagating in the medium (e.g. air), and the receiver is the reactor chamber. The waveguide line can be considered as the line transporting the microwave energy from the transmitter to the receiver.

Typical microwave beams, apart from the elements presented on the diagram (Figure 19.), have in their construction the circulator element (Figure 20.). Due to the operations specificity it serves mostly the security function by redirecting the returned energy from the load, directed towards the generator, to the substitute load. This prevents the magnetron head from the damage caused by miss adjustment in the transmitter - receiver system.

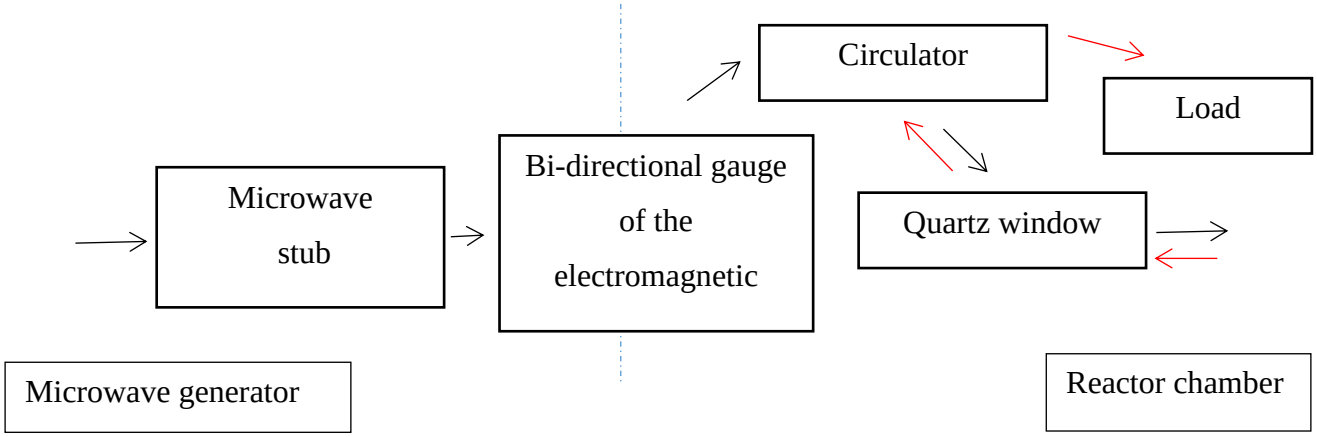

Figure 20. The diagram of the waveguide track with the circulator (red marked reflected energy returning to the microwave generator)

In the presented waveguide truck was used the three column stub of type E - AG340M3 produced by the Alter Power Systems of the maximum acceptable power of 1,6 kW and the other parameters described in the note sheet (Appendix 2.). This element belongs to the main elements of the waveguide track, whose function is to tune the microwave system in order to obtain the desired effects of plasma generation within the area of the reactor chamber and, to be more precise, inside the rotary drum. The tuning provides the strengthening of the electromagnetic wave generated in the reactor chamber with a defined approximate location, thus in this process it is possible to partially control the plasmoactive area. This element is made of aluminium corresponding to the WR340 waveguide with the R26 flange.

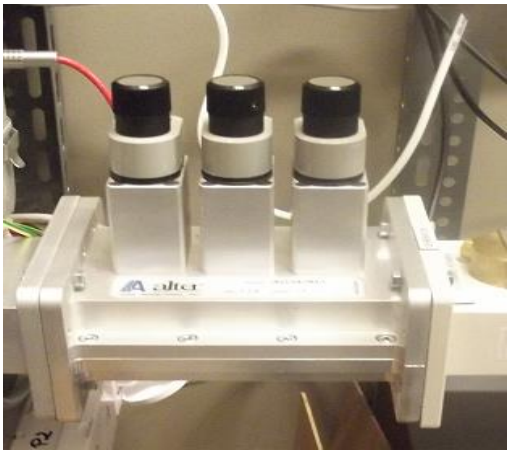

Figure 21. Three column microwave stub type E

In order to monitor the real power of the generated electromagnetic radiation and the fitting of the electromagnetic system MW PACVD + R was used the Bi-directional gauge of the microwave **(**Appendix 3.**)**.

4.1.4.3 The microwave generator

The microwave generator consists essentially of the magnetron head TMA1.2V52 of the power of 1,3 kW, dedicated power supply SM445G.5 and a set of cables connecting those two elements. All components were provided by Alter Power Systems. The microwave generator is the key element of the system and its main task is to generate the stable beam of the microwave radiation at a frequency of 2,45 GHz and a set power point that is necessary to carry out the CVD processes.

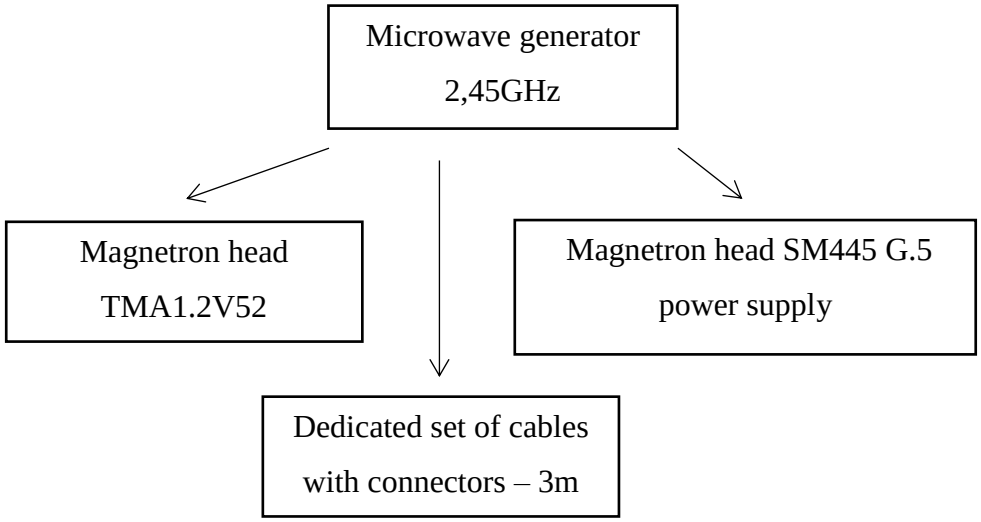

Figure 22. The components of microwave generator

The magnetron head is the activator of the generator system that is responsible for the generation of the stable electromagnetic wave. The head construction is based of 2M137 magnetron from Panasonic, air-cooled and of the maximum power of 1,3kW.

The magnetron is the main component of the described magnetron head and determines its basic parameters. The head is also equipped with aluminium waveguide connector WR340 of PDR26 style, two high-voltage connector sockets with the dedicated power supply and a range of control and regulating systems (Figure 22.).

The author placed the note sheet in the appendices of this dissertation (Appendix 4.).

Figure 23. Magnetron head TMA1.2V52 from Alter Power Systems

The proper functioning of the head is ensured by the SM445G.5 power supply from ALTER company. This power supply, beyond its basic task (to supply and regulate the power) thanks to mutual communications with the head, also serves as the steering – control panel. It also controls the basic critical paremetres of the head, overheating, exceeding the permissible load and, if necessary, is able to turn the head off. The whole is signalized by the corresponding LED diode located in front of the control panel. SM445G.5 is the version of power supply operating in the *CW* (continuum wave mode) with the possibly of puls operations up to 1kHz, which increases the potential and the range of possible applications.

By the use of biocomponent set it is possible to install the magnetron head freely in a wide number of various spatial orientations. The large size of the power supply and the requirements regarding working conditions are not the dominant factor. The only limit is brought by the cables that connect those two devices. This provides a great comfort and freedom in the implementation of systems that use microwave radiation. The note sheet has been placed by the author in the annexes to this dissertation (Appendix 5.).

The cables constitute an integrative part of the microwave generator system. They combine two basic components allowing at the same time their proper functioning. For the implementation of the system was used dedicated wiring kit of the length of three metres.

4.1.4.4 The vacuum system

In the presented system, due to the nature of microwave electromagnetic radiation – high energy density – in order to initiate the activation of the plasma, the sufficient is low of average vaccum. Therefore, it is reasonable to use a single-stage vacuum system with rotary one-stage vaccum oil pump. Below is presented a simplified diagram (Figure 24.).

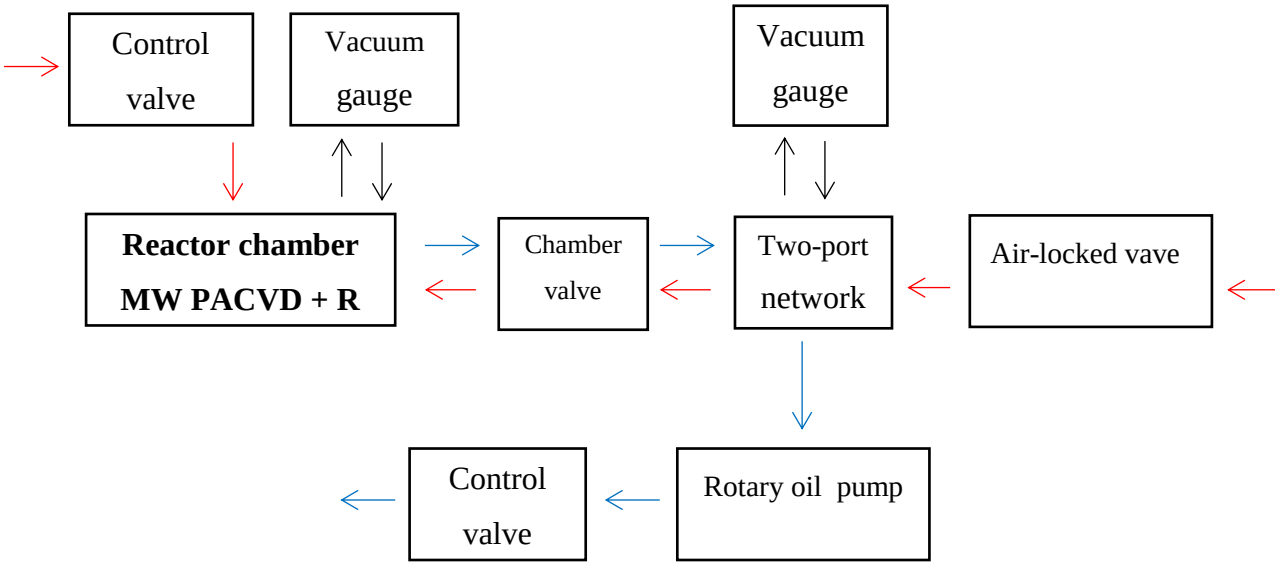

Figure 24. Schematic diagram of the vacuum system used in MW PACVD+R

4.1.4.5 Gas distribution system

The construction of MW PACVD + R reactor enables to use any system of process gas distribution. The proposed system consists of a manual valve that regulates the flow of gases and the gauge based on the Pirani Gauge Head. Process gases are supplied directly to the interior of the rotary drum by means of the wire made of stainless steel. Such solution allows for greater control over the gas composition of the plasma-creating area and improving the efficiency of the modification process.

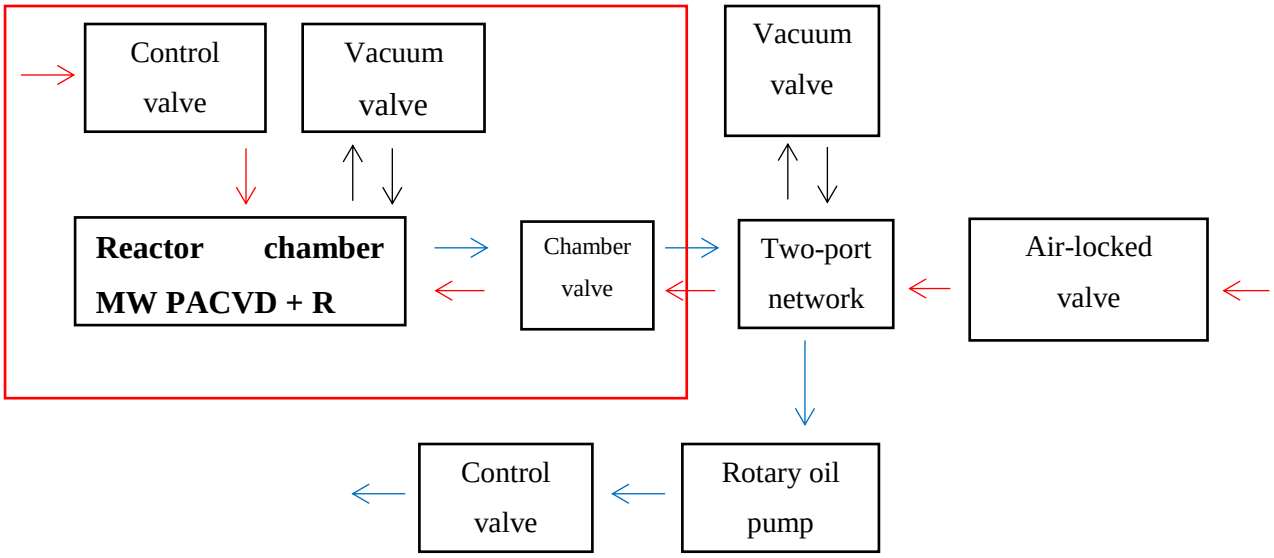

Figure 25. Schematic diagram of reactive gases dispersion in MW PACVD+R system

4.1.4.6 The system of control and regulation

In order to control and verify the parameters of the MW PACVD + R system at work, there is used a range of specialist measurement devices and controllers. These include the following: gauges for classic heads ELVAC MP211, pressure regulator RP-3 as well as the system for temperature regulation RT-2PID with the heating tape 1600x40mm.

The vacuum system was equipped with solenoid valves that control the system with the use of driver based on microcomputer Raspberry Pi. For measuring the temperature inside the chamber was used the MAX 31855 electronic circuit.

The realization of the control panel is presented in the picture below (Figure 26.).

Figure 26. The control panel with a set of gauges

The microprocessor driver of MW PACVD system is based on Raspberry Pi microcomputer – computer platform created by Raspberry Pi Foundation. The device is based on the Broadcom BCM2835 SoC system, which consists of the processor ARM1176JZF-S 700 MHz, VideoCore IV GPU and 512 megabytes (MB) of random access memory (RAM). The device does not have the hard disc, however, in order to load the operating system and to store the data it offers SD card slot. Raspberry Pi also has the USB connector to plug in any external devices.

Raspberry Pi runs on operating systems based on Linux and RISC OS. The latest model, Raspberry Pi 2 B, also operates under Windows 10.

The development of web user interface was based on the dedicated set, web remote control package *webiopi*, having friendly system for creating user interfaces; full control and support for GPIO ports, Serial, I2C, SPI; the ability to control over 30 defined devices; built-in HTTP server and CoAP; built-in Javascript client; built-in Python libraries.

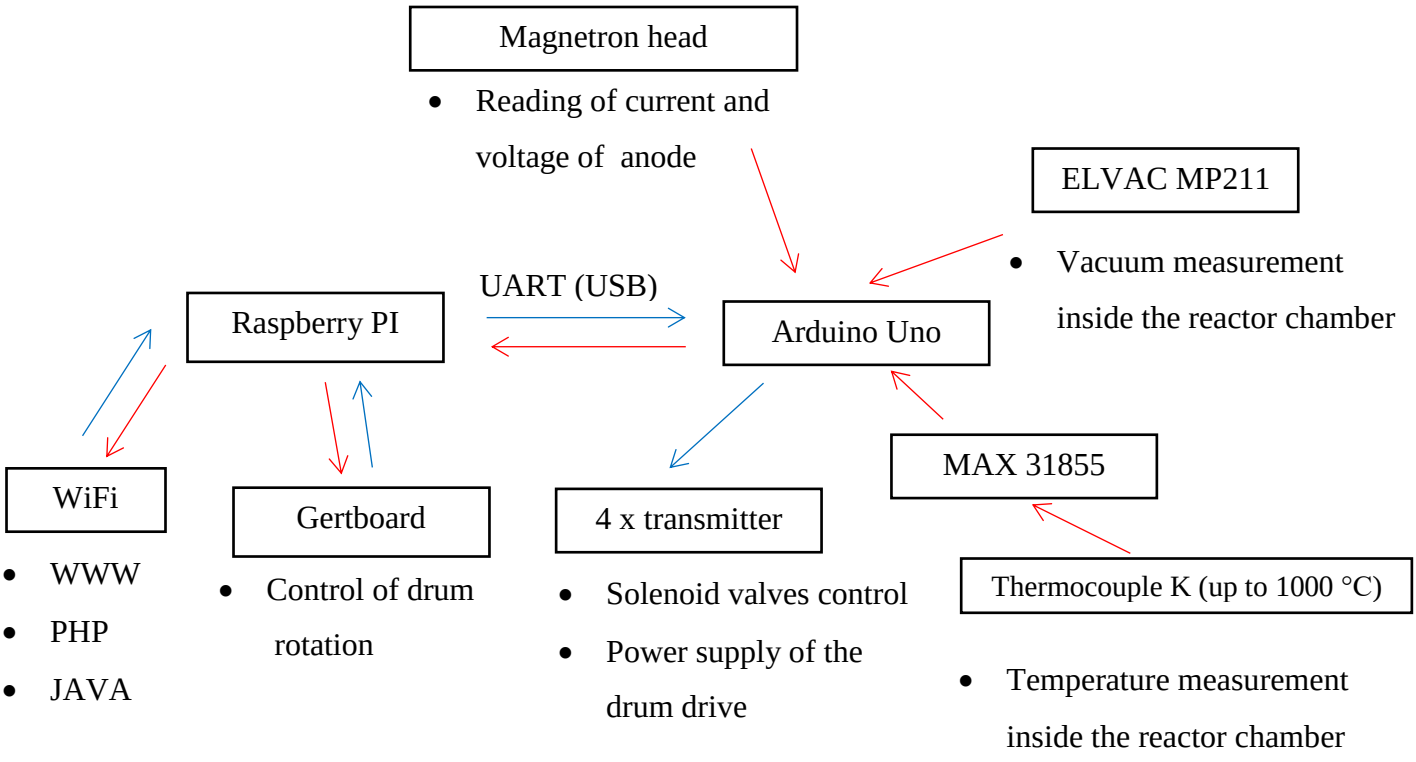

Figure 27. The schematic diagram of the microprocessor control of MW PACVD + R system

In order to increase the possibility of the driver, in this concept anticipated the cooperation with equally popular Arduino UNO system. The communication between those devices is done using suitably configurated USB (UART) ports. This type of solution provides the Raspberry Pi communications via Arduino UNO with the vacuum gauge ELVAC MP211 (dynamic read of the measure values), the control of the set of four transmitters, communication with MAX31855 system (dynamic read of the measure values), communication with the magnetron head (dynamic read current and voltage of anode).

In addition, the driver was equippped with Gertboard expansion card having a number of systems that can significantly increase the utility value of Raspberry Pi. For his own purposes, the author used, located on the board, the DC motor driver chip, used to control directly the rotational speed of the rotary drum vacuum chamber.

Below is the photography illustrating the driver in the test phase (Figure 28.)

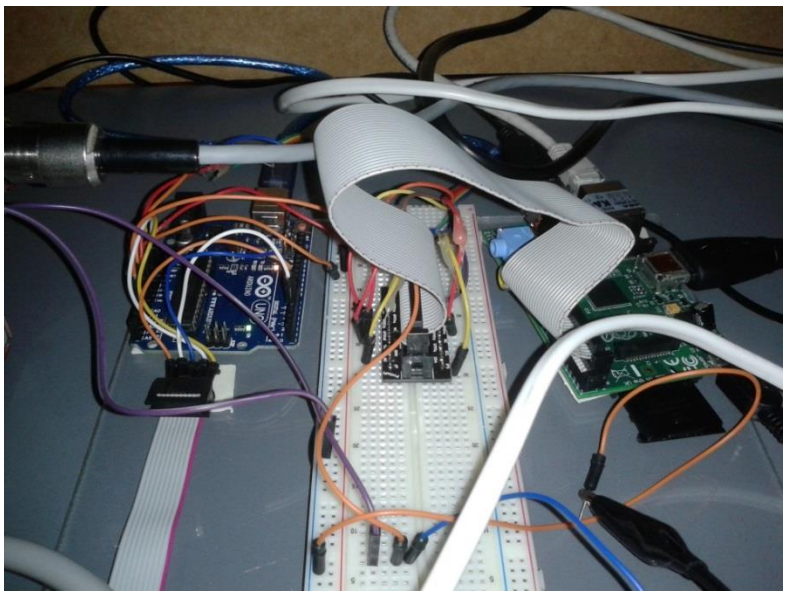

Figure 28. The microprocessor driver of the MW PACVD + R system

The initial configuration of hardware and technical assistance required, at the later stage, to programme Raspberry Pi, Arduino UNO and other components of the driver, to provide them with the mutual and proper functioning.

On the Raspberry Pi was installed the open version of LINUX – RASPBIAN especially for the purpose of this type of device, which was then enriched with the software

enabling remote control - WEBIOPI, under which was created the web user interface. The fragment of the source code is placed below, file *index.html* (Table 3.), whole to be found in the appendices (Appendix 6.)

Table 3. The fragment of the source code of http website – user interface

```
<!DOCTYPE html PUBLIC "-//W3C//DTD HTML 4.01 Transitional//EN"
"http://www.w3.org/TR/html4/loose.dtd">
<html>
<head>
<meta http-equiv="Content-Type" content="text/html; charset=UTF-8">
<title>WebIOPi | Sterownik Komory MWPACVD</title>
<script type="text/javascript" src="webiopi.js"></script>
<script src="js/raphael.2.1.0.min.js"></script>
<script src="js/justgage.1.0.1.min.js"></script>
        <script src="js/highcharts.js"></script>
        <script src="js/modules/exporting.js"></script>

                <script type="text/javascript">
    // Javascript code will go here
    // declare variable for Serial object
    var serial;

    webiopi().ready(init);

    // defines function passed to webiopi().ready()
    function init() {
        // define Serial object, must be configured in /etc/webiopi/config
        serial = new Serial("uno");

        // automatically refresh UI each 5 seconds
        setInterval(updateUI, 1000);

        // update UI now
        updateUI();
}
```

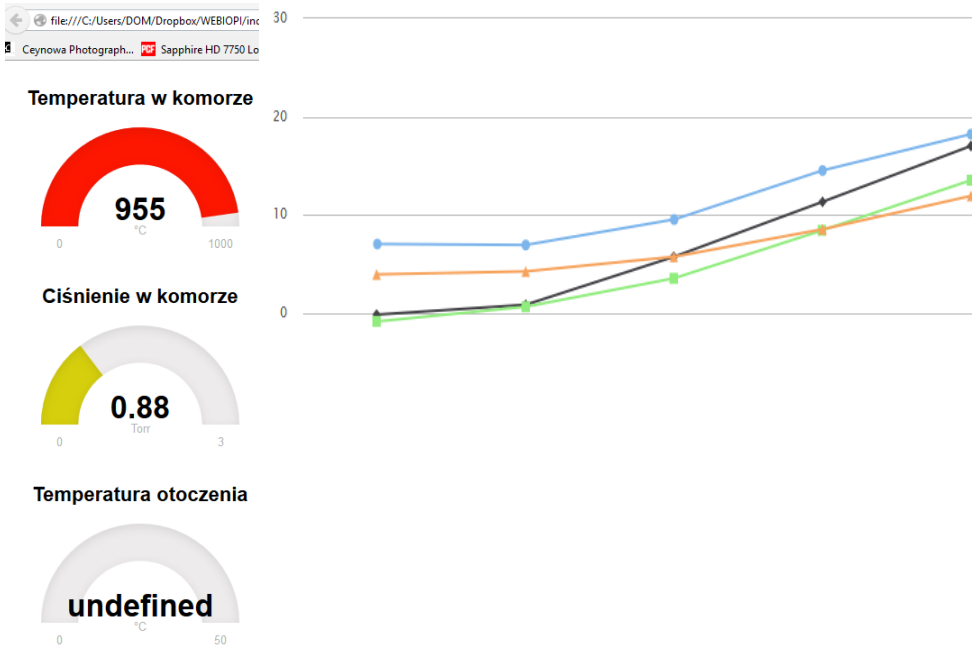

Figure 29. User interface in the WWW browser

The proper functioning of the driver required to program the Arduino UNO. The fragment of the source code is placed below (Table 4.), whole to be found in the appendixes (Appendix 7.)

Table 4. The fragment of the source code for Arduino UNO.

```
char input;

void setup() {
  // open the serial port at 9600 bps:
  Serial.begin(9600);
  pinMode(2, INPUT);
}

void loop() {
  if (Serial.available() > 0) {
    input = Serial.read();
    switch (input) {

  //************************ TIME *********************************
```

```
    // "t" command: returns time in millis since reset/powerup
    case 't':
      Serial.println(millis());
      break;
 //************************ ANALOG ******************************
    // "a0" command: read and returns analog channel 0
    case 'a0':
      Serial.println(analogRead(0));
      break;

    // "a1" command: read and returns analog channel 1
    case 'a1':
      Serial.println(analogRead(1));
break;
```

4.2 Methods used to study the properties of diamond nanopowders

In order to obtain more information on specific properties of diamond nanopowders it is necessary to select the appropriate test method.

Raman Spectroscopy

Raman spectroscopy is a research technique that provides information on the structure of nanopowders. Using this method, it is possible to identify all carbon allotropes. Individual phases of carbon generate spectra that are characteristic for each of them, which can determine their mutual relationship in the tested nanopowder. Thanks to Raman spectroscopy it is possible to determine the degree of defect of the crystal. Deterioration in the quality of the crystal, increases the width of the Raman scattering line.

For testing diamond nanopowders was used the Raman *Renishaw InVia* spectroscope. The wavelength of the excitation beam was 532 nm, and the laser Power of 1.5 mW. The measurement range was between 900 cm^{-1} and 2100 cm^{-1}. All measurements were performed at the room temperature in the air atmosphere. Raman spectroscopy tests

were performed in order to analyze the various carbon allotropes that are present in the tested nanodiamond powders.

The research was conducted in the Institute of Materials Science and Engineering at Lodz University of Technology. The aim of the study was to determine the size and shape of the grains of nanodiamond powders and their agglomerates, and to determine their chemical composition.

Fourier transform infrared spectroscopy (FTIR)

Fourier transform infrared spectroscopy FT–IR provides information on the chemical structure of the tested compounds by the identification of functional groups and the analysis of the spectra in terms of the fingerprint area.

The study was performed with the use of the reflective technique with the use of snap-DRIFT. During the test was used the *Thermo Scientific Nicolet IS50 FT-IR* spectrometer. The range of measurement was between 400 and 4000 cm^{-1}. The research was conducted in the Institute of Materials Science and Engineering at Lodz University of Technology. The absorption spectra of FT–IR were carried out for nanodiamond samples before and after the chemical functionalization. The study was carried out in order to determine the function groups present on the surface of diamond nanopowder.

The electron microscopy

The structural analysis at the level of agglomerates and their crystalline structure is possible to be made by HRTEM technique (High-Resolution Transmission Electron Microscopy) [17,33–35]. Both, SEM (Scanning Electron Microscopy), and HRTEM technique allows to examine the structure of the surface and to determine the chemical composition of the sample. The restriction is the fact that the determination of the phase composition is possible to be conducted only by means of SEM technique [25].

Sizes of the tested nanomaterial cause certain restrictions to the above mentioned techniques, it is mainly due to the heterogeneity of the structure and structural defects. These studies are often combined with other techniques in order to obtain more detailed information.

Characterization of diamond powders in the biological tests

Biological tests of diamond powders belong to the group of specialized tests with a high level of difficulty and complexity. Usually the tests are implemented for future biological applications mainly in the field of medicine (drugs, cosmetics, biosensors, etc.). The main difficulty, when it comes to the implementation, is the fact that the functionalization process itself changes the biological properties of diamond powders obtained by a given method. Thus, it is difficult to control, at the same time, both parameters that so strongly dependent on each other.

In vitro tests- examination with human blood and detonation nanodiamond particles.

For the investigation were used four types of detonation nanodiamond in biological tests: *ND-0 "Danilenko", ND-1 "Gdansk", ND-2 "Koszalin", modified ND-3 "Koszalin".*

Nanodiamonds ND-1, ND-2 (Adamas Company) were manufactured by detonation method and they have the grain size from 2 to 4 nm (Table 5. – Section 4.3). ND-0 detonation nanodiamond has been received directly form dr V. Danilenko from Chelyabinsk and the grain size is from 2 to 5 nm.

Detonation nanodiamonds were incubated for 4 hours in 37 degrees Celsius. Next, 1 milligram of nanodiamond powder was dissolved in 1 millilitre of deionised water. The suspensions of nanodiamonds were added to samples of full human blood collected on the citrate in amounts: 20 ul to 500 ul full human blood. An attempt to reference: full human blood without nanodiamonds. Histological preparations were prepared of living drop of blood and have been observed after 10 minutes. The blood came from volunteers from Regional Blood Center and Transfusion in Gdańsk.

The histological preparations have been observed in optical microscope OLYMPUS CX31, 400 times of magnification and have been performed the pictures of these.

4.3 Modification of diamond powders

In order to carry out the modification process were used 5 milligrams of diamond powder manufactured by Adamas Nanotechnologies. Below are presented the technical specifications of the diamond powder used for the test.

Table 5. Technical specifications of the diamond powder

Parameter	
Structure	Cubic diamond
Average particle size	4.0 nm
Agglomerate size in aqueous solutions	200 nm
The density of the powder	0.3 - 0.7 g/cm^3
SSA (ang. specific surface area)	300 - 400 m^2/g
Colour	grey
Cleanliness	> 98%

Below is the photography of the diamond nanopowder taken before the process. The photography was taken by SEM technique.

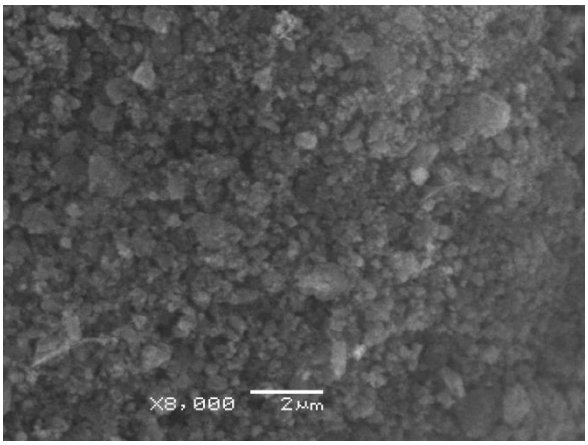

Figure 30. SEM of the diamond nanopowder

The above shown photography from SEM indicates the characteristic, for powders, parameter – the specific surface area, providing, inter alia, the high susceptibility to the effective functionalization (great amount of free atomic bonds). The specific surface are from 285,4 to 295,7 [m^2/g] [11].

The modification of nanodiamond powder

The modification of nanodiamond particles was carried out of plasma innovative chemical system (MW PACVD), having a rotary drum within the vacuum chamber. The system was initially prepared in the process - an initial chamber pressure reduction and annealing at about 300 K for about 3 days (in order to clean the inside of the chamber).

Then, the target is loaded (5g nanopowder diamonds) into the chamber (rotating drum). Other parameters of the process are shown in Table 6.

Table 6. Modyfication process parameter

Parameter	
pressure	1.0 Torr (133.32 Pa)
Temperature	460 degrees Celsius
MW power	900 W
process time	60 min
gas environment	mixture of nitrogen (78.09%) and oxygen (20.93%)
rev /min	60

Stages of modification of nanodiamond powder:

1. The first step of the process is the initial preparation and verification of MW PACVD + R system. It consists of checking the functioning of separate systems, control of the MW generator and the vacuum system.
2. Secondly, the inside of the MW PACVD + R reactor chamber is annealed at the temperature of about 200 K and under a lowered vacuum of 1 Torr for about 72 hours – in order to pre-clean the inside of the chamber and the rotary drum from pollutants.
3. Then, starts the MW generator (350W), for about 20 minutes along with the vacuum system that lowers the pressure inside the chamber to 135 Pa – another step of purification of the inside of the reactor chamber.
4. The next step is to load the substrate (diamond nanopowders) subjected to the MW PACVD process into the inside of the chamber and, to be more precise, to the interior of the rotary drum inside its interior.

5. Further step is to seal the lid of the chamber, to connect the wires of the vacuum system and to transfer the powertrain of the rotary drum. This is followed by the re-check of the connection of all components of the system.
6. Another step is to run the control panel and all peripherals gauges and regulators. At this stage the microcomputer driver is also activated and the control of its functioning is being carried out (the test of remote-controlled vacuum solenoid valves, read test of measurement data from the connected measuring devices).
7. Subsequently, the vacuum system starts to run. Vacuuming of the system takes place in two stages. The first step is to vacuum the vacuum system, so that in further step, the MW reactor chamber is vacuumed.
8. Later, there comes the control of the pressure parameters of the MW reactor chamber.
9. Following, when the pressure in the reactor chamber reaches the predetermined value there appears the remote switch-off of the magnetron head, which power is initially set to the minimum.
10. Another step is to gradually increase the power of the MW generator until it reaches the set value, taking into account the full control vacuum parameters in the MW PACVD + R system.
11. Further step is to generate the MW plasma in the system at the given parameters of the process – the power of MW and the pressure for the set period of time. This is accompanied by the launch of the rotary drum driver system, which functioning is coupled with the time-generation of MW.
12. The consequent step is to switch off the MW generator system (stopping the rotating driver of the drum), and then to gradually air-lock the vacuum system.
13. The final step is to disconnect the vacuum system and to open the lid of the reactor chamber. In the rotary drum is a metal subjected to the process. The metal can be, in an easy way, brought out from the interior of the rotary drum.

5 Description and the test results

The implementation of the aim of the dissertation, described in details in chapter 3, required to carry out the series of experiments aimed to confirm changes in biological properties of the material modified by the presented author`s MW PACVD + R system. This chapter contains research work and interpretation of the results along with the summary of the described reactions.

5.1.1 Biological Studies

Within the studies were used three types of nanodiamonds obtained by the detonation method. ND-0 is the Danilenko powder, ND-2 "Koszalin powder" and ND-3 is the "modified Koszalin powder". ND-0 received its direct shape from dr Danilenko. ND-2 was obtained by the detonation method and ND-3 was modified in the microwave reactor MW PACVD + R.

Figures 31-37 shows the results of biological tests with full human blood without nanodiamond particles as a control (Fig. 34) and in presence of nanodiamond particles (Fig. 31-36). Figure 31 shows the normal human red blood cells (erythrocytes) without any damages.

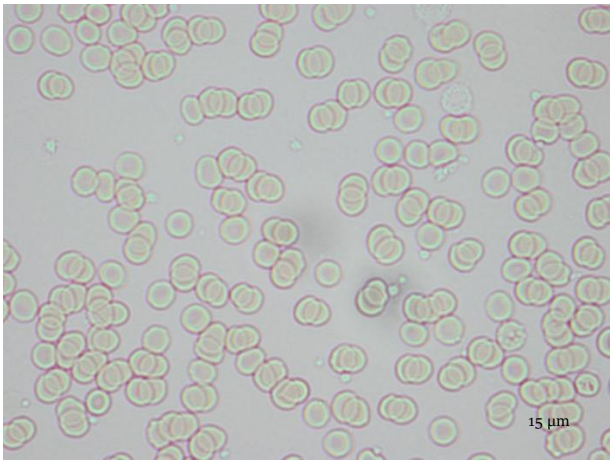

Figure 31. The normal erythrocyte without detonation nanodiamonds particles after 10 minutes. Optical microscope OLYMPUS CX31

Figure 32 shows the rouleaux of erythrocytes in contact with ND-0 nanodiamond particles. This is probably dependent on the presence of nanodiamond particles as the biomaterial and have caused the change in shape of human red blood cells but the physiological function of these is preserved.

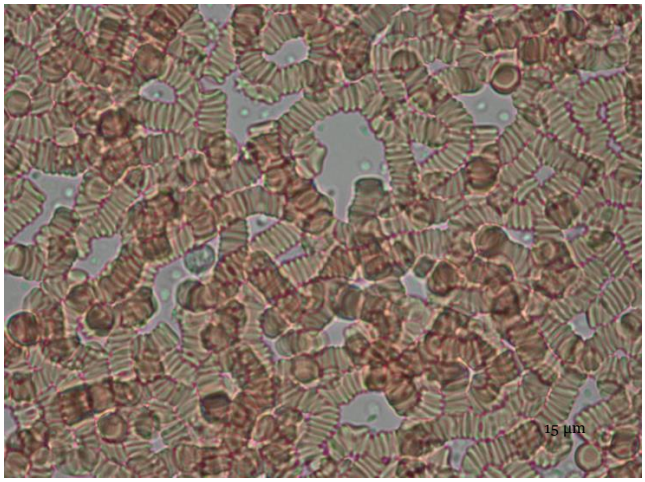

Figure 32. Rouleaux of erythrocytes in contact with ND-0 nanodiamond particles after 10 minutes. Optical microscope OLYMPUS CX31

Figure 33 shows the agglutination of human red blood cells in contact with ND-1 nanodiamond particles. This process is connected with the reaction on the presence of nanodiamond particles agglomerates (clusters). This process can be presented in normal erythrocytes.

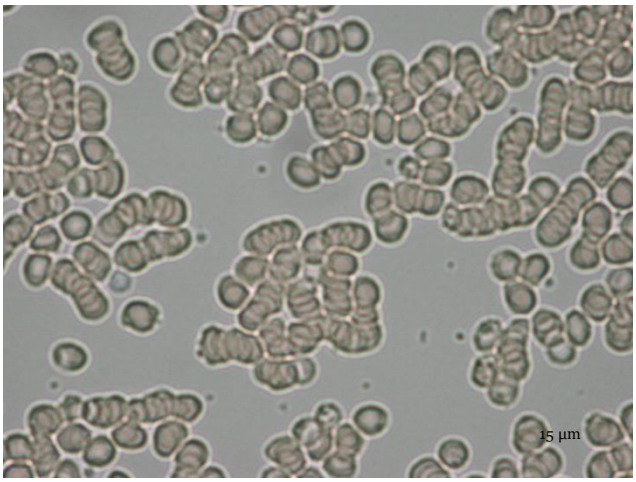

Figure 33. Agglutination of red blood cells in contact with ND-1 nanodiamond particles after 10 minutes. Optical microscope OLYMPUS CX31

Figure 34 shows the haemolysis of human red blood cells in contact with the presence of ND-1 nanodiamond particles. We have observed the spherical shape of erythrocytes (spherocytes) responsible for pathological image and function of blood.

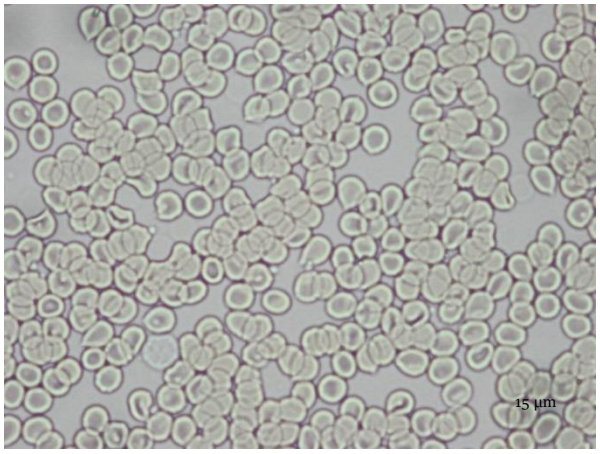

Figure 34. The haemolysis of red blood cells (the presence of spherocytes) in contact with the presence of ND-1 nanodiamond particles after 10 minutes. Optical microscope OLYMPUS CX31

Figure 35 shows the normal human red blood cells and the shadows of erythrocytes and the presence of schistocytes in contact with ND-2 nanodiamond particles. This blood picture corresponds to physiology of blood function.

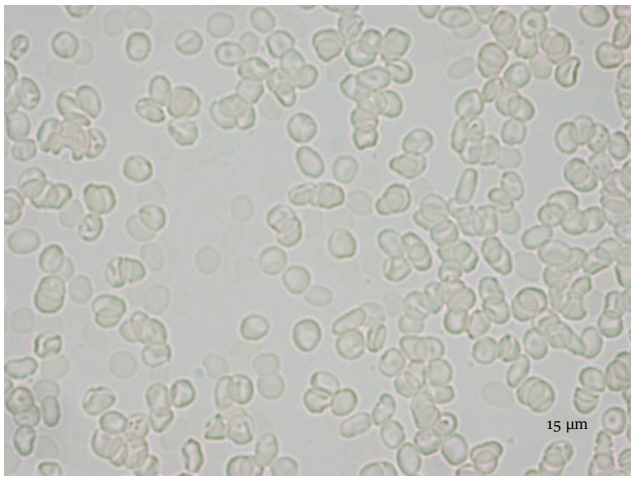

Figure 35. The normal human red blood cells and the shadows of erythrocytes and the presence of schistocytes in contact with ND-2 nanodiamond particles after 10 minutes. Optical microscope OLYMPUS CX31

Figure 36 shows the normal erythrocytes in contact with modified ND-3 nanodiamond particles.

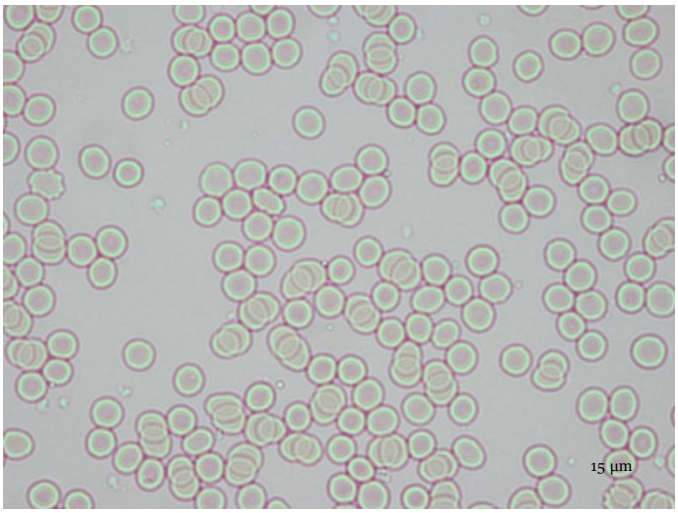

Figure 36. The normal erythrocyte in contact with modified ND-3 nanodiamond particles after 10 minutes. Optical microscope OLYMPUS CX31

5.1.2 HR TEM

Shape and size of nanoparticles (2–10 nm) were inspected by high-resolution transmission electron microscopy (HR TEM - Figures 37. shows that the grains of nanoparticles forming conglomerates).

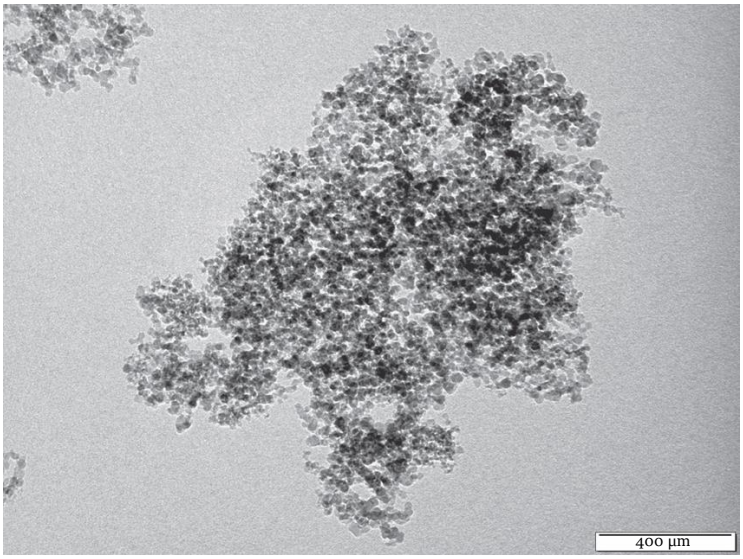

Figure 37. HR TEM image of nanodiamond particles manufactured by detonation method

5.1.3 SEM

In the research were used 3 samples of the nanodiamond powder: PD – the reference powder not subjected to any modification and powders subjected to the modification by the MW PACVD + R system, respectively PDM_30 and PDM_60. The samples differ in the time of modification, the other parameters are identical (Table 6.)

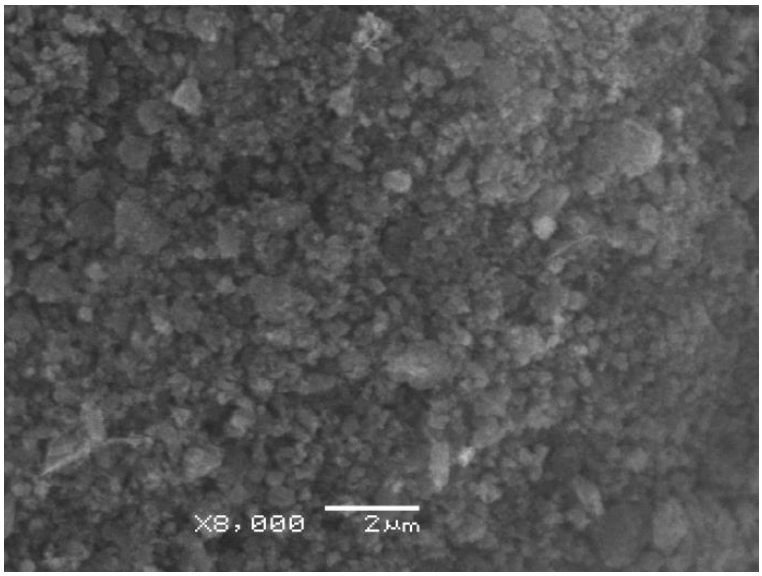

Figure 38. SEM detonation diamond nanopowder - PD

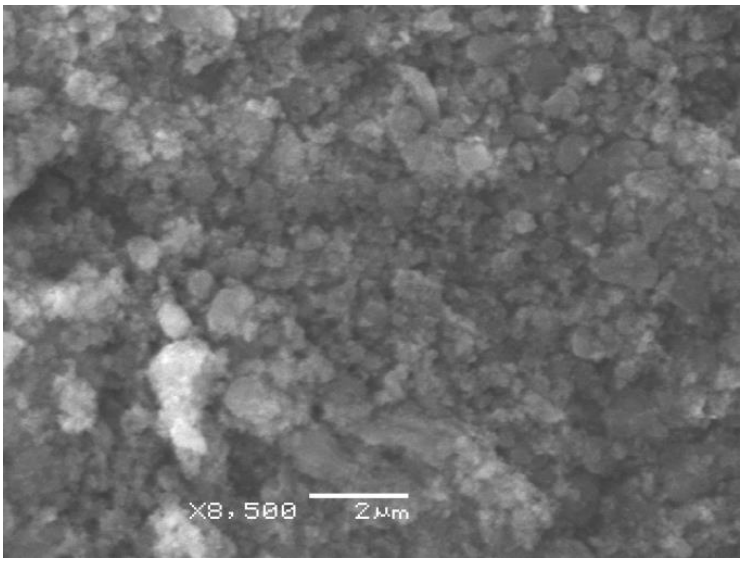

Figure 39. SEM detonation diamond nanopowder after the modification - PDM_30

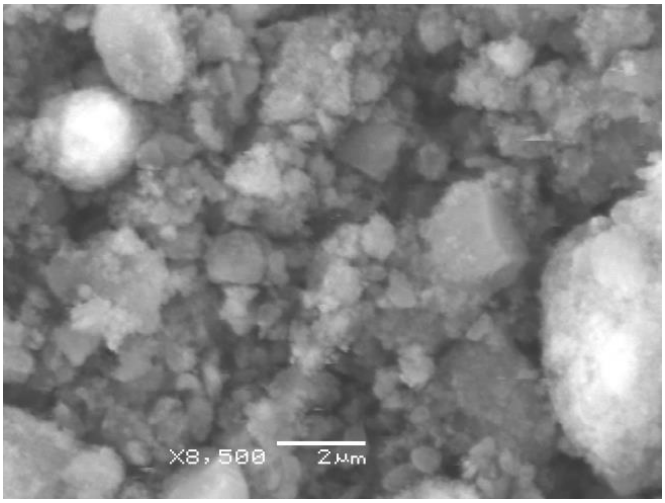

Figure 40. SEM detonation diamond nanopowder after the modification - PDM_60

Images of the surface of the carbon powder grains, modified by the MW PACVD + R method taken by the scanning electron spectroscopy, show the irregular structure of the shape of flakes with the tendency to form dense particles and the lack of regularity in the appearance of their edges. It is highly probable that such large differences are due to the tendency to form conglomerates or the degradation process being the result of the action of the internal stress. The images also show structural differences of the powders subjected to the modification, PDM_30 and PDM_60, in comparison to the reference material, PD. There is observed the increase of the "feathery" of conglomerates with the significant increase in their size, particularly visible for the PDM_60 image (Figure 41.).

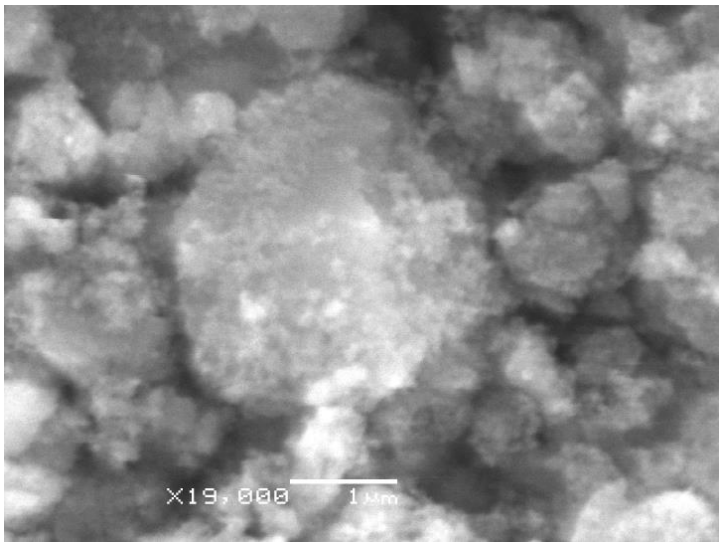

Figure 41. SEM conglomerate of the detonation diamond after modification - PDM_60

5.1.4 FTIR

The picture below (Figure 42.) presents the FTIR spectrum for all the examined nanodiamond particles after they are obtained and after they are subjected to the modification process. On all courses the peak has its peak at 3423 cm^{-1}, which responds to the presence of the hydroxyl group (OH). The intensity of the band 1140 cm^{-1} responds in the carbon-oxygen single chemical bond. The presence of the peak of hydroxyl group gives the ability of functionalization of the surface of the nanodiamond particles in the plasma modification processes.

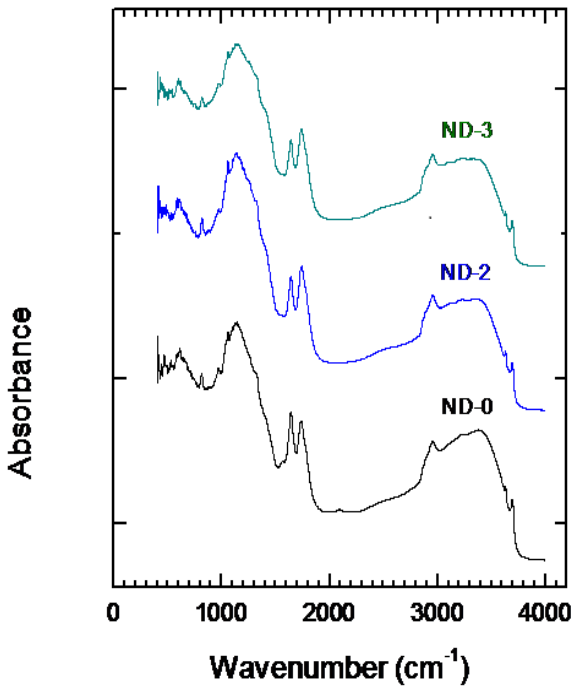

Figure 42. Comparison of the FTIR spectrum of the detonation powder of all tested powders (ND-0 "Danilenko powder", ND-2 „Koszalin", ND-3 „Modified ND Koszalin"

Due to the slight differences in the results of the analysis by the FTIR, studies were carried out again. There were used 2 representative samples of the detonation diamond nanopowder: the reference powder not subjected to the modification (ND-2), and the powder (ND-3) subjected to the modification by the MW PACVD + R system.

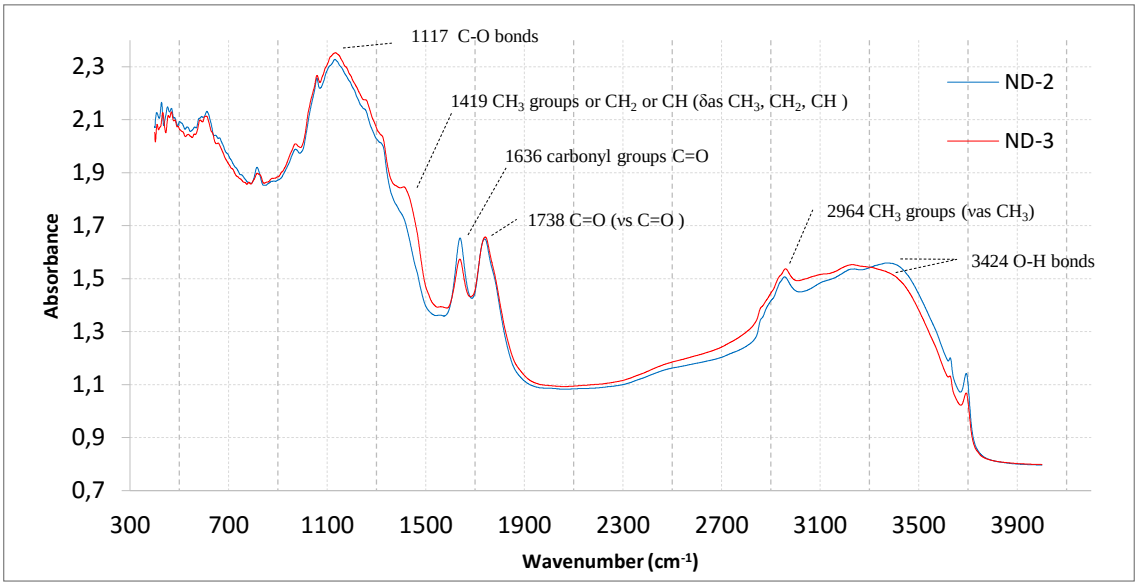

Figure 43. Comparison of the FTIR spectrum of the detonation powder before and after the modification

In the infrared spectrum of the diamond powder there can be observed characteristic peaks at a wavenumber 3424 cm^{-1}, 2964 cm^{-1},1738 cm^{-1}, and 1117 cm^{-1}. The first broad signal at 3424 cm^{-1} indicates the presence of the O–H bonds in the tested material. The presence of oxygen-hydrogen bonds also confirms the strong absorbance band at 1117 cm^{-1} that is characteristic for vibrations stretching the C–O bonds. The signal, present in the spectrum, at a wavenumber 1636 cm^{-1}, may indicate the presence of carbonyl groups, C=O, on the surface of diamond powders. The appearance of peaks at wavenumbers 1738 cm^{-1} and 1117 cm^{-1}, respectively for bonds C=O and C–O, may also suggest the presence of the ester bonds on the nanodiamonds surface. It should also be noted that in the literature signals at a wavenumber 1636 cm^{-1} are described as characteristic for vibrations stretching the C=O bonds of the amide group or C=C bond. The weak signal, present in the spectrum, at a wavenumber 1419 cm^{-1}, may indicate the presence of the CH_3 groups or CH_2 or CH on the surface of the diamond powders.

The analysis of the spectrum obtained in the infrared, confirmed the presence of function groups, containing oxygen and hydrogen, on the surface of the diamond nanopowders. The functional groups and the bonds between the atoms absorb the infrared radiation in a relatively narrow area of frequency, irrespective of the construction of the rest of the molecule, thereby enabling the accurate determination of functional groups that are present on the surface of the nanopowders.

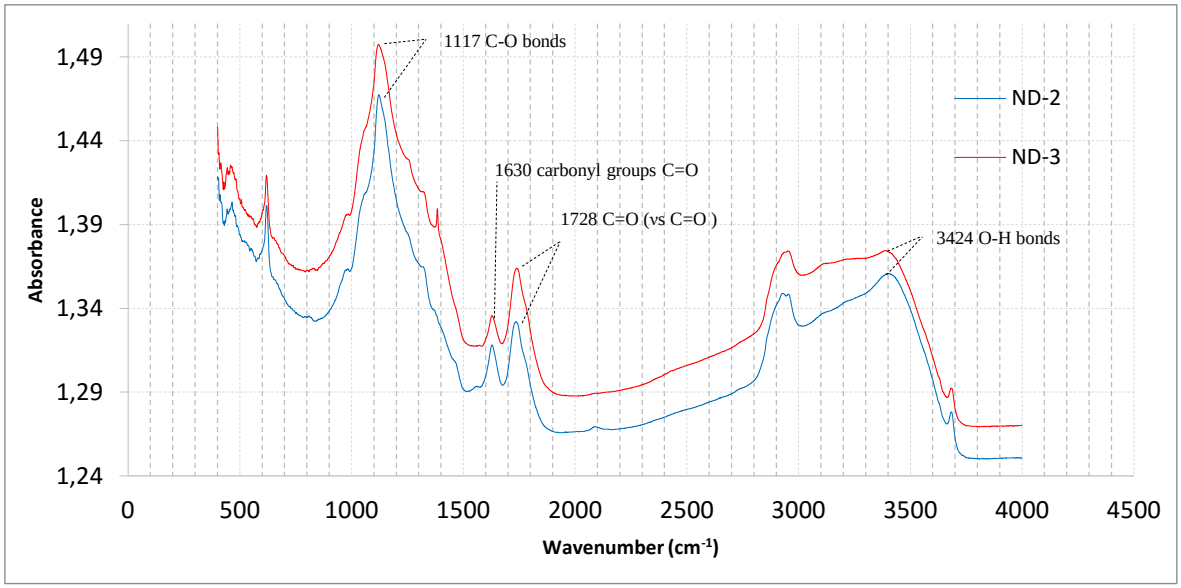

Figure 44. Comparison of the FTIR spectrum of the detonation powder before (ND-2) and after the modification (ND-3)

On the basis of the analysis were determined locations, which would indicate the difference in the course of FTIR spectroscopy. Those locations were marked on the graph below (Figure 45.).

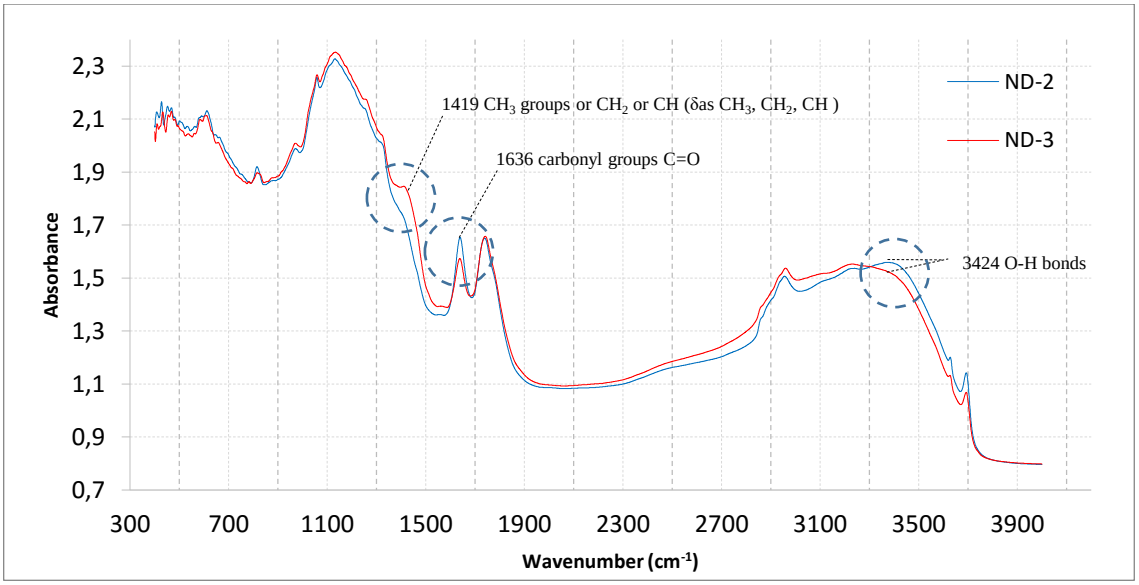

Figure 45. Comparison of the FTIR spectrum of the detonation powder before (ND-2) and after the modification (ND-3)

According to the author, the differences indicating the modification of the carbon powder should be searched around the wavenumber 1419 cm^{-1} ,1636 cm^{-1} and 3424 cm^{-1}.

For the deeper analysis, the obtained courses were divided into 3 ranges and were redistributed over the individual peaks components.

Range 900-1500 cm^{-1}

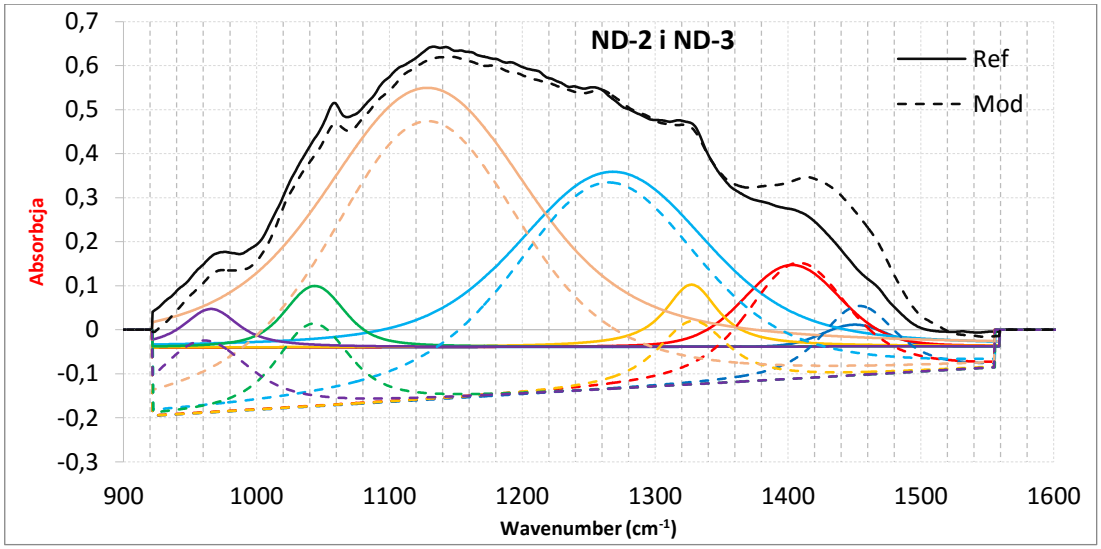

Figure 46. Distribution of the spectrum at the range of 900-1500cm^{-1} for ND-2 and ND-3

In order to illustrate the changes in a more detailed way, the individual components of ND-2 and ND-3 were subjected to the quantitative analysis. The results are shown in the table below (Table 7. and Table 8.)

Table 7. Ref peak distribution (ND-2)

PEAK DISTRIBUTION:					
Spectrum: Ref					
Range: 1559,236 921,743					
Baseline: Linear					
List of peaks:					
Name	**Centre X**	**Height**	**Width**	**Other**	**Area**
Ref7	965,826	0,0876	20,27	39,81	6,2764
Ref 6	1043,957	0,1395	36,624	25,73	9,4566
Ref 5	1128,624	0,5893	124,228	93,815	139,9935
Ref 4	1268,199	0,3979	129,548	61,729	81,4163
Ref 3	1327,445	0,1411	14,135	42,804	10,1308
Ref 2	1403,265	0,1854	77,512	11,556	17,4931
Ref 1	1450,35	0,0496	56,082	0,005	2,9651

Table 8. Mod peak distribution (ND-3)

PEAK DISTRIBUTION:					
Spectrum: Mod					
Range: 1555,544 921,807					
Baseline: Linear					
List of peaks:					
Name	**Centre X**	**Height**	**Width**	**Other**	**Area**
Mod7	959,626	0,1646	44,1	57,658	19,0681
Mod6	1042,165	0,1887	36,793	42,433	16,8241
Mod5	1127,776	0,6339	112,263	96,762	145,5142
Mod4	1262,936	0,4709	107,582	96,088	105,5797
Mod3	1328,356	0,1452	22,734	54,486	13,7069
Mod2	1407,458	0,2635	56,066	53,71	32,0387
Mod1	1453,082	0,1576	38,408	43,377	14,4776

The comparison of the percentage differences between the two distribution peaks are presented in the table below (Table 9.) .

Table 9. Percentage comparison of the differences in the distribution of peak Ref (ND-2) and peak Mod (ND-3)

PEAK DISTRIBUTION:					
Spectrum: Mod /Ref					
Range: 1555,544 921,743					
Baseline: Linear					
List of peaks:					
Name	**Centre X**	**Height**	**Width**	**Other**	**Area**
Mod7/Ref7	-0,65%	46,78%	54,04%	30,95%	67,08%
Mod6/Ref6	-0,17%	26,07%	0,46%	39,36%	43,79%
Mod5/Ref5	-0,08%	7,04%	-10,66%	3,05%	3,79%
Mod4/Ref4	-0,42%	15,50%	-20,42%	35,76%	22,89%
Mod3/Ref3	0,07%	2,82%	37,82%	21,44%	26,09%
Mod2/Ref2	0,30%	29,64%	-38,25%	78,48%	45,40%
Mod1/Ref1	0,19%	68,53%	-46,02%	99,99%	79,52%

The table presents the level of change of the modified carbon powder (ND-3) in a ratio of the reference material, which is a detonation nanodiamond not subjected to the

modification (ND-2). The individual peaks have centres located in a similar way, the difference in the size, of the fraction of the percent, may be the result of the measurement errors and does not affect the final result. The differences are clearly visible when it comes to the level of the absorption, as evidenced by the height and width of the peak, particularly evident in the case of peaks Mod1/Ref1, Mod2/ Ref2, Mod6/Ref6 and Mod7/ Ref7. The differences are illustrated on the area under the graph. Taking into consideration the above-mentioned criteria, the biggest impact of the shape of the main peak (appearance of a slope of the peak at 1419cm $^{-1}$) have the peaks of Mod1 appearing at around 1453 cm^{-1} and Mod2 appearing at 1408 cm^{-1} .

Range 1500-1900 cm^{-1}

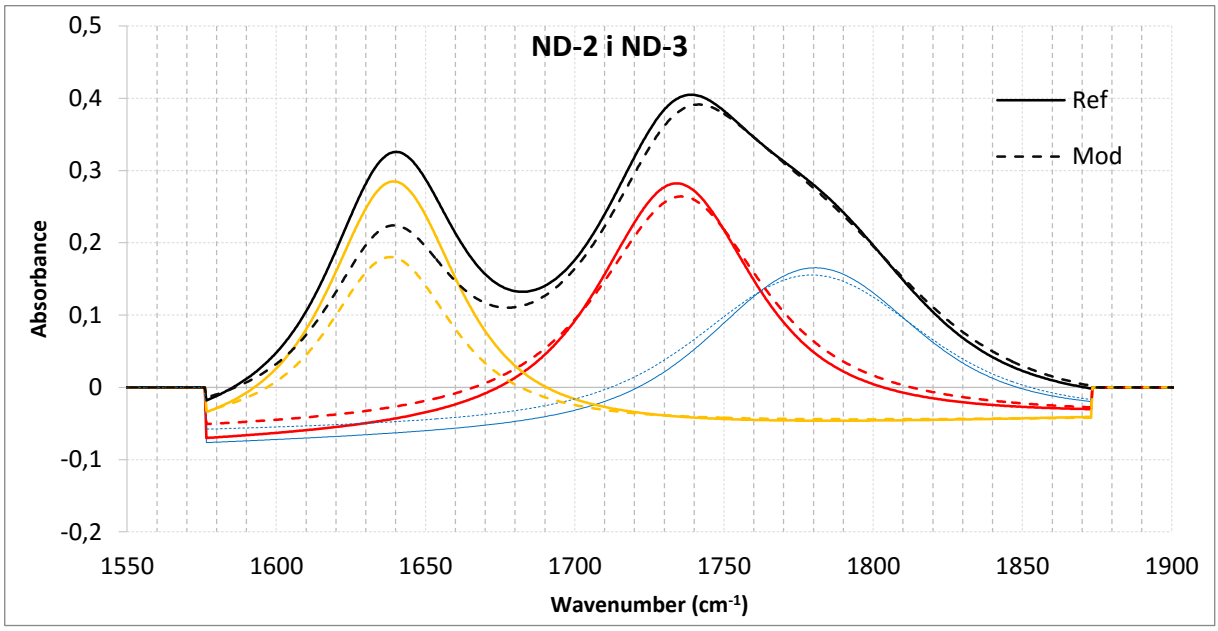

Figure 47. Spectrum distribution at the range of 1500-1900cm^{-1} for ND-2 and ND-3

In order to illustrate the changes in a more detailed way, the individual components of ND-2 and ND-3 were subjected to the quantitative analysis. The results are shown in the table below (Table 10. and Table 11.)

Table 10. Ref peak distribution (ND-2)

PEAK DISTRIBUTION:
Spectrum: Ref
Range: 1872,870 1576,282
Baseline: Linear

List of peaks:					
Name	**Centre X**	**Height**	**Width**	**Other**	**Area**
Ref 3	1639,208	0,3584	18,546	45,201	27,9611
Ref 2	1733,956	0,344	21,678	55,066	32,4603
Ref 1	1780,004	0,2214	48,864	51,019	24,6282

Table 11. Mod peak distribution (ND-3)

PEAK DISTRIBUTION:					
Spectrum: Mod					
Range: 1872,870 1576,282					
Baseline: Linear					
List od peaks:					
Name	**Centre X**	**Height**	**Width**	**Other**	**Area**
Mod3	1638,168	0,2397	16,68	44,768	18,2616
Mod2	1735,667	0,3173	16,306	63,05	32,7014
Mod1	1779,07	0,2057	53,67	55,618	25,0245

The percentage comparison of the differences in the distribution of the two distributions is presented in the table below (Table 12.) .

Table 12. Percentage comparison of the differences in the distribution of peak Ref (ND-2) and Mod (ND-3)

PEAK DISTRIBUTION:					
Spectrum: Mod /Ref					
Range: 1872,870 1576,282					
Baseline: Linear					
List of peaks:					
Name	**Centre X**	**Height**	**Width**	**Other**	**Area**
Mod3/Ref3	-0,06%	-49,52%	-11,19%	-0,97%	-53,11%
Mod2/Ref2	0,10%	-8,41%	-32,94%	12,66%	0,74%
Mod1/Ref1	-0,05%	-7,63%	8,95%	8,27%	1,58%

The table presents the level of change of the modified carbon powder (ND-3) in a ratio of the reference material, which is a detonation nanodiamond not subjected to the modification (ND-2). The individual peaks have centres located in a similar way, the difference in the size, of the fraction of the percent, may be the result of the measurement

errors and does not affect the final result. The differences are clearly visible when it comes to the level of the absorption, as evidenced by the height and width of the peak, particularly evident in case of peaks Mod3/Ref3 and Mod2/ Ref2. The differences are illustrated on the area under the graph. Taking into consideration the above-mentioned criteria, the biggest impact on the shape of the main peak has the peak of Mod3 appearing at around 1736cm $^{-1}$.

Range 2800-3000 cm^{-1}

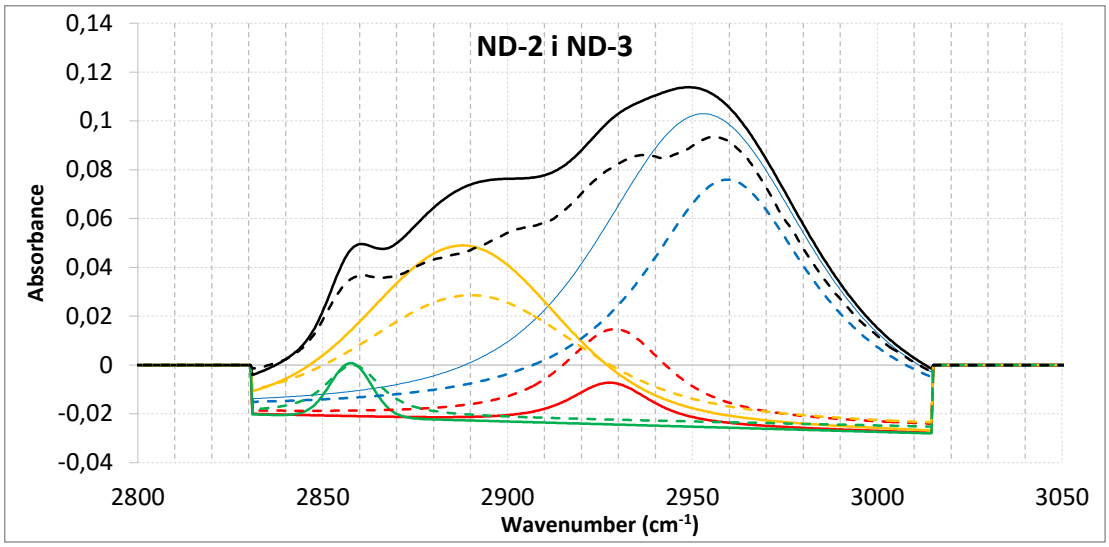

Figure 48. Distribution of the spectrum at the range of 2800-3000cm^{-1} for ND-2 and ND-3

In order to illustrate the changes in a more detailed way, the individual components of ND-2 and ND-3 were subjected to the quantitative analysis. The results are shown in the table below (Table 13. and Table 14.)

Table 13. Ref peak distribution (ND-2)

PEAK DISTRUBUTION:					
Spectrum: Ref					
Range: 1559,236 921,743					
Baseline: Linear					
List of peaks:					
Name	**Centre X**	**Height**	**Width**	**Other**	**Area**
Ref 4	2858,216	0,0203	8,337	13,514	0,5183
Ref 3	2890,51	0,05	47,162	35,704	4,5171
Ref 2	2929,169	0,0373	10,801	30,212	1,9086
Ref 1	2959,515	0,0995	4,137	55,758	8,7148

Table 14. Mod peak distribution (ND-3)

PEAK DISTRIBUTION:					
Spectrum: Mod					
Range: 1555,544 921,807					
Baseline: Linear					
List of peaks:					
Name	**Centre X**	**Height**	**Width**	**Other**	**Area**
Mod4	2857,616	0,022	12,695	0,408	0,3062
Mod3	2887,982	0,0714	48,713	20,53	5,2744
Mod2	2927,998	0,0174	10,973	20,312	0,6424
Mod1	2953,198	0,1293	33,628	50,458	12,5331

The percentage comparison of the differences in the distribution of the two distributions is presented in the table below (Table 15.) .

Table 15. Percentage comparison of the differences in the distribution of peak Ref (ND-2) and Mod (ND-3)

PEAK DISTRIBUTION:					
Spectrum: Mod /Ref					
Range: 1555,544 921,743					
Baseline: Linear					
List of peaks:					
Nazme	**Centre X**	**Height**	**Width**	**Other**	**Area**
Mod4/Ref4	-0,02%	7,73%	34,33%	-3212,25%	-69,27%
Mod3/Ref3	-0,09%	29,97%	3,18%	-73,91%	14,36%
Mod2/Ref2	-0,04%	-114,37%	1,57%	-48,74%	-197,10%
Mod1/Ref1	-0,21%	23,05%	87,70%	-10,50%	30,47%

The table above presents the level of change of the modified carbon powder (ND-3) in a ratio of the reference material (ND-2). These differences are significant in comparison to the examined ranges. This is particularly evident with regard to peak Mod2, whose area is almost 200 times smaller than the reference one. The differences are also visible when it comes to the level of absorption, as evidenced by the width and height of the peak, particularly in case of peaks of Mod2 discussed earlier. Taking into consideration the above-mentioned criteria, the biggest impact on the shape of the main peak has the peak of Mod3 appearing at around 2928cm $^{-1}$.

Peak at 2953,198 cm^{-1} (Mod1) indicates the presence of CH_2 symmetric vibrations.

Peak at 2927,998 cm^{-1} (Mod2) indicates the presence of CH_3 symmetric vibrations..

Peak at 2887,982 cm^{-1} (Mod3) indicates the presence of CH_2 asymmetric vibrations..

Peak at 2953,198 cm^{-1} (Mod4) indicates the presence of CH_3 asymmetric vibrations..

5.1.5 Raman spectroscopy

In the study, as before, were used 3 kinds of the nanodiamond obtained by the detonation method (ND-0 – Danilenko powder, ND-2 „Koszalin" and ND-3 – modified by MW PACVD + R).

The Raman spectra of the examined diamond nanopowders, carried out by Raman spectrometer, are shown below (Figure 49.). The collected spectra point out the unnoticeable differences in the analyzed powder. In all spectra there is observed the peak at position 1332 cm^{-1} that is typical for the nanodiamond particles of the graphite phase, whose existence is indicated by peak G and peak D. Peak G is at the level of about 1580-1600 cm^{-1}, and peak D at about 1350 cm^{-1}.

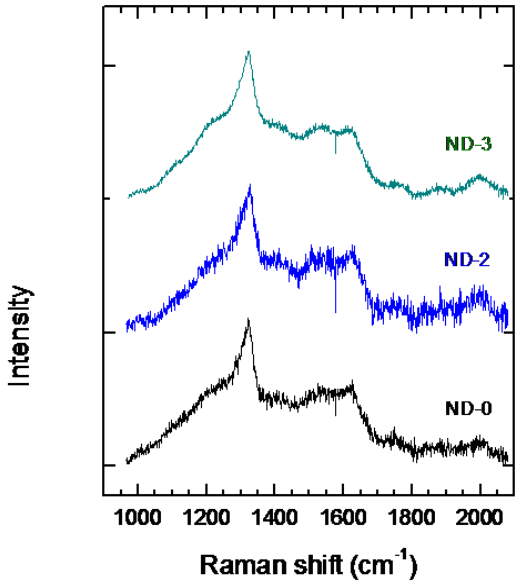

Figure 49. Comparison of all examined particles in Raman spectroscopy (ND-0 "Damilenko powder", ND-2 „Koszalin", ND-3 „modified ND Koszalin")

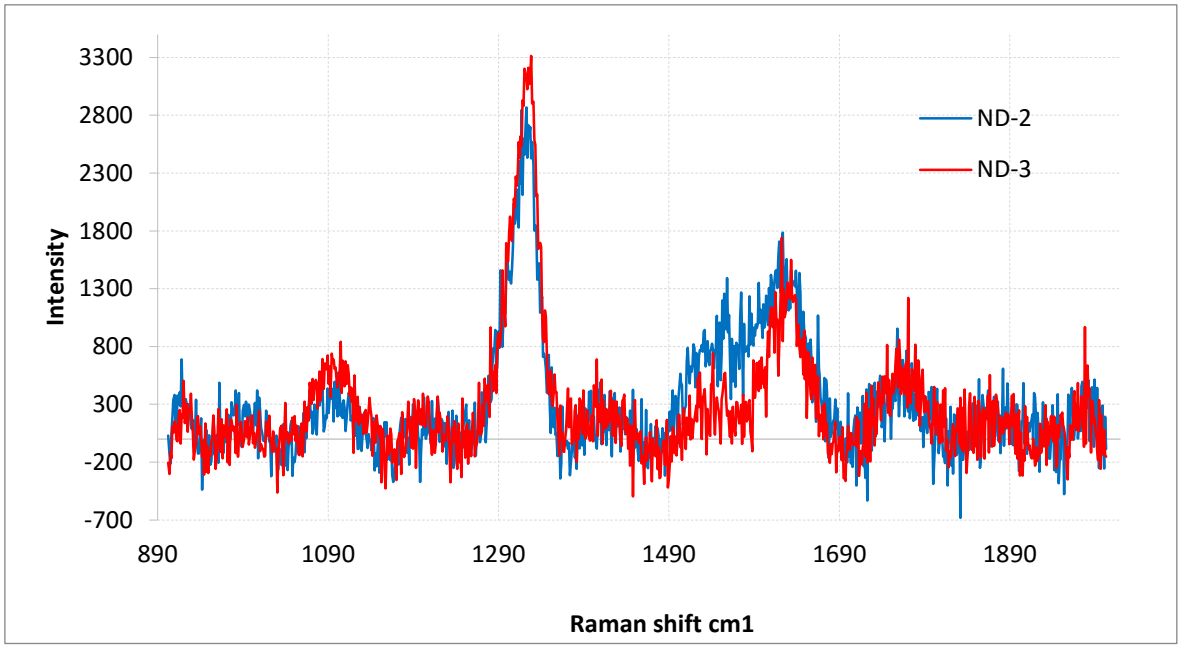

Figure 50. Comparison of examined particles in Raman spectroscopy before ND-2 and after modification ND-3

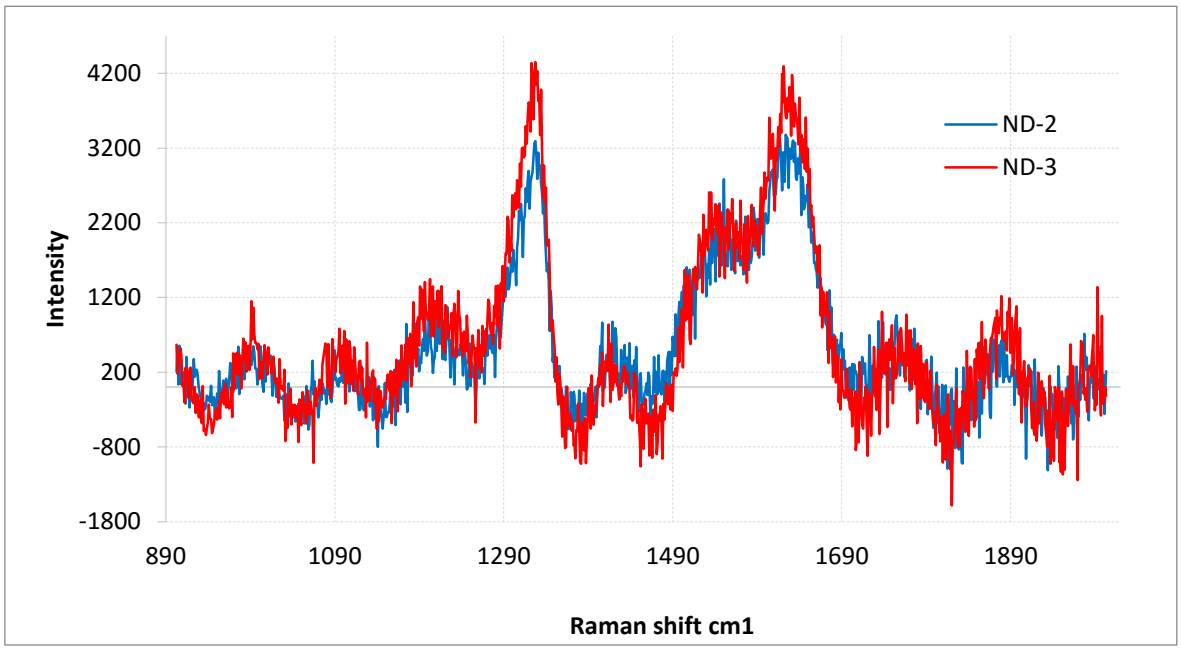

Figure 51. Comparison of examined particles in Raman spectroscopy before ND-2 and after modification ND-3

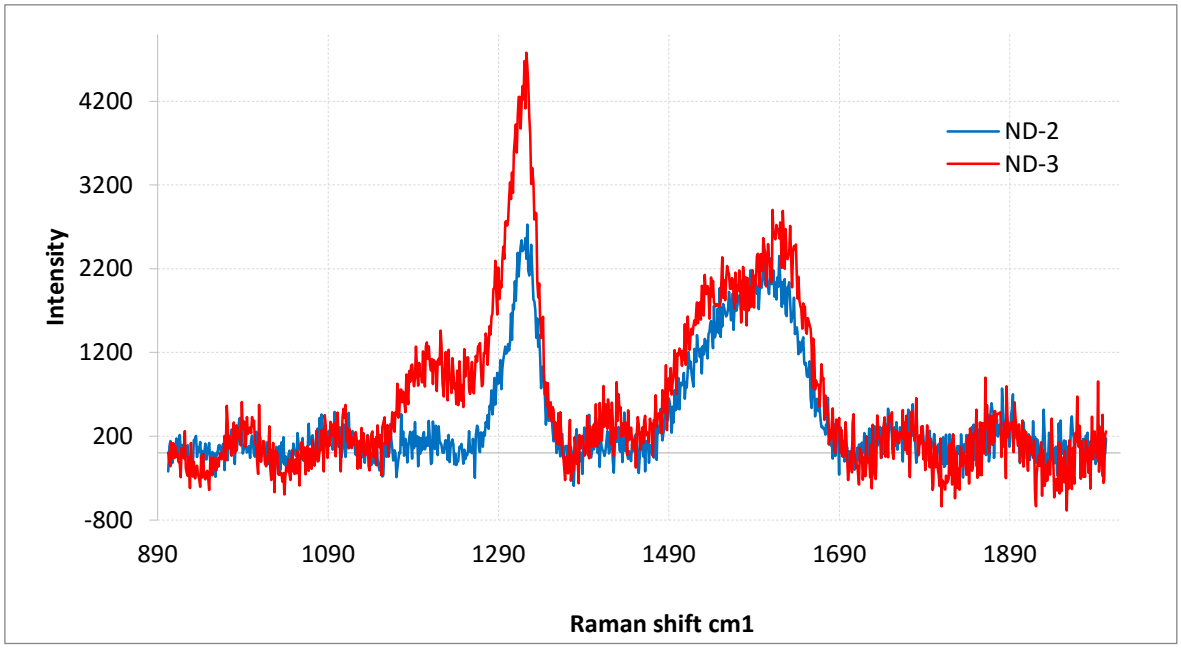

Figure 52. Comparison of examined particles in Raman spectroscopy before ND-2 and after modification ND-3

6 Discussion of results

Currently, there is a great interest in methods of modifying carbonaceous materials by which they gain new properties. There are known methods of mechanical, chemical [53] or plasma functionalization. This dissertation is devoted to the construction of the innovative MW PACVD + R system for plasma-chemical modification of diamond nanopowders, thanks to which it gains new – biological properties. The carbonaceous material obtained in the process was subjected to a series of tests that are to verify and determine its new features.

In order to conduct the study, three types of nanodiamond, obtained by the detonation method, were used:

- *ND-0* – not modified Danilenko`s nanodiamond powder,
- *ND-2* – not modified nanodiamond powder
- *ND-3* – nanodiamond powder modified by the microwave reactor MW PACVD + R.

Biological test were carried out by *in vivo* method on cells of the human blond haemoglobin for all three types of nanodiamond. The images of the optical microscope indicate the following:

- The result of contact of human haemoglobin with not modified nanodiamond powder marked *ND-0,* is the rouleaux of erythrocytes (Figure 32.). The result obtained after 10 minutes contact.
- The result of contact of human haemoglobin with not modified nanodiamond powder marked *ND-1,* is the agglutination of erythrocytes (Figure 33.). The result obtained after 10 minutes contact (Figure 34.) clearly show the process of hemolysis of the erythrocytes.
- The result of contact of human haemoglobin with not modified nanodiamond powder marked *ND-2,* in ten minutes time is the occurrence of the schistocytosis (decomposition) of erythrocytes (Figure 35.) In the photography are visible shadows of the destroyed biological cells.
- The result of contact of human haemoglobin with not modified nanodiamond powder marked *ND-3,* in ten minutes time no changes are observed (Figure 36.)

- The analyzed photography indicates a good condition of erythrocytes as compared to the reference photography (Figure 31.) of the haemoglobin without the carbonaceour material, thus showing a high biocompatibility of the modified diamond nanopowder.

The analysis of diamond powder by HR TEM allows to specify the size of grains. Shown in the pictures individual particles have the size ranging from 2 to 10 nm, however, the formation of agglomerates considerably hinders to actually determine the size of a single diamond grain. It was estimated that the size of the agglomerates reaches the size of 10 to 400 nm.

Another method used to analyze the detonation diamond nanopowders was infrared spectroscopy. Figure 43 presents a summary of FTIR spectra of not modified nanodiamonds and nanodiamond modified by MW PACVD + R system. In all graphs the peak has its peak at 3423 cm^{-1}, which corresponds to the presence of the hydroxyl group. The intensity of the band (width) at 1140 cm^{-1} corresponds to single bond carbon-oxygen. These results indicate an unnoticeable difference in the results between various powders, which may indicate the negative modification process in case of *ND-3* sample.

The small differences in the results of the FTIR presents on Figure 45. (three locations marked on the graph). This peak are located on the wavenumber 1419 cm^{-1}, 1636 cm^{-1} and 3424 cm^{-1}.

The location of the peak at the position of 1332 cm^{-1} in the spectrum of Raman spectroscopy (Figure 50.) shows graphite phases that are typical for nanodiamond particles, whose existence indicates also peak G and peak D. Peak G is at the level of about 1580-1600 cm^{-1}, and peak D at about 1350 cm^{-1}. The collected spectra show unnoticeable differences in the analyzed powder.

Positively completed stages of this dissertation:

1. The project of the research station for plasma modification of diamond nanopowders (MW PACVD + R).

2. The proper selection of ready-made elements of the construction (microwave generator composed of the basic part which is the magnetron head and correct power supply).
3. The adaptation of the possessed chamber: the original system of transferring the rotation on the plane vacuum – atmospheric pressure and the microwave spigot with the quartz window.
4. Adjusting the microwave system (the microwave generator to the load – the vacuum chamber).
5. The successful implementation of the designed system.
6. Tight and stable vacuum system.
7. The ability to adopt the measuring and regulating system for the automatic operations (microcomputer Raspberry PI) – web-based system and MySQL data backup.
8. The generation of stable plasma.
9. Due to the generated high energy density (up 1,2kW) in the relatively small reactor volume, the ability to carry out the CVD process to an extent unattainable for standard solutions.
10. The novel method using the rotary drum inside the MW PACVD reactor chamber - unique in the world (prepared utility model).
11. The possibility of further expansion and the use in material CVD processes.
12. Starting from the concept through the design (visualization) to the actual implementation – the idea was presented on a number of international and national conferences, meeting at the same time with the great interest and the positive feedback.
13. The modification of diamond powders in the rotary plasma-chemical reactor chamber (MW PACVD) confirmed by the results.

Analyses indicate that the modification process was carried out positively. It clearly confirms the basic assumption of the project and proves such concept of the construction solution. Even though the project focuses mainly on constructing the device for plasma-chemical modification of diamond powders, the obtained results of the modification by the use of the device, explicitly prove the success of the concept.

For the purpose of the analysis was used the diamond nanopowder manufactured by ADAMAS company, of known parameters that were analyzed by the Raman spectroscopy. The obtained result was compared to the analogous analysis on the modified powder in the described MW PACVD system. The result was ambiguous and indicated almost unnoticeable structural changes both in the morphology of the surface and the atomic composition. Only the conducted biological tests on human haemoglobin by *in vivo* method, clearly indicate that the modification occurred and resulted in the change of biological properties of the modified carbonous material.

7 Conclusions

The research work carried out within the framework of this doctoral thesis as well as the achieved results allow to formulate the conclusions that are presented below.

- The analysis, performed as a part of the research, of diamond nanopowders using Raman spectroscopy show unnoticeable differences within the analyzed spectrum. It signifies that despite the modification by the MW PACVD + R method, the structure of nanodiamond was fully preserved (no increase in the content of σsp^2 diamond phase providing for overlapping potential partial graphitization of the substrate).
- The analysis of diamond nanopowders using FTIR method show small differences in the peaks located on the wavenumber 1419 cm^{-1}, 1636 cm^{-1} and 3424 cm^{-1}, which cause spectacular differences in the biological properties of the modified diamond nanopawders.
- Despite the unnoticeable differences in the results of the Raman and small differences characterizing diamond nanopowders by FTIR method, in the biological tests carried out by in vivo method on the human haemoglobin, the results are evident and clearly indicate high biocompatibility of the modified carbon material.
- The realized original MW PACVD system for the modification of diamond nanopowders, accomplishes the assumed tasks as evidenced by presented the biological results.
- The biological results may be a positive forecast for the application of the MW PACVD + R system to create biocompatible carbon materials for medical needs.

8 Abstract

Modern technologies, used in material engineering, are the source of modern biomaterials. At present, there is observed a significant increase in the interest of plasma chemical methods of nanodiamond modification thanks to which it gains new spectacular properties.

This dissertation concerns the modification of diamond powders (DPP – *diamond powders particles*) in order to achieve the specific physical and chemical properties that would be beneficial for various applications in biomedical engineering. That was the reason why the innovative MW PACVD rotary reactor chamber (MW PACVD – *Microwave Plasma Activated Chemical Vapour Deposition*) was designed and constructed. The material modified in the reactor chamber was tested for potential applications.

The initial phase of work was focused mainly on the construction of the system MW PACVD equipped with a rotary drum. It dealt with a number of solutions commonly used in this field, both in science and in industry. Definitively established main concept fulfilling the basic assumptions, which are in effect, been fully realized.

The next step was to carry out the modification process of diamond nanopowders using a system constructed MW PACVD + R. The completion of the process was preceded by a series of test trials and the work starts control and calibration. Yield was satisfactory output at a relatively stable plasma generation MW.

The next stage of the study was a comparative analysis of carbon materials (detonation diamond nanopowders) undergoing surface modification using the present system of unmodified materials. They conducted a study into Raman spectroscopy, and FTIR. The results indicated a noticeable difference in the analyzed waveform which could indicate a malfunction of the system (expected noticeable change). However, only biological research shed new light on the issue. It turned out that in vivo studies of human hemoglobin modified in the reporting system, the detonation diamond nanopowder shows odmnienne of reference materials, good biological properties. The high degree of biocompatibility indicates practically negligible negative effect on the hemoglobin as shown in image 37 (Figure 37). It can be assumed that used to analyze the conventional

method (Raman and FTIR) are methods which are able to detect subtle changes which clearly indicate the biological tests.

The paper presents results of research on plasma-detonation modification of nanopowders diamond implemented in the author's reactor design MW PACVD + R and the impact of these modifications on their biological properties.

Keywords: diamond particles powder, detonation nanodiamond, modification, CVD process, plasma-chemical process, rotary drum, microwave, MW PACVD system, biological properties, biomaterial.

9 Publications of the author

1. Patryn A., Doroshenko J., **Ceynowa P**., L. Bychto: „Optical Coupling Block for Discrete Pseudomonochromator", poster-conference after the International Conference IMAPS 2011

2. P. **Ceynowa,** W. Zink, W. Kaczorowski, K. Mitura: „Biomedical and mechanical properties of diamond powder particles (DPP), produced by RF PACVD method with a Mechanically modified particle size." NANOSMAT 2011, ed. N.Ali, p. 32-33,

3. K. Adach, J.Skolimowski, **P.Ceynowa**, K.Mitura:"Chemical modification of bioactive nanodiamondsby the reaction with ampicillin.", NANOSMAT 2011, ed. N.Ali, p. 28,

4. R. Woś, J.Skolimowski, **P.Ceynowa**, K.Mitura:"Modyfication of carbon powder obtained by RF PACVD method using microwave reactor.", NANOSMAT 2011, ed. N.Ali, p. 28-29

5. J. Soukupová, D. Lucas, **P. Ceynowa**, K. Mitura:" The fabrication and characterization of nanofibrous scaffold with nanodiamonds by electrospinning method.", NANOSMAT 2012, ed. N.Ali, p. 19

6. P**. Ceynowa**, W. Zink. Siddiqui, S. Mitura:" Modification of diamond powder particles (DPP) by using the new construction MP CVD reactor.", NANOSMAT 2012, ed. N.Ali, p. 19

7. P**. Ceynowa**: "Modification of diamond powder particles (DPP) by using the new construction MP CVD reactor." Nomination: Young Scientist Lecture Competition (4 place), w: Proc. NANOSMAT 2012, ed. N.Ali, p. 21-22,

8. S. Mitura, **P. Ceynowa**, K.Adach, K. Mitura, P. Louda, "Plasmachemical modification of diamond", w: Proc. 68thIUVSTA WORKSHOP Hong Kong - "Multifunctional Surface Engineering for Advanced Energy Applications", ed. Prof. Wenjun Zhang, p. 6,

9. K. Mitura, I. Gisterek, **P.Ceynowa**, G.Pich, R.Woś, K.Adach , "Microbiological testing of bioactive powders nanodiamentowych chemically modified" ,w: Postępy inżynierii biomedycznej, ed. L. Leniowska, Z. Nawrat, 2013, pp. 157-168, **ISBN 978-83-63151-02-7**

10. P**. Ceynowa**, K. Mitura , S.Mitura, "System modyfikacji nanoproszków diamentowych (DPP) w rotacyjnej komorze reaktora plazmo-chemicznego (MW PACVD)" , w: Elektronika, 2014 R.55 nr 10 p.17-18 **DOI : 10.15199/ELE-2014-170**

11. P**. Ceynowa**, K. Kubiak, K. Mitura, M.Bielecki, S.Krzewiński, K.Symonowicz, S.Bielecki, S. Mitura, " Synteza nanowłókna z bionanocelulozy (BNC)" , w: Elektronika, 2014 R.55 nr 10 p.47-50 **DOI: 10.15199/ELE-2014-161**

12. P**. Ceynowa**, K.Wyrębski ,W. Zinka, K. Mitura, S. Mitura, " The detonation diamonds nanopowder (DND) modified with MW PECVD+R system " , w: Proc. ITMED 2015, ed. prof. Stanisław F. Mitura , p. 17,

13. P**. Ceynowa**, K.Wyrębski ,W. Zinka, K. Mitura, S. Mitura, " Properties of the detonation diamonds nanopowder (DND) modified with MW PECVD+R system " , w: Proc. 9th Symposium on Vacuum based Since and Technology , Kołobrzeg, 2015

14. P**. Ceynowa**, M. Dudek, Z. Ociepa, W. Zinka, S. Mitura:" Monochromatic monitoring of microwave plasma source in MW PACVD + R system.", NANOSMAT 2015, ed. N.Ali, p. 21,

15. P. Wilczek, **P. Ceynowa** , K. Cabała, P. Bajko, M. Kosik, K. Kozłowski, S. Mitura:" Mesenchymal stromal cells onto polycaprolactone nanofiber", NANOSMAT 2015, ed. N.Ali, p. 22,

16. P**. Ceynowa**, K.Wyrębski, A.Balcer, M. Sobaszek, R. Bogdanowicz, M.Dudek , W. Zinka, S. Mitura:" Diamond sensor for special applications in breath control", Smart Engineering of New Materials SENM 2015, ed. P.Niedzielski,

17. K. Mitura, M. Jedrzejewska-Szczerska, **P. Ceynowa**, M. Dudek, M. Cicha, I. Kotela, S. Mitura, „Haemocompatibility of Non-Functionalized and

Plasmachemical Functionalized Detonation Nanodiamond Particles", w: Archives of Metallurgy and Materials vol.60 issue 3-2015, pp. 2183-2190

10 Bibliography

[1] S.Mitura, Nucleation of diamond powder particles in an RF methane plasma, Journal Crystal Growth 80 (1987) 417-424.

[2] S. Mitura, The role of electrons in low-pressure diamondsynthesis, Scientific Bulleutin of Technology Univesity of Lodz 666 (1992).

[3] P. Niedzielski, *Wytwarzanie i zastosowanie proszków diamentowych*, Wydawnictwo Politechniki Łódzkiej, Łódź (2011)

[4] K. Mitura, *HR TEM examinations of nanodiamond particles for biomedical application*, Journal of Achievements in Materials and Manufacturing Engineering, 37, 317 – 322, (2009)

[5] S. Mitura, P. Ceynowa *The project of the National Center for Science No. UMO-2011/03 / N / ST8 / 06184* (2012-2014)

[6] B.S. Lewis, M. Tang, J.F. Walker, E. Anders, E. Steel, Interstellar grains in meteorites, Nature 326 (1987) 160-162.

[7] I. Sigalas, R. J. Caveney, M. W. Bailey Diamond Materials and their Applications, Handbook of Ceramic Hard Materials, Weinheim 2000, t.2, s. 479-481

[8] Tillmann W. , Trends and market perspectives for diamond tools in the construction of industry. Corporate Research, Hilti AG, FL-9494 Schaan, Principality of Liechtenstein, 27 February 2001.

[9] James C. Sung, Shao Chung Hu, I Chiao Lin, Chia Cheng Tsai, The Revolution of Diamond Synthesis Technology, Materials Science Forum t. 534-536, 2007, s. 1141-1144

[10] Hall H.T., Strong H.M., Wentorf R.M., Method of making diamonds, U.S. Patent 2,947, 610 (August 2, 1960)

[11] K. Adach, J. Skolimowski, K. Mitura, Chemical modification of nanodiamond particles, manufacture of detonation method,N.Ali, S.Mitura (eds); Nanosmat Abstracts Book, Krakow, 17-20 Oct. 2011, p. 34

[12] W.Z. Kaczorowski, T.Kaźmierczak, Micro and Nano Carbon Powders Manufactured Using Dual Frequency CVD Plasma, N.Ali, S.Mitura (eds); Nanosmat Abstracts Book, Krakow, 17-20 Oct. 2011, pp. 72-73

[13] P. Ceynowa, W. Zinka, W.Kaczorowski, K. Mitura, Biomedical and mechanical properties of diamond powder particles (DPP), produced by RF PACVD method with a mechanically modified particle size, N.Ali, S.Mitura (eds); Nanosmat Abstracts Book, Krakow, 17-20 Oct. 2011, pp. 284-285

[14] K. Bakowicz-Mitura, G. Bartosz, S. Mitura, Surf. Coat. Tech., 201, 6131 (2007).

[15] M. Czerniak-Reczulska, P. Niedzielski, A. Balcerczyk, G. Bartosz, A. Karowicz-Bilinska, K. Mitura, Journal of Nanoscience and Nanotechnology, 10, 1065, (2010)

[16] K. Bakowicz (Mitura), PhD, Thesis, Technical University of Lodz, Poland, (2003).

[17] O. Shenderova, V.V. Zhirnov, D.W. Brenner, *Carbon Nanostructures*, Critical Reviews in Solid State and Materials Sciences, 27, 227–356 (2002)

[18] O. Shenderova, I. Petrov. J. Walsh, V. Grichko, V. Grishko, T. Tyler, G. Cunningham, Modification of detonation nanodiamonds by heat treatment in air, Diamond and Related Materials 15 (2006) 1799 - 1803

[19] E. Osawa, *Monodisperse single nanodiamond particulates*, Pure Appl. Chem., Vol. 80, No. 7, 1365–1379, (2008)

[20] R. B. Heimann, S. E. Evsyukov, Y. Koga, *Carbon allotropes: a suggested classification scheme based on valence orbital hybridization*,Carbon35,1654–1658, (1997)

[21] Q. Zou, Y. G. Li, L. H. Zou, M. Z. Wang, *Characterization of structures and surface states of the nanodiamond synthesized by detonation*, Materials Characterization, 60, 1257 – 1262, (2009)

[22] A. Krueger, *The structure and reactivity of nanoscale diamond*, Journal of Materials Chemistry, 18, 1485-1792, (2008)

[23] P. Chen, F. Huang, S. Yun, *Structural analysis of dynamically synthesized diamonds*, Diamond and Related Materials 39, 1589-1597, (2004)

[24] R. C. Fort, P. R. Schleyers, *Adamantane: Consequences Of The Diamondoid Structure*, Chem. Rev., 64 (3), 277–300, (1964)

[25] J. B. Donnet, C. Lemoigne, T. K. Wang, C.-M. Peng, M. Samirant, A. Eckhardt, Bull. Soc. Chim. Fr., 134, 875,(1997)

[26] A. Krueger, F. Kataoka, M. Ozawa, T. Fujino, Y. Suzuki, A. E. Aleksenskii, A. Ya. Vul, E. Osawa, Unusually tight aggregation in detonation nanodiamond: Identification and disintegration, Carbon, 43, 1722–1730, (2005)

[27] A. E. Aleksenskii, M. V. Baidakova, A. Ya. Vul' and V. I. Siklitskii, Phys. Solid State, 41, 668–671, (1999)

[28] A.E. Aleksenskii, V.Y. Osipov, A.T. Dideykin, A.Y. Vul , G.J. Adreaenssens, V.V. Afanasev, Ultradisperse diamond cluster aggregation studied by atomie force microscopy. Tech Phys Lett 26 (2000) 819 - 821.

[29] G. L. Bilbro, Diamond Relat. Mater., 11, 1572–1577, (2002)

[30] X. Xu, Z. Yu, Y. Zhu and B. Wang, J. Solid State Chem., 178, 688–693, (2005)

[31] A. P. Demnt'ev, K. I. Maslakov, *Chemicalstate of carbon atoms on the surface of nanodiamond particles*, Phys. Sol. State 46, 678–680, (2004)

[32] B. Palosz, C. Pantea, E. Grzanka, S. Shelmakh, T. Proffen, T. W. Zerda, W. Palosz, *Investigation of relaxation of nanodiamond surface in real and reciprocal spaces*, Diam. Relat. Mater. 15, 1813–1817, (2006)

[33] Y. Liu, Z. Gu, J. L. Margrave, V. N. Khabashesku, *Functionalization of Nanoscale Diamond Powder: Fluoro-, Alkyl-, Amino-, and Amino Acid-Nanodiamond Derivatives*, Chem. Mater., 16, 3924-3930, (2004)

[34] Alexander Y. Vul', Characterisation and Physical Properties of UNCD Particles, Ultra Nanocrystalline Diamond, Synthesis, Properties and Applications, Ed. O.A. Shenderova, D.M. Gruen, Wiliam Andrew Publishing, 2006

[35] Pengwan Chen, Fenglei Huang, Shourong Yun, Characterization of the condensed carbon in detonation soot, Carbon 41(2003) 2093 - 2099

[36] J. Qian, C. Pantea, J. Huang, T.W Zerda, Y. Zhao, Graphitization of diamond powders of different sizes at high pressure-high temperature, Carbon 42(2004) 2691-2697

[37] S. Osswald, M. Havel, V. Mochalin, G. Yushin, Y. Gogotsi, Increase of nanodiamond crystal size by selective oxidation, Diamond and Related Materials 17(2008) 1122 - 1126

[38] B. Palosz, E. Grzanka, Y. Wang, J. Gubicza, T. Ungar, Microstructure of nanocrystalline diamond powders studiem by powder diffractometry, Journal of Applied Physics 97(2005)

[39] B. Palosz, E. Grzanka, S. Gierlotka, S. Stel'makh, R. Pielaszek, U. Bismayer, J. Neuefeind, H.-P. Weber, Th. Proffen, R. Von Dreele, and W. Palosz, "Analysis of

short and long range atomic order in nanocrystalline diamonds with application of powder diffractometry", Zeitschrift fur Kristallographie217 (2002) 497

[40] C. Pantea, J. Gubicza, T. Ungar, G. A. Voronin, T. W. Zerda, Dislocation density and graphitization of diamond crystals, Physical Review B 66 (2002)

[41] A.C. Ferrari, J. Robertson, Raman Spectroscopy of amorphous, nanostructured, diamond-like carbon and nanodiamond, Philosophical Transactions of the Royal Society A 362 (2004) 2477

[42] A. Karczemska, M. Szurgot, M. Kozanecki, M. I. Szynkowska, V. Ralchenko, V.V. Danilenko, P. Louda, S. Mitura, Extraterrestrial, terrestrial and loboratory diamonds - Differences and similarities, Diamond and Related Materials, 17 (2008) 1179 – 1185

[43] S. A. Solin, A. K. Ramadas, Raman Spectrum of Diamond, Phys. Rev. B 1 (1970) 1687 - 1698

[44] A. N. Obraztsov, M. A. Timofeyev, M. B. Guseva, V. G. Babaev, Z. Kh. Valiullova, V.M. Babina, Compratative study of microcrystalline diamond, Diamond and Related Materials 4 (1995) 968 - 971

[45] S. Reich, C. Thomsen, Raman spectroscopy of graphite, Philosophical Transactions of the Royal Society A 362 (2004) 2271- 2512

[46] S. M. Leeds, T. J. Davis, P. W. May, C. D. O Pickard, M. N. R. Ashfold, Use of different excitation wavelengths for the analysis of CVD diamond by laser Raman spectroscopy, Diamond and related Materials 7 (1998) 233 - 237

[47] A. C. Ferrari, J. Robertson, Resonant Raman spectroscopy of disordered, amorphous, and diamondlike carbon, PHYSICAL REVIEW B, VOLUME 64, 075414,

[48] S. Piscanec, F. Mauri, A.C. Ferrari, M. Lazzeri, J. Robertson, Ab initio resonant Raman spectra of diamond-like carbons, Diamond & Related Materials 14 (2005) 1078- 1083]

[49] V. Mochalin, S. Osswald, Y. Gogotsi, Contribution of Functional Groups to the Raman spectrum of nanodiamond powders, Chem. Mater. 21 (2009) 273 - 279

[50] A.I. Shames, A.M. Panich, W. Kempiński, A.E. Alexenskii, M.V. Baidakova, A.T. Dideikin, V.Yu. Osipov, V.I. Siklitski, E. Osawa, M. Ozawa, A.Ya. Vul', Defects and impurities in nanodiamonds: EPR, NMR and TEM study, Journal of Physics and Chemistry of Solids 63 (2002) 1993 - 2001

[51] I. Petrov, O. Shenderova, V. Grishko, V. Grichko, T. Tyler, G. Cunningham, G. McGuire, Detonation nanodiamonds simultaneously purified and modified by gas treatment, Diamond and Related Materials 16 (2007) 2098 - 2103

[52] J.L Peng, R.P Fehlhaber, L.A. Bursill, D.G. McCulloch, Analysis of nanocrystalline diamond powder by scanning transmission electron microscopy, Journal of Applied Physics 89 (2001) 6204 – 6213

[53] K. Adach, J. Skolimowski, K. Mitura, *Chemiczna modyfikacja nanoproszków diamentowych otrzymywanych metodą detonacyjną*, Wiadomości Chemiczne, 67, 1-2, (2013)

[54] S. Osswald, G, Yushin, V. Mochalin, S. O. Kucheyev, Y. Gogotsi, *Control of sp2/sp3 Carbon Ratio and Surface Chemistry of Nanodiamond Powders by Selective Oxidation in Air*, J. AM. CHEM. SOC., 128, 11635-11642, (2006)

[55] A. I. Shames, A. M. Panich, W. Kempiński, A. E Alexenskii, M. V. Baidakova, A. T. Dideikin, V. Yu. Osipov, V. I. Siklitski, E. Osawa, M. Ozawa, A. Ya. Vul, *Defects and impurities in nanodiamonds: EPR, NMR and TEM study*, Journal of Physics and Chemistry of Solids, 63, 1993-2001, (2002)

[56] J. Qian, C. Pantea, J. Huang, T. W. Zerda, Y. Zhao, Carbon, 42, 2691-2697, (2004)

[57] S. Osswald, M. Havel, V. Mochalin, G. Yushin, Y. Gogotsi, *Increase of nanodiamond crystal size by selective oxidation*, Diamond & Related Materials, 17, 1122-1126, (2008)

[58] V. Mochalin, S. Osswald, Y. Gogotsi, *Contribution of Functional Groups to the Raman Spectrum of Nanodiamond Powders*, Chemistry of Materials, 21, 273 – 279, (2009)

[59] P. Atkins, J. de Paula, *Physical Chemistry*. 8th ed: Oxford ; New York : Oxford University Press, (2006)

[60] K. Bąkowicz, Bioaktywność diamentu, Praca doktorska, Politechnika Łódzka, Łódź 2003

[61] W.Kopaliński, Słownik wyrazów obcych i zwrotów obcojęzycznych z almanachem, Wydawnictwo Muza, Warszawa 2003

[62] P. Niedzielski, Wytwarzanie warstw nanokrystalicznego diamentu na potrzeby medycyny, Praca doktorska, Politechnika Łódzka, Łódź 1998

[63] A. Kruger, F. Kataoka, M. Ozawa, T. Fujino, Y. Suzuki, A.E. Aleksenskii, A.Ya Vul, E. Osawa, Unusually tight aggregation in detonation nanodiamond: indetification and disintegration"; Carbon; 43(2005) 1722-1730

[64] V.Y. Dolmatov, Synthesis and Post-Synthesis Treatment of Detonation Nanodiamonds, Ultra Nanocrystalline Diamond, Synthesis, Properties and Applications, Ed. O.A. Shenderova, D.M. Gruen, Wiliam Andrew Publishing, 2006

[65] D.F. Williams, Biomaterials, Vol.19, Issue 20, (2008), 2941-2953

[66] L.A. Thompson, et al., Biocompatibility of diamond-like carbon coating. Biomaterials. 12(1991), 37-40

[67] W. Jakubowski, G. Bartosz, P. Niedzielski, W. Szymański, B. Walkowiak, Nanocrystalline diamond surface is resistant to bacterial colonization; Diamond and Related Materials; 13 (2004) 1761-1763

[68] S Mitura, et al., Nanokrystaliczny diament dla medycyny Inżynieria Materiałowa. 3(2000) NANODIAM. New technologies for medical applications: studying and production of carbon surfaces allowing for controlable bioactivity, w: S. Mitura, P. Niedzielski, B. Walkowiak (red.), PWN, Warszawa, 2006

[69] M. Allen, B. Myer, N. Rushton, In vitro and in vivo investigations into the biocompatibility of diamond-like carbon (DLC) coatings for orthpoedic applications. Journal of Biomedical Materials Research. 58(2001), 319-328

[70] J. Drzymała, Podstawy mineralurgii, Oficyna Wydawnicza Politechniki Wrocławskiej, Wrocław, 2001

[71] R. Koch, A. Noworyta, Procesy mechaniczne w inżynierii chemicznej, Wyd. II; Wydawnictwo Naukowo-Techniczne, Warszawa 1995

[72] M. Ozawa, M. Inakuma, M. Takahashi, F. Kataoka, A. Krueger, E. Osawa, Preparation and Behavior of Brownish, Clear Nanodiamond Colloids, Adv. Mater. 19 (2007), 1201 – 1206

[73] A. Krueger, D. Lang, Functionality is Key:Recent Progress in the Surface Modification of Nanodiamond, Adv.Funct.Mater.,2012,1-17

[74] T. Hasebe, et al., Fluorinated Diamond-like carbon as antithrombogenic coating for blood-contacting devices., J. Biomed., Mater., 76A (2006), 86-94

[75] R. Hauert, et al., Surface analysis and bioreactions of F and Si containing a-C:H., Thin Solid Films, 308-309 (1997),191-194

[76] T. Saito, et al., Antithronbogenicity of fluorinated diamond-like carbon films. Diamond Relat. Mater. 14 (2005), 1116-1119

[77] G.Q. Yu, et al., Properties of fluorinated diamond like carbon films by PECVD. Applied Surface Science. 219(2003), 228-237

[78] M.Kamińska, Modyfikacja warstw nanokrystalicznego diamentu (NCD) dla zastosowań w medycynie, Praca doktorska, Politechnika Łódzka, Łódź 2006

[79] B.V. Spitsyn , S.A. Denisov , N.A. Skorik , A.G. Chopurova , S.A. Parkaeva , L.D. Belyakova , O.G. Larionov, The physical – chemical study of detonation nanodiamond application in adsorption and chromatography, Diamond Relat. Mater., 2010, 19, 123 – 127

[80] M.B. Smith, J. March, March's Advanced Organic Chemistry, 6 th ed. , John Wiley & Sons , Hoboken 2007

[81] W.S. Yeap , S. Chen , K.P. Loh, Detonation Nanodiamond: An Organic Platform for the Suzuki Coupling of Organic Molecules, Langmuir 2009, 25, 185–191

[82] T. Penkala, Postawy chemii ogólnej, Warszawa, PWN, 1979

[83] Stuart Turner, Oleg I. Lebedev, Olga Shenderova, Igor I. Vlasov, Jo Verbeeck, Gustaaf Van Tendeloo, Determination of Size, Morphology, and Nitrogen Imp, urity Location in Treated Detonation Nanodiamond by Transmission Electron Microscopy, Adv. Funct. Mater. 2009, 19, 2116–2124

[84] S. Osswald, G. Yushin, V. Mochalin, S. O. Kucheyev, Y. Gogotsi, Control of sp2/sp3 Carbon Ratio and Surface Chemistry of Nanodiamond Powders by Selective Oxidation in Air, J. Am. Chem. Soc., 2006, 128 (35), 11635–11642

[85] V. Pichot, M. Cornet, E. Fousson, C. Baras, A. Senger, F. Le Normand, D. Spitzer, An efficient purification method for detonation nanodiamonds, Diamond Relat. Mater., 2008, 17, 13-22

[86] A.V. Karabutov, S.K. Gordeev, V.G. Ralchenko, S.B. Korchagina, K.I. Maslakov, A.P. Dementjev, Oxidation improvement of field electron emission from diamond nanomaterials, Surf. Interface Anal. 2004; 36: 455–460

[87] A. Krueger, M. Ozawa, G. Jarre, Y. Liang, J. Stegk, L. Lu, Deagglomeration and functionalisation of detonation diamond Phys. Stat. Sol. A 2007, 204, 2881–2887

[88] W.-W. Zheng, Y.-H. Hsieh, Y.-C. Chiu, S.-J. Cai, C.-L. Cheng, C. Chen, Organic functionalization of ultradispersed nanodiamond: synthesis and applications, J. Mater. Chem. 2009, 19, 8432–8441

[89] S. Ciftan Hens, G. Cunningham, T. Tyler, S. Moseenkov, V. Kuznetsov, O. Shenderova, Nanodiamond bioconjugate probes and their collection by electrophoresis Diamond Relat. Mater., 2008, 17, 1858–1866

[90] R. Martin, M. Alvaro, J. R. Herance, H. Garcia, Fenton – Treated Functionalized Diamond Nanoparticles as Gene Delivery System, Journal of American Chemical Society, 4, (2010), 65-74

[91] R. Martın, P. Concepcion Heydorn, M. Alvaro, H. Garcia, General Strategy for High-Density Covalent Functionalization of Diamond Nanoparticles Using Fenton Chemistry, Chem. Mater., 21(2009), 4505–4514

11 Figures list

Figure 1. The range of different morphologies of a large single crystal of the synthetic diamond 12
Figure 2. CHO phase diagram summarising 70 experiments with the use of gas mixtures for diamond deposition and with the use of CVD method [Bachmann et al., 1991]. 23
Figure 3. Stages of the detonation synthesis process of diamond nanopowders [17] 25
Figure 4. Model of possible structure of diamond particles obtained by the detonation process [5] 26
Figure 5. Diffractogram of diamond powders obtained by detonation of mixture of TNT-RDX in the amount of 50 / 50 in various environments (1-N_2, 2-NH_4CHO_3, 3-H_2O) [35]; 29
Figure 6. Raman spectroscopy of nanocrystalline diamond powders [49]..... 30
Figure 7. Diamond nanopowders surface examined by SEM 31
Figure 8. AFM image of detonation diamond conglomeration on the silicon surface [28] 32
Figure 9. Graphical record of the Fenton reaction carried out in the nanodiamond powder [62]. 38
Figure 10. 3D model of the waveguide line with magnetron head (1) and vacuum chamber equipped with a rotary drum inside (2) 41
Figure 11. The photography of the author while removing the lid of the vacuum chamber. 43
Figure 12. The block diagram of MW PACVD + R system 44
Figure 13. The initial concept of MW reactor chamber with the rotary drum. 45
Figure 14. MW PACVD vacuum reactor chamber 46
Figure 15. Photography of the rotary drum. 47
Figure 16. Photography showing vacuum ratio of the rotary drum..... 47
Figure 17. Photography of the quartz window during the process of plasma generation. .. 48
Figure 18. The rotary drum propulsion system. 48
Figure 19. The diagram of the waveguide line. 49
Figure 20. The diagram of the waveguide track with the circulator (red marked reflected energy returning to the microwave generator) 50

Figure 21. Three column microwave stub type E 50
Figure 22. The components of microwave generator 51
Figure 23. Magnetron head TMA1.2V52 from Alter Power Systems 52
Figure 24. Schematic diagram of the vacuum system used in MW PACVD+R 53
Figure 25. Schematic diagram of reactive gases dispersion in MW PACVD+R system ... 54
Figure 26. The control panel with a set of gauges 54
Figure 27. The schematic diagram of the microprocessor control of MW PACVD + R system 55
Figure 28. The microprocessor driver of the MW PACVD + R system 56
Figure 29. User interface in the WWW browser 58
Figure 30. SEM of the diamond nanopowder 62
Figure 31. The normal erythrocyte without detonation nanodiamonds particles after 10 minutes. Optical microscope OLYMPUS CX31, 400 times of magnification. 65
Figure 32. Rouleaux of erythrocytes in contact with ND-0 nanodiamond particles after 10 minutes. Optical microscope OLYMPUS CX31, 400 times of magnification. 66
Figure 33. Agglutination of red blood cells in contact with ND-1 nanodiamond particles after 10 minutes. Optical microscope OLYMPUS CX31, 400 times of magnification 66
Figure 34. The haemolysis of red blood cells (the presence of spherocytes) in contact with the presence of ND-1 nanodiamond particles after 10 minutes. Optical microscope OLYMPUS CX31, 400 times of magnification. 67
Figure 35. The normal human red blood cells and the shadows of erythrocytes and the presence of schistocytes in contact with ND-2 nanodiamond particles after 10 minutes. Optical microscope OLYMPUS CX31, 400 times of magnification. 67
Figure 36. The normal erythrocyte in contact with modified ND-3 nanodiamond particles after 10 minutes. Optical microscope OLYMPUS CX31, 400 times of magnification 68
Figure 37. HR TEM image of nanodiamond particles manufactured by detonation method 68
Figure 38. SEM detonation diamond nanopowder - PD 69
Figure 39. SEM detonation diamond nanopowder after the modification - PDM_30 69
Figure 40. SEM detonation diamond nanopowder after the modification - PDM_60 70
Figure 41. SEM conglomerate of the detonation diamond after modification - PDM_60 .. 70

Figure 42. Comparison of the FTIR spectrum of the detonation powder of all tested powders (ND-0 "Danilenko powder", ND-2 „Koszalin", ND-3 „Modified ND Koszalin" 71
Figure 43. Comparison of the FTIR spectrum of the detonation powder before and after the modification 72
Figure 44. Comparison of the FTIR spectrum of the detonation powder before (ND-2) and after the modification (ND-3) 73
Figure 45. Comparison of the FTIR spectrum of the detonation powder before (ND-2) and after the modification (ND-3) 73
Figure 46. Distribution of the spectrum at the range of 900-1500cm^{-1} for ND-2 and ND-3 74
Figure 47. Spectrum distribution at the range of 1500-1900cm^{-1} for ND-2 and ND-3 76
Figure 48. Distribution of the spectrum at the range of 2800-3000cm^{-1} for ND-2 and ND-3 78
Figure 49. Comparison of all examined particles in Raman spectroscopy (ND-0 "Damilenko powder", ND-2 „Koszalin", ND-3 „modified ND Koszalin") 80
Figure 50. Comparison of examined particles in Raman spectroscopy before ND-2 and after modification ND-3 81
Figure 51. Comparison of examined particles in Raman spectroscopy before ND-2 and after modification ND-3 81
Figure 52. Comparison of examined particles in Raman spectroscopy before ND-2 and after modification ND-3 82

12 Tables list

Tabel 1. The features of varietes of carbon materials [5] 10
Table 2. Some extreme properties of natural diamonds [Field, 1992, Maj, 2000]. 11
Table 3. The fragment of the source code of http website – user interface 57
Table 4. The fragment of the source code for Arduino UNO. 58
Table 5. Technical specifications of the diamond powder 62
Table 6. Technical specification of diamond powder 63
Table 7. Ref peak distribution (ND-2) 74
Table 8. Mod peak distribution (ND-3) 75
Table 9. Percentage comparison of the differences in the distribution of peak Ref (ND-2) and peak Mod (ND-3) 75
Table 10. Ref peak distribution (ND-2) 76
Table 11. Mod peak distribution (ND-3) 77
Table 12. Percentage comparison of the differences in the distribution of peak Ref (ND-2) and Mod (ND-3) 77
Table 13. Ref peak distribution (ND-2) 78
Table 14. Mod peak distribution (ND-3) 79
Table 15. Percentage comparison of the differences in the distribution of peak Ref (ND-2) and Mod (ND-3) 79

13 Appendix

Appendix 1

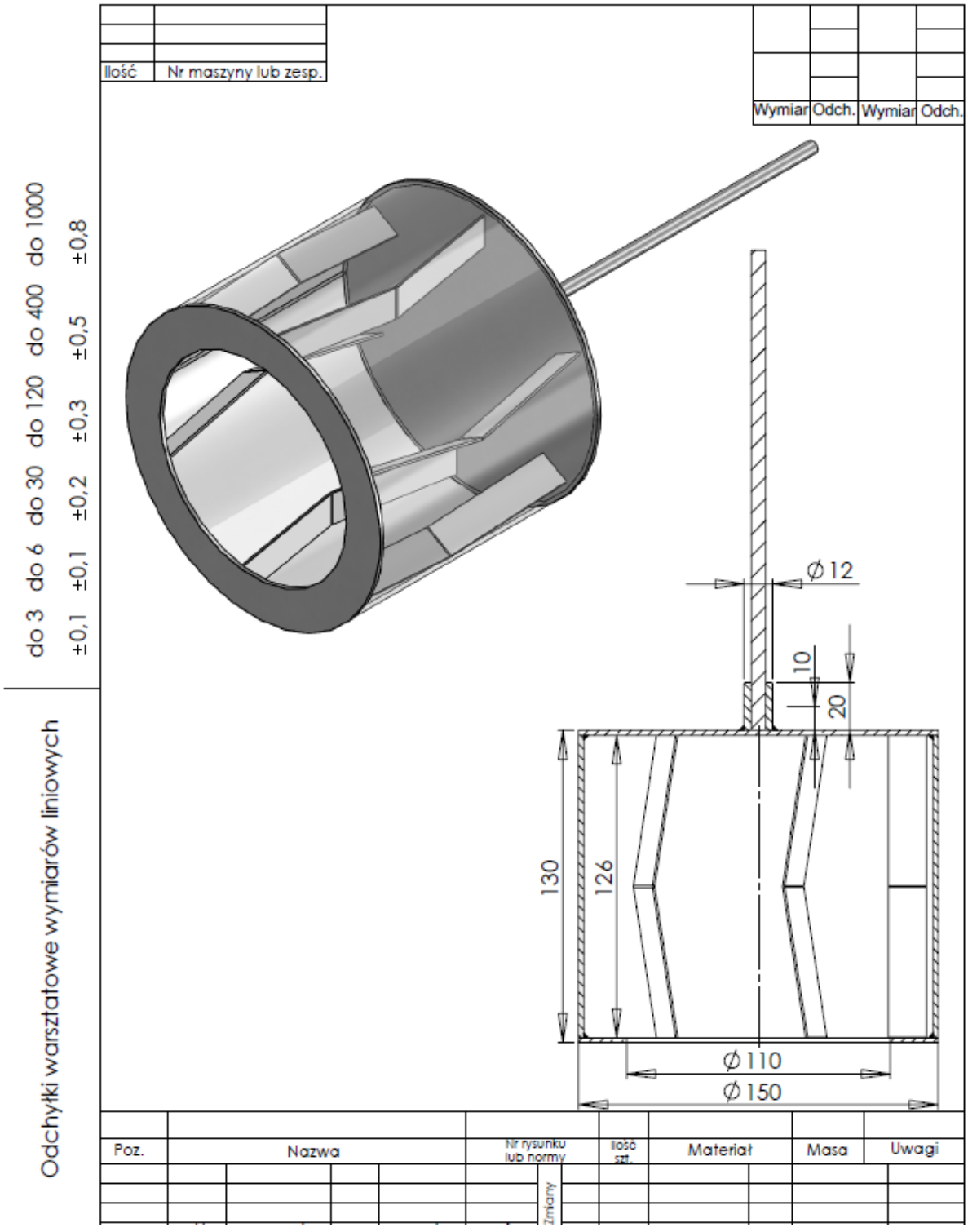
Ilość
Nr maszyny lub zesp.
Wymiar
Odch.
Wymiar
Odch.
do 3 ±0,1
do 6 ±0,1
do 30 ±0,2
do 120 ±0,3
do 400 ±0,5
do 1000 ±0,8
Odchyłki warsztatowe wymiarów liniowych
Ø12
10
20
130
126
Ø110
Ø150
Poz.
Nazwa
Nr rysunku lub normy
Ilość szt.
Materiał
Masa
Uwagi
Zmiany

Appendix 2

alter Power Systems

AG340M3 **3-Stub Tuner**

General description:

Waveguide type:	WR 340 (RETMA)
Flange type:	R 26 (IEC 153)
Frequency:	2450 Mhz +/- 50 Mhz
Power:	Look at graph
Material:	Aluminium (waveguide and stubs)
Finishing:	Alodine

AG340M3 Working graph

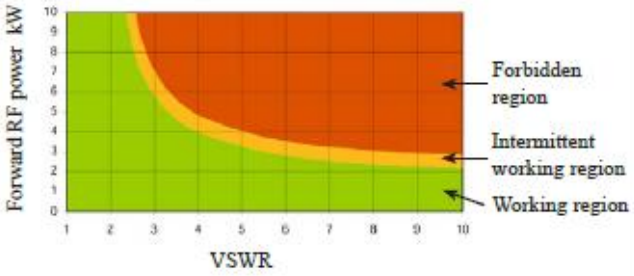

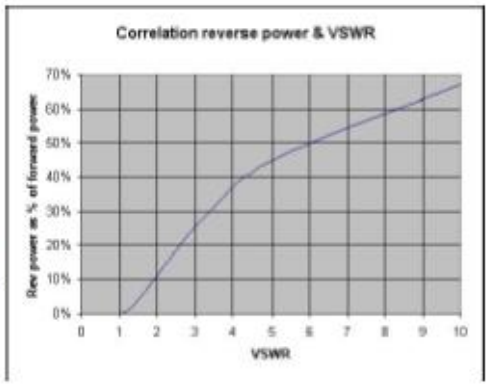

Outside dimensions

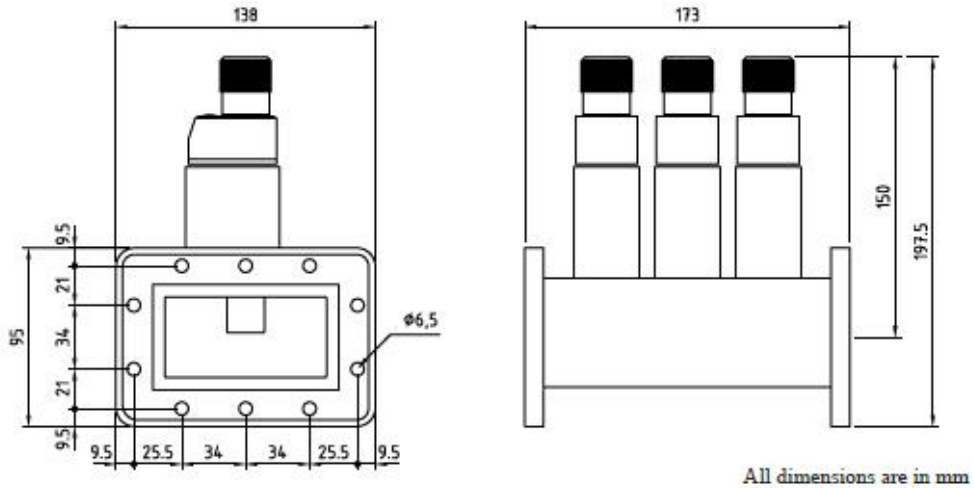

All dimensions are in mm

Appendix 3

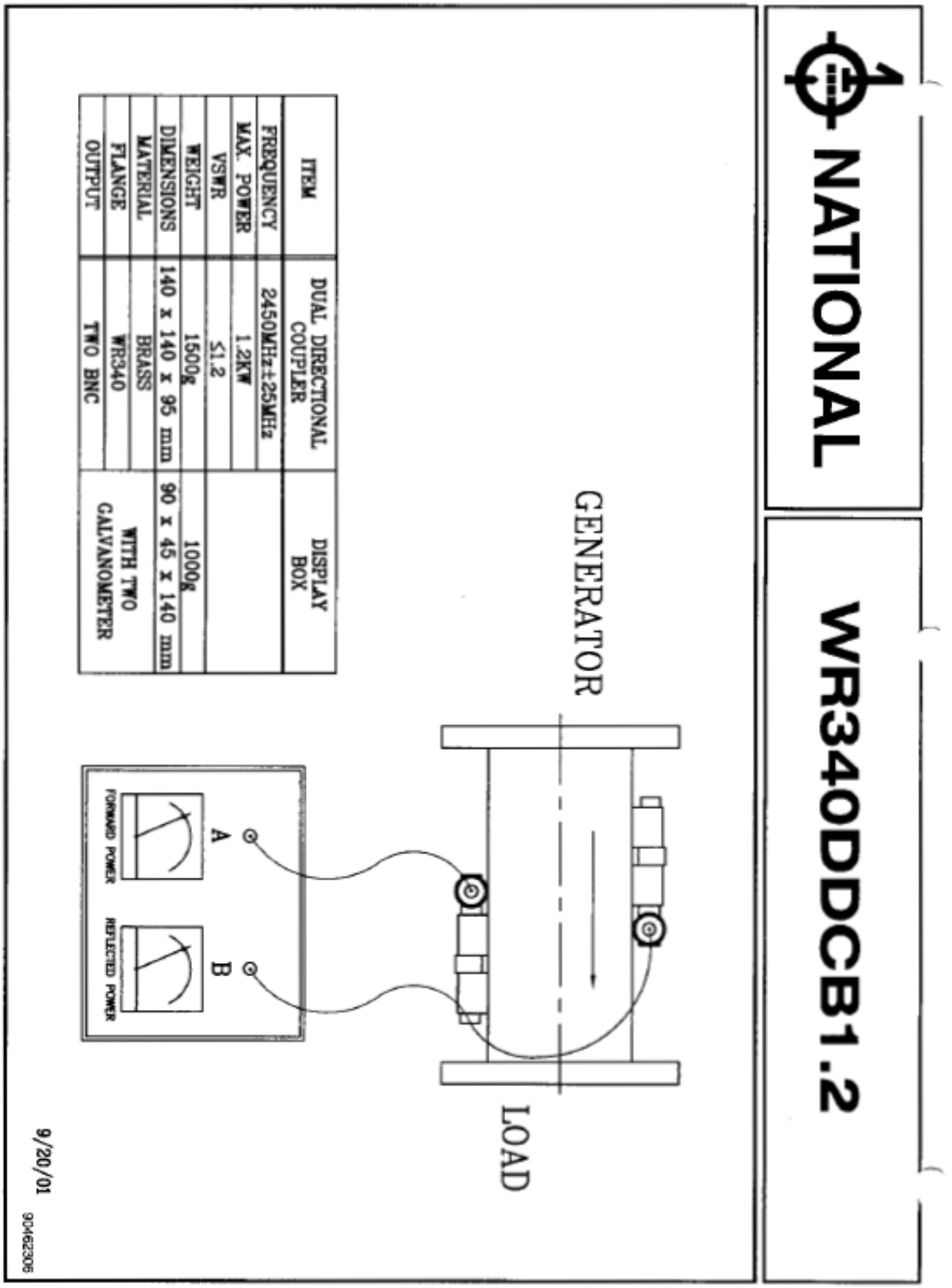
NATIONAL
WR340DDCB1.2
GENERATOR
LOAD
A
B
FORWARD POWER
REFLECTED POWER
ITEM
DUAL DIRECTIONAL COUPLER
DISPLAY BOX
FREQUENCY
2450MHz±25MHz
MAX. POWER
1.2KW
VSWR
≤1.2
WEIGHT
1500g
1000g
DIMENSIONS
140 x 140 x 95 mm
90 x 45 x 140 mm
MATERIAL
BRASS
FLANGE
WR340
WITH TWO GALVANOMETER
OUTPUT
TWO BNC
9/20/01
NATIONAL ELECTRONICS • A Division of Richardson Electronics, Ltd. • LaFox, IL 60147 (630) 208-2300

Appendix 4

alter Power Systems TM0 - TMA

COMPONENTS LAYOUT

Air cooled microwave generator up to 2 kW

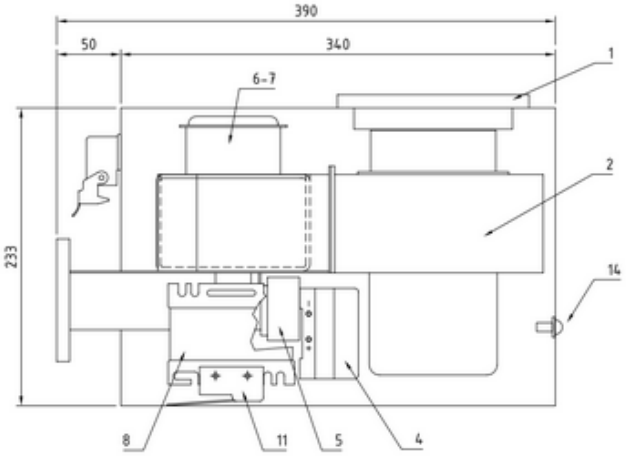

SIDE VIEW (WITHOUT COVER)
VISTA LATERALE (SENZA COPERCHIO)

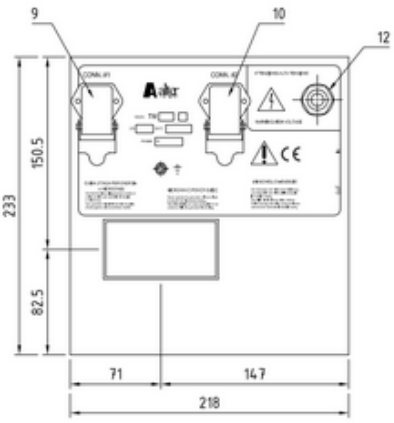

FRONT VIEW (WITHOUT FLANGE)
VISTA FRONTALE (SENZA FLANGIA)

Air cooled microwave generator 3 kW - TMA31

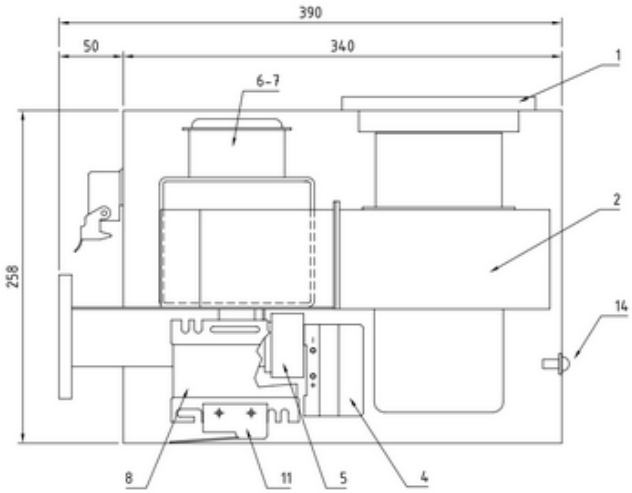

SIDE VIEW (WITHOUT COVER)

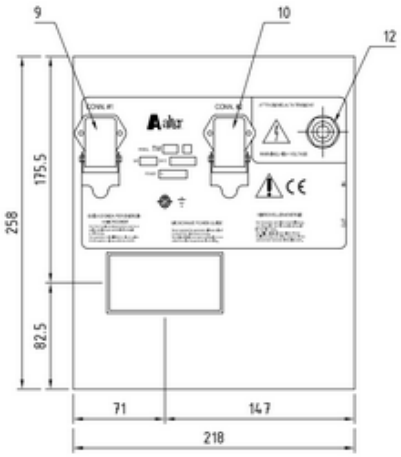

FRONT VIEW (WITHOUT FLANGE)

Appendix 5

alter SM445G & SM745G

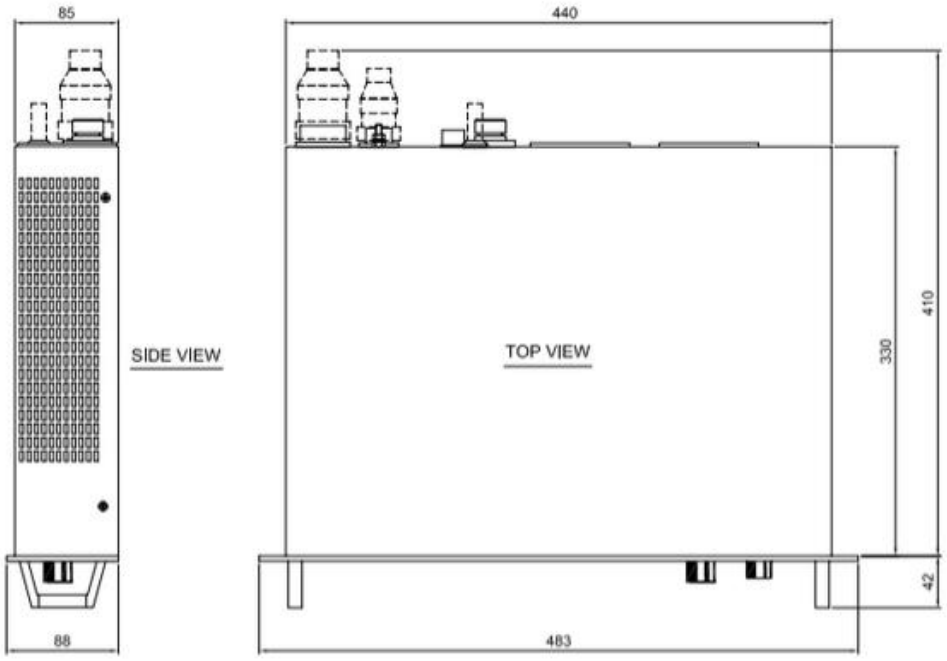

Power supply installation

Before use, the SMx45 must be installed in a proper cabinet like a commercial 19" standard rack.
The power supply must be safely fixed to the rack by means of 4 screws through the 4 holes provided on the front panel and supported by means of two angle (L shape) supports on the bottom.

Usually two "L" shape angle supports, one on each side is adequate.

The rear side of the power supply must be protected by a fixed panel which can be removed only by means of a special tool or by a security micro-switch so that when the door is opened the micro-switch will shut-off the mains. This safety precautions must be taken to prevent operations on rear fuses or on the connectors while the power supply is still powered.

Note that each equipment has its own fans on the rear side which intakes approx 150 m³/h: the exhaust outlets are on both sides of the power supply.

When designing a rack to house several units, we recommend adopting the following criteria:
1. use a standard 19" wide rack with a minimum depth of 600 mm (24");
2. allow free air intake from the rear of the rack;
3. if the ambient air contains dust and moisture, install an heat exchanger or proper filters with regular maintenance;
4. keep a separation between the air intake duct and the air outlets, to avoid recirculation;
5. when the air flow that exits from power supply cannot be exhausted directly into ambient, then a suitable fan must be used to remove the exhausted air.

Appendix 6

```
<!DOCTYPE html PUBLIC "-//W3C//DTD HTML 4.01 Transitional//EN" "http://www.w3.org/TR/html4/loose.dtd">
<html>
<head>
<meta http-equiv="Content-Type" content="text/html; charset=UTF-8">
<title>WebIOPi | Sterownik Komory MWPACVD</title>
<script type="text/javascript" src="webiopi.js"></script>
<script src="js/raphael.2.1.0.min.js"></script>
<script src="js/justgage.1.0.1.min.js"></script>
            <script src="js/highcharts.js"></script>
            <script src="js/modules/exporting.js"></script>
                        <script type="text/javascript">
      // Javascript code will go here
      // declare variable for Serial object
      var serial;
      webiopi().ready(init);
      // defines function passed to webiopi().ready()
      function init() {
            // define Serial object, must be configured in /etc/webiopi/config
            serial = new Serial("uno");
            // automatically refresh UI each 5 seconds
            setInterval(updateUI, 1000);
            // update UI now
            updateUI();
      }
//************************************* TIME ***************************************
      // function called through setInterval
      function updateUI() {
            // retrieve Time
            getTime();
      }
      // function to use "t" command
      function getTime() {
            serial.write("t");
            serial.read(timeCallback);
      }
      // function that will process received data from getTime function
      function timeCallback(data) {
            // rounds milliseconds to seconds
            millis = parseInt(data);
            seconds = parseInt(millis/1000);

            // use jQuery to display seconds elapsed since Arduino reset
            $("#time").text(seconds+" s");
            getAnalog();
      }

//************************************* ANALOG ***************************************
      // function to use "a0" command
```

```
function getAnalog() {
        serial.write("a0");
        serial.read(analogCallback);
}
// function that will process received data from getAnalog function
function analogCallback(data) {
        // scales analog value to percent and to 0-255 range
        value0 = parseInt(data);
        percent0 = parseFloat(value0 * 0.00515);
        red0 = parseInt(value0/1024 * 255);
        // use jQuery to display percent value
        $("#analog0").text(percent0+" V");
        // use jQuery to change color from black to red
        $("#analog0").css("background-color", "rgb(" + red0 + ", 0, 0)");
        getDigital();
}
                        // function to use "a1" command
function getAnalog() {
        serial.write("a1");
        serial.read(analogCallback);
}
// function that will process received data from getAnalog function
function analogCallback(data) {
        // scales analog value to percent and to 0-255 range
        value1 = parseInt(data);
        percent1 = parseFloat(value1 * 0.00515);
        red1 = parseInt(value1/1024 * 255);
        // use jQuery to display percent value
        $("#analog1").text(percent1+" V");
        // use jQuery to change color from black to red
        $("#analog1").css("background-color", "rgb(" + red1 + ", 0, 0)");
        getDigital();
}
// function to use "a2" command
function getAnalog() {
        serial.write("a2");
        serial.read(analogCallback);
}
// function that will process received data from getAnalog function
function analogCallback(data) {
        // scales analog value to percent and to 0-255 range
        value2 = parseInt(data);
        percent2 = parseFloat(value2 * 0.00515);
        red2 = parseInt(value2/1024 * 255);

        // use jQuery to display percent value
        $("#analog2").text(percent2+" V");
```

```
        // use jQuery to change color from black to red
        $("#analog2").css("background-color", "rgb(" + red2 + ", 0, 0)");
        getDigital();
}
// function to use "a3" command
function getAnalog() {
        serial.write("a3");
        serial.read(analogCallback);
}
// function that will process received data from getAnalog function
function analogCallback(data) {
        // scales analog value to percent and to 0-255 range
        value3 = parseInt(data);
        percent3 = parseFloat(value3 * 0.00515);
        red3 = parseInt(value3/1024 * 255);

        // use jQuery to display percent value
        $("#analog3").text(percent3+" V");

        // use jQuery to change color from black to red
        $("#analog3").css("background-color", "rgb(" + red3 + ", 0, 0)");
        getDigital();
}
                // function to use "a4" command
function getAnalog() {
        serial.write("a4");
        serial.read(analogCallback);
}
// function that will process received data from getAnalog function
function analogCallback(data) {
        // scales analog value to percent and to 0-255 range
        value4 = parseInt(data);
        percent4 = parseFloat(value4 * 0.00515);
        red4 = parseInt(value4/1024 * 255);

        // use jQuery to display percent value
        $("#analog4").text(percent4+" V");

        // use jQuery to change color from black to red
        $("#analog4").css("background-color", "rgb(" + red4 + ", 0, 0)");
        getDigital();
}
                // function to use "a5" command
function getAnalog() {
        serial.write("a5");
        serial.read(analogCallback);
}
// function that will process received data from getAnalog function
```

```
    function analogCallback(data) {
        // scales analog value to percent and to 0-255 range
        value5 = parseInt(data);
        percent5 = parseFloat(value5 * 0.00515);
        red5 = parseInt(value5/1024 * 255);
        // use jQuery to display percent value
        $("#analog5").text(percent5+" V");
        // use jQuery to change color from black to red
        $("#analog5").css("background-color", "rgb(" + red5 + ", 0, 0)");
        getDigital();
    }
//************************************** DIGITAL ****************************************
    // function to use "d" command
    function getDigital() {
        serial.write("d");
        serial.read(digitalCallback);
    }
    // function that will process received data from getDigital function
    function digitalCallback(data) {
        value = parseInt(data);

        // set appropriate color and text depending on value
        if (value == 1) {
            $("#digital").css("background-color", "Red");
            $("#digital").text("ON");
        }
        else if (value == 0) {
            $("#digital").css("background-color", "Black");
            $("#digital").text("OFF");
        }
    }
</script>
                    <script>
                    var g0, g1, g2, g3, g4, g5;
                    window.onload = function(){
                        var g0 = new JustGage({
                            id: "g0",
                            min: 0,
                            max: 5.242,
                            title: "Analog 0",
                            titleFontColor: "Black",
                            label: " Volt [V]",
                        });
                        var g1 = new JustGage({
                            id: "g1",
                            min: 0,
                            max: 5.242,
                            title: "Analog 1",
```

```
                titleFontColor: "Black",
                label: " Volt [V]",
});
var g2 = new JustGage({
                id: "g2",
                min: 0,
                max: 5.242,
                title: "Analog 2",
                titleFontColor: "Black",
                label: " Volt [V]",
});

var g3 = new JustGage({
                id: "g3",
                min: 0,
                max: 5.242,
                title: "Analog 3",
                titleFontColor: "Black",
                label: " Volt [V]",
});

var g4 = new JustGage({
                id: "g4",
                min: 0,
                max: 5.242,
                title: "Analog 4",
                titleFontColor: "Black",
                label: " Volt [V]",
});

var g5 = new JustGage({
                id: "g5",
                min: 0,
                max: 5.242,
                title: "Analog 5",
                titleFontColor: "Black",
                label: " Volt [V]",
});

setInterval(function() {
                g0.refresh(percent0);
                g1.refresh(percent1);
                g2.refresh(percent2);
                g3.refresh(percent3);
                g4.refresh(percent4);
                g5.refresh(percent5);

}, 1000);
```

```
};
</script>

<script type="text/javascript">
$(function () {
    $('#wykres').highcharts({
        title: {
            text: 'Monthly Average Temperature',
            x: -20 //center
        },
        subtitle: {
            text: 'Source: WorldClimate.com',
            x: -20
        },
        xAxis: {
            categories: ['Jan', 'Feb', 'Mar', 'Apr', 'May', 'Jun',
                'Jul', 'Aug', 'Sep', 'Oct', 'Nov', 'Dec']
        },
        yAxis: {
            title: {
                text: 'Temperature (°C)'
            },
            plotLines: [{
                value: 0,
                width: 1,
                color: '#808080'
            }]
    },
        tooltip: {
            valueSuffix: '°C'
        },
        legend: {
            layout: 'vertical',
            align: 'right',
            verticalAlign: 'middle',
            borderWidth: 0
        },
        series: [{
            name: 'Tokyo',
            data: [7.0, 6.9, 9.5, 14.5, 18.2, 21.5, 25.2, 26.5, 23.3, 18.3, 13.9, 9.6]
        }, {
            name: 'New York',
            data: [-0.2, 0.8, 5.7, 11.3, 17.0, 22.0, 24.8, 24.1, 20.1, 14.1, 8.6, 2.5]
        }, {
            name: 'Berlin',
            data: [-0.9, 0.6, 3.5, 8.4, 13.5, 17.0, 18.6, 17.9, 14.3, 9.0, 3.9, 1.0]
        }, {
            name: 'London',
```

```
                                                data: [3.9, 4.2, 5.7, 8.5, 11.9, 15.2, 17.0, 16.6, 14.2, 10.3, 6.6, 4.8]
                                        }]
                                });
                        });
                        </script>
<style type="text/css">
      #time, #analog0, #analog1, #analog2, #analog3, #analog4, #analog5, #digital {
            margin: 5px 5px 5px 5px;
            width: 160px;
            height: 45px;
            font-size: 24pt;
            font-weight: bold;
            color: white;
            text-align: center;
            background-color: Blue;
}
</style>
                        <style type="text/css">
                        #g0, #g1, #g2, #g3, #g4, #g5 {
                                        width:150px; height:78px;
                                        display: inline-block;
                                        margin: 0em;
    }
                        </style>
</head>
<body>
<div align="center">
<div id="time"></div>
                        <div id="analog0"></div>
                        <div id="analog1"></div>
                        <div id="analog2"></div>
                        <div id="analog3"></div>
                        <div id="analog4"></div>
                        <div id="analog5"></div>
                        <div id="digital"></div>
                        <div id="g0" style="width:300px; height:220px"></div>
                        <div id="g1" style="width:300px; height:220px"></div>
                        <div id="g2" style="width:300px; height:220px"></div>
                        <div id="g3" style="width:300px; height:220px"></div>
                        <div id="g4" style="width:300px; height:220px"></div>
                        <div id="g5" style="width:300px; height:220px"></div>
                        <div id="wykres" style="min-width: 310px; height: 400px; margin: 0 auto"></div>
</div>
</body>
</html>
```

Appendix 7

```
#include <SPI.h>
#include "Adafruit_MAX31855.h"
#define DO   3
#define CS   4
#define CLK  5
Adafruit_MAX31855 thermocouple(CLK, CS, DO);

char input;
float e;
float d;
void setup() {
  // open the serial port at 9600 bps:
  Serial.begin(9600);
 // delay(500);
}
void loop() {
  if (Serial.available() > 0) {
    input = Serial.read();
    switch (input) {
 //************************** TIME *********************************
      // "t" command: returns time in millis since reset/powerup
      case 't':
        Serial.println(millis());
        break;
 //************************** ANALOG *******************************
      // "a0" command: read and returns analog channel 0
      case 'a0':
        Serial.println(analogRead(0));
        break;

      // "a1" command: read and returns analog channel 1
      case 'a1':
        Serial.println(analogRead(1));
        break;

              // "a2" command: read and returns analog channel 2
      case 'a2':
        Serial.println(analogRead(2));
```

```
      break;

            // "a3" command: read and returns analog channel 3
    case 'a3':
      Serial.println(analogRead(3));
      break;

            // "a4" command: read and returns analog channel 4
    case 'a4':
      Serial.println(analogRead(4));
      break;

            // "a5" command: read and returns analog channel 5
    case 'a5':
      Serial.println(analogRead(5));
      break;
 //************************ THERMOCOUPLE *******************************
    // "e" command: read and returns thermocuple internal
    case 'e':
           //Serial.parseFloat();
            e = thermocouple.readInternal();
                  Serial.println(e);
                  break;
//---------------------------------------------------------------------
          // "d" command: read and returns thermocuple internal
    case 'd':
                  //Serial.parseFloat();
            d = thermocouple.readCelsius();
            Serial.println(d);
                  break;
    default:
break;
   }
  }
}
```